MEASUREMENTS VERSUS PREDICTIONS FOR ROTORDYNAMIC

COEFFICIENTS AND LEAKAGE RATES FOR A NOVEL HOLE-PATTERN

GAS SEAL

A Thesis

by

BRENT ALAN SEIFERT

Submitted to the Office of Graduate Studies of
Texas A&M University
in partial fulfillment of the requirements for the degree of

MASTER OF SCIENCE

December 2005

Major Subject: Mechanical Engineering

MEASUREMENTS VERSUS PREDICTIONS FOR ROTORDYNAMIC

COEFFICIENTS AND LEAKAGE RATES FOR A NOVEL HOLE-PATTERN

GAS SEAL

A Thesis

by

BRENT ALAN SEIFERT

Submitted to the Office of Graduate Studies of
Texas A&M University
in partial fulfillment of the requirements for the degree of

MASTER OF SCIENCE

Approved by:

Chair of Committee,   Dara Childs
Committee Members,   John Vance
                                   Paul Cizmas
Head of Department,   Dennis L. O'Neal

December 2005

Major Subject: Mechanical Engineering

ABSTRACT

Measurements versus Predictions for Rotordynamic Coefficients and Leakage

Rates for a Novel Hole-Pattern Gas Seal. (December 2005)

Brent Alan Seifert, B.S., Texas A&M University

Chair of Advisory Committee: Dr. Dara W. Childs

Results are presented for measured and predicted rotordynamic coefficients and leakage for hole-pattern seals with a hole depth that varies axially along the seal. Testing was done to discover how pressure ratio, inlet preswirl, and rotor speed affect the seals' rotordynamic characteristics and leakage. The results were compared to a constant hole depth hole-pattern seal.

Experimental results show that the seals' rotordynamic characteristics are not strongly influenced by pressure ratio.

There were three preswirl conditions tested, each separated by a 6.9 bar (100 psi) difference in inlet pressure. Therefore, normalized preswirl results were compared. The normalized results indicate that introducing inlet fluid preswirl affects the cross-coupled stiffness and effective damping coefficients. Inlet preswirl increases the magnitude of cross-coupled stiffness. Effective damping decreases with inlet preswirl, as well as the effective damping cross-over frequency increasing. These results indicate that swirl brakes would be of great value.

Rotor speed had a significant effect on the cross-coupled coefficients; both increased with speed.

Experimental results were compared to results for a constant hole depth hole-pattern seal. The variable hole-depth seal has higher direct damping. The cross-coupled stiffness and cross-coupled damping coefficients were very similar. The direct stiffness was always lower at lower frequencies and higher at higher frequencies for the variable hole depth hole-pattern seal. This was also the case for effective stiffness. The effective damping of the variable hole-depth seal was not only larger than for the

constant hole depth seal, it also had a drastically lower cross-over frequency. The difference in cross-over frequency was 40 percent on average.

Experimental results for rotordynamic characteristics and leakage were compared to theoretical predictions by ISOTSEAL 2, a modified version of ISOTSEAL. Both cross-coupled stiffness and damping are reasonably predicted. Direct damping is always under-predicted. ISOTSEAL 2 does a poor job of predicting direct stiffness. Direct stiffness is over-predicted at lower frequencies and under-predicted at higher frequencies. This is also the case for effective stiffness. ISOTSEAL 2 under-predicts the direct damping, but does an excellent job of predicting the direct damping cross-over frequency. Seal leakage is well predicted by ISOTSEAL 2.

ACKNOWLEDGEMENTS

I would like to thank Dr. Childs for allowing me the opportunity to work under him at the turbomachinery laboratory. It has been a great learning experience. All the advice and guidance from Dr. Childs has been invaluable.

I would like to thank Brad Kerr for all his help and guidance with the seal testing. I would also like to thank Zach Zutavern and Stephen Phillips for all their help during our many trouble-shooting sessions. I could not have completed my testing if not for these individuals.

I thank my wife for her support in all that I do. I never would have accomplished this, if not for her.

TABLE OF CONTENTS

LIST OF FIGURES

FIGURE   Page

LIST OF TABLES

NOMENCLATURE

A_{ij}	-	Stator acceleration	$[L/T^2]$
C_r	-	Radial Clearance	$[L]$
C	-	Direct damping	$[FT/L]$
c	-	Cross-coupled damping	$[FT/L]$
C_{ij}	-	Damping Coefficient	$[FT/L]$
C_{eff}	-	Effective Damping	$[FT/L]$
CHD	-	Constant Hole Depth	$[-]$
D_s	-	Seal Diameter	$[L]$
D_r	-	Rotor Diameter	$[L]$
D_{ij}	-	Relative Displacement	$[L]$
F_s	-	Seal reaction forces	$[F]$
F_{ij}	-	Force	$[F]$
g	-	Acceleration due to gravity	$[L/T^2]$
H_{ij}	-	Impedance	$[F/L]$
H_w	-	Inches of water	$[L]$
j	-	$\sqrt{-1}$	$[-]$
K	-	Direct stiffness	$[F/L]$
k	-	Cross-coupled stiffness	$[F/L]$
K_{ij}	-	Stiffness Coefficient	$[F/L]$
K_{eff}	-	Effective Stiffness	$[F/L]$
L	-	Seal Length	$[L]$
m_s	-	Stator mass	$[M]$
N	-	Rpm	$[1/T]$
P	-	Pressure	$[F/L^2]$
P_i	-	Inlet Pressure	$[F/L^2]$
P_e	-	Exit Pressure	$[F/L^2]$
PR	-	Pressure ratio	$[-]$
PS	-	Preswirl ratio	$[-]$

R	-	Gas constant	[FL/(MT)]
$\ddot{R}$	-	Stator acceleration vector	[L/T^2]
T_i	-	Inlet Temperature	[Θ]
T_e	-	Exit Temperature	[Θ]
V_t	-	Inlet tangential (swirl) velocity	[L/T]
VHD	-	Variable Hole Depth	[-]
X,Y	-	Displacement directions	[L]
$\dot{X},\dot{Y}$	-	Velocities	[L/T]
ΔP	-	Differential Pressure	[F/L^2]
$\dot{m}$	-	Mass flow rate	[M/T]
$\dot{Q}$	-	Flow Rate	[L^3/T]
ρ	-	Density of gas	[M/L^3]
ρ_a	-	Density of air at STP	[M/L^3]
ρ_w	-	Density of water	[M/L^3]
Ω	-	Excitation Frequency	[1/T]
ω	-	Running speed	[1/T]

Subscripts

ij	-	Direction of force and response	[-]

INTRODUCTION

Gas seals are used in compressors and turbines to control the leakage of the working fluid. They can also have a major effect on the stability of the system. There are many different types of gas seals, each with its own leakage and rotordynamic characteristics. A hole-pattern seal is basically a smooth seal with a hole-pattern drilled into the seal stator. Hole-pattern seals have been shown to have leakage and rotordynamic characteristics similar to honeycomb seals, Yu and Childs [1]. Honeycomb and hole-pattern seals have been shown to increase the stability of a rotordynamic system. This was demonstrated when labyrinth seals were replaced with honeycomb seals in the High Pressure Oxygen Turbopump of the Space Shuttle Main Engine, to solve synchronous and subsynchronous vibration problems, Childs and Moyer [2]. Hole-pattern seals have gained popularity in industry over honeycomb seals for two main reasons. First, honeycomb seals are much more difficult and expensive to manufacture. Second, honeycomb seals are very abrasive to the rotor if a rub occurs. The hole-pattern design, as well as the fact that hole-pattern seals can be made out of much softer material (e.g.: aluminum), make it much less abrasive. A typical hole-pattern seal and rotor configuration is shown in Fig. 1. The direction of the rotor as well as the preswirl rotation is shown.

This thesis follows the style and format of the ASME Journal of Engineering for Gas Turbines and Power.
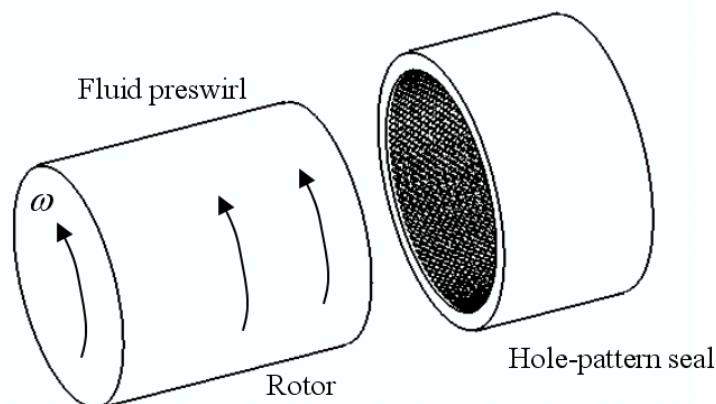
Fig. 1 Typical rotor annular seal configuration

The model for the reaction forces produced by hole-pattern seals is given in equation 1.

$$-\begin{Bmatrix} f_{sX} \\ f_{sY} \end{Bmatrix} = \begin{bmatrix} K(\Omega) & k(\Omega) \\ -k(\Omega) & K(\Omega) \end{bmatrix} \begin{Bmatrix} X \\ Y \end{Bmatrix} + \begin{bmatrix} C(\Omega) & c(\Omega) \\ -c(\Omega) & C(\Omega) \end{bmatrix} \begin{Bmatrix} \dot{X} \\ \dot{Y} \end{Bmatrix} \tag{1}$$

In this equation K is the direct stiffness, k is the cross-coupled stiffness, C is the direct damping and c is the cross-coupled damping. All variables are a function of the rotor precession frequency (Ω).

The effects of pressure ratio, preswirl, and rotor speed on the rotordynamic characteristics, as well as the leakage will be investigated. It was desired to also investigate the effect of two clearances on the seal. This was not done due to a seal instability that did not allow testing at the smaller clearance. The seals were tested under different conditions so that an understanding of the seals' behavior could be gained.

There has been much work done to discover the behavior of hole-pattern seals. However, to date there has been no experimental work published regarding the affect of varying the hole depth on a hole-pattern seal. Shin [3] predicted that almost any

variation in the hole depth would produce desirable rotordynamic characteristics over constant hole depth hole-pattern seals. One of the main advantages of variable hole depth seals is in the effective damping. Effective damping is a combination of the seal's tangential forces, direct damping and cross-coupled stiffness, which greatly influences the stability of a rotordynamic system. As effective damping increases, so does the system's stability. There is also a cross-over frequency associated with effective damping. The cross-over frequency is the frequency at which the effective damping goes from a negative, destabilizing force, to a positive, stabilizing force. Shin [3] predicted that varying the hole depth would increase the effective damping, as well as decrease the cross-over frequency. Therefore, the other main goal of this experimentation was to investigate how these seals compared to constant hole depth hole pattern seals.

LITERATURE REVIEW

Nelson [4] was one of the first to develop a computational model for smooth rotor, roughened stator seals. Nelson [4] was particularly interested in honeycomb seals. His model predicted that honeycomb seals would decrease cross-coupled stiffness, while at the same time increasing direct damping and stiffness.

Childs, Elrod, and Hale [5] were the first to dynamically test honeycomb seals. They found that with any inlet fluid rotation, honeycomb seals are more stable than both labyrinth and smooth seals. The characteristics of honeycomb seals were found to vary with cell dimension, although a trend was not discovered. They also found that rotordynamic characteristics for honeycomb seals vary with frequency.

Kleynhans and Childs [6] found that the acoustic influence of cell depth caused frequency depended rotordynamic characteristics. Their analysis showed that the cells of honeycomb seals reduce the effective acoustic velocity of the flow within the seals. This brought the seal's lower acoustic natural frequency into the frequency range of interest for rotordynamics. The two control volume model of Ha and Childs [7] was used to demonstrate that the rotordynamic characteristics could not be modeled as frequency independent.

Dawson [8] compared a straight bore and a convergent bore honeycomb seal. He found that the convergent bore seal had significantly more direct stiffness but significantly less direct damping. The convergent bore seal also had a severe leakage penalty. He also showed that the rotordynamic characteristics of honeycomb seals are frequency dependent.

Yu and Childs [1] compared hole-pattern seals to honeycomb seals. Three hole-pattern seal designs were compared to a honeycomb seal. They found that the hole-pattern seal configurations provided higher effective damping. Also, hole-pattern seals leaked less at zero inlet preswirl. The main conclusion was that honeycomb and hole-pattern seals behave similarly. Thus, hole-pattern seals are an attractive alternative to honeycomb seals.

Holt [9] tested two sets of hole-pattern seals with different hole depths. He showed that an increase in hole depth increases the effective stiffness, while

decreasing the effective damping. He also found that as hole depth increases leakage decreases.

Weatherwax [10] tested smooth and honeycomb seals at different eccentricities to find the effect of eccentricity on rotordynamic characteristics and leakage. He showed that the eccentricity of the rotor did not affect rotordynamic or leakage characteristics, up to a 50% eccentricity ratio. This is important because rotors and seals will never truly run centered.

Wade [11] tested hole-pattern gas seals under both choked and unchoked conditions. He found that there is not a significant change in seal behavior when the seals transition to the choked condition.

Shin [3] analytically studied the influence of hole depth variation on annular gas seals. He found that varying the hole depth axially has a dramatic impact on the frequency dependent rotordynamic characteristics.

THEORY AND MATHEMATICAL MODEL

The Laplace transform model from Kleynhans and Childs [6], shown in equation 2, was used to model the reaction forces of the seal.

$$-\begin{Bmatrix} F_x(s) \\ F_y(s) \end{Bmatrix} = \begin{bmatrix} D & E \\ -E & D \end{bmatrix} \begin{Bmatrix} x(s) \\ y(s) \end{Bmatrix} \tag{2}$$

In this equation **D** and **E** are the direct and cross-coupled impedance, respectively. **F_s** is the seal reaction force and **x**(s) and **y**(s) represent the reaction force between the rotor and stator. This model is good for small motion about a centered position. It is used for seals where the acoustic velocity of the main flow is within the rotordynamic range of interest, usually hole-pattern or honeycomb seals. This drop in the acoustic flow causes the seals to be frequency dependent, and they must be modeled as such. Once this frequency dependence is included in the seal model, equation 3 results.

$$-\begin{Bmatrix} f_{sX} \\ f_{sY} \end{Bmatrix} = \begin{bmatrix} K(\Omega) & k(\Omega) \\ -k(\Omega) & K(\Omega) \end{bmatrix} \begin{Bmatrix} X \\ Y \end{Bmatrix} + \begin{bmatrix} C(\Omega) & c(\Omega) \\ -c(\Omega) & C(\Omega) \end{bmatrix} \begin{Bmatrix} \dot{X} \\ \dot{Y} \end{Bmatrix} \tag{3}$$

To go from one form to the other the conversion in equation 4 is used.

$$D(j\Omega) = K(\Omega) + jC(\Omega)$$
$$E(j\Omega) = k(\Omega) + jc(\Omega) \tag{4}$$

In equation 4 $j = \sqrt{-1}$.

Effective stiffness and effective damping are two other coefficients that are very useful in comparing the rotordynamic characteristics of seals. The conversions for these coefficients are shown in equations 5 and 6.

$$K_{eff}(\Omega) = K(\Omega) + c(\Omega)\Omega \qquad (5)$$

$$C_{eff} = C(\Omega) - \frac{k(\Omega)}{\Omega} \qquad (6)$$

DESCRIPTION OF THE TEST RIG

The test rig was originally designed to test high-speed hydrostatic bearings. A complete description of the original test stand configuration is included in Childs and Hale [12]. The rig was later altered to accommodate the testing of gas seals [11]. Dawson et al. [13] describe how the test rig was altered to allow the testing of annular gas seals with an inlet pressure of up to 17.2 bar (250 psi). Later the test rig was modified yet again to allow testing of annular gas seals at much higher inlet pressures of up to 84 bar-a (1235 psi-a). Weatherwax and Childs [11], explain how the test rig was altered to handle this high pressure testing. The drive assembly rig can spin the test rotor up to 29,000 RPM. There is a throttling valve down stream of the test seals and upstream of the exit labyrinth seals that can be used to control the pressure drop across the test seals. The pressure ratio is defined as the exit pressure divided by the inlet
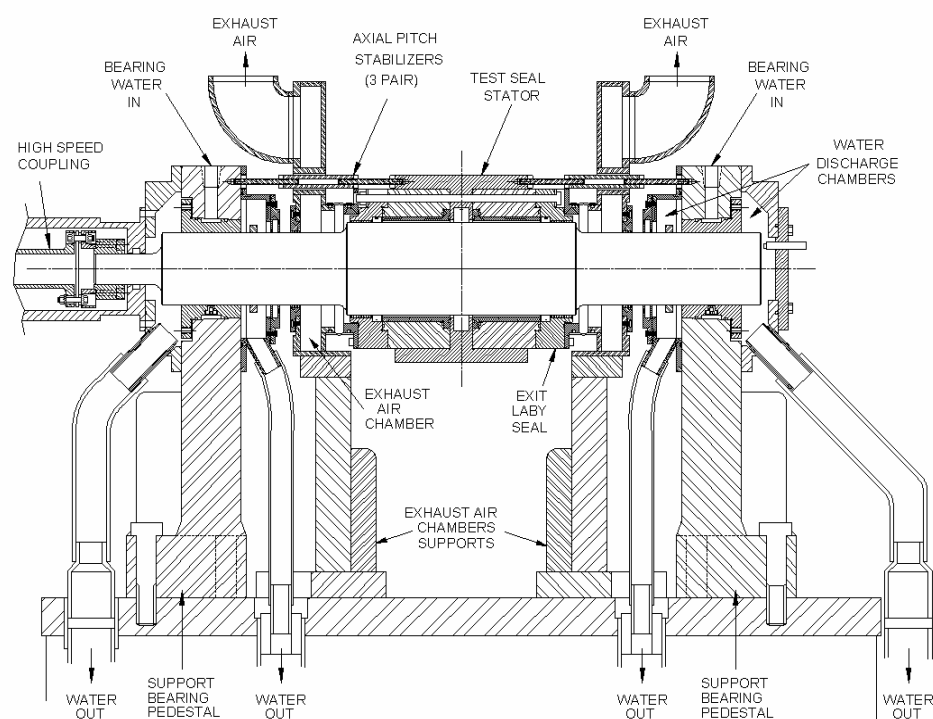
Fig. 2 Cross-section of the test rig

pressure. The pressure ratios that can be achieved with the backpressure valve are from 0.1 to 0.7, depending on the leakage of the test seals. Figure 2 shows a cross section view of the test rig [11].

The rotor is supported on hydrostatic bearings. The hydrostatic support bearings are supplied with water at 69 bar-a (1000 psi-a). Two rotors are used to provide the two seal clearances. These rotors both have the same axial measurements [11]. The only significant difference between the two rotors is their diameters under the test seals; one of the rotors has a 0.2 mm (8 mils) larger diameter than the other. The smaller rotor has a diameter of 114.3 mm (4.500 in). These dimensions result in a rotor-to-seal radial clearance of 0.2 mm (8 mils) for the seals tested. The larger rotor gives a radial clearance of 0.1 mm (4 mils). This clearance was not used due to a seal instability that did not allow testing at this condition [11].
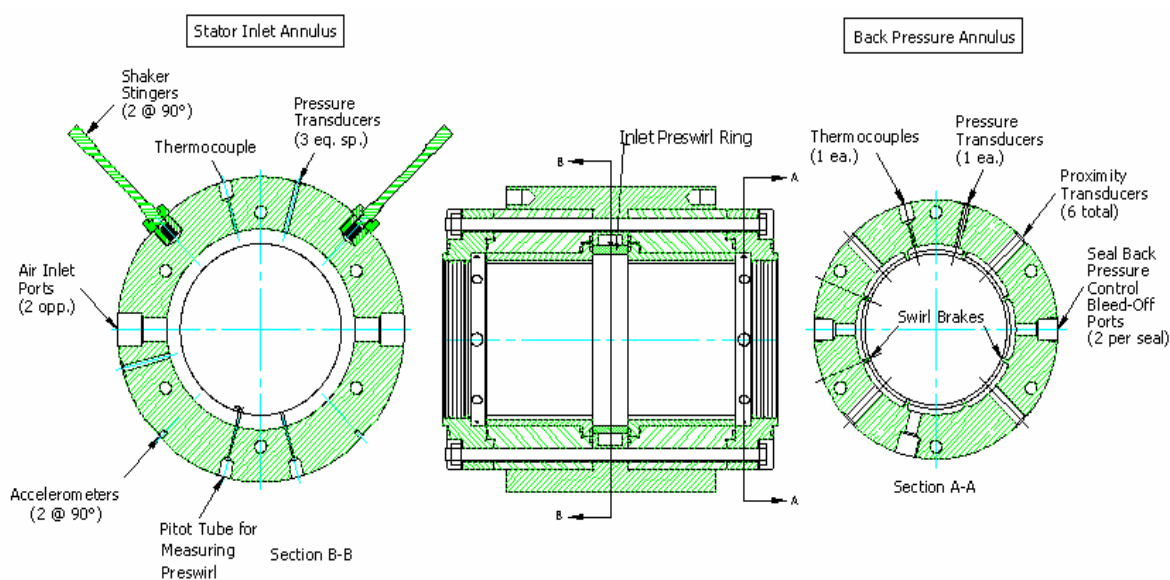
Fig. 3 Test stator

The seals are held in the stator assembly during testing. Two orthogonal hydraulic shakers support the stator assembly and control the seal's radial position relative to the rotor [11]. The stingers that the hydraulic shakers act through can be seen in Fig. 3 Section B-B. Force transducers that are in series with the stingers

measure the force exerted on the stator by the hydraulic shakers. Inline with the stingers, on the other side of the stator, there are accelerometers to measure the acceleration of the test stator in the two orthogonal directions corresponding to the directions the stator is shaken in.

There are three pitch stabilizers on each end of the stator; they are located in 120-degree increments around the rotor. The pitch stabilizers are constructed in three pieces so they can be preloaded. The pitch stabilizers attach axially between the stator and the hydrostatic bearing mounts.   The pitch stabilizers control the stator's axial position.   They also align the stator with the rotor so that there is not a pitch misalignment between the rotor and stator [11]. By tightening the pitch stabilizers in the appropriate manner, the stator can be positioned so that it is aligned with the rotor.

During a test, high-pressure air enters at the middle of the stator through the inlet pre-swirl ring, and then exits through the two test seals. The exiting air then passes through swirl brakes before the exit labyrinth seals. The swirl brakes before the exit labyrinth seals are provided to minimize the cross coupled forces from the exit labyrinth seals [11].

The stator is instrumented to obtain the inlet and exit air pressure and temperature. At the inlet to the test seals, the circumferential velocity of the air is measured using a pitot tube. Once the circumferential velocity of the air is known, the fluid pre-swirl can be calculated. The motor used to control the speed of the rotor is a 93 kW (125 hp) AC electric motor. The rotor can be rotated at up to 29,000 RPM because it is driven by the electric motor through a Lufkin 6.960:1 step-up gearbox. A high-speed flexible coupling is used to link the test rotor to the gearbox [11].

Parameter identification

The stator is excited in two orthogonal directions as stated before. The equation for the stator's motion is

$$\begin{Bmatrix} f_X \\ f_Y \end{Bmatrix} - \begin{Bmatrix} m_s \ddot{R}_{sX} \\ m_s \ddot{R}_{sY} \end{Bmatrix} = - \begin{Bmatrix} f_{sX} \\ f_{sY} \end{Bmatrix} \qquad (7)$$

where f is the measured excitation force, f_s is the seal reaction force, $\ddot{R}_s$ is the measured acceleration of the stator, and m_s is the stator mass. Restating equation 7 in the frequency domain yields,

$$\begin{Bmatrix} F_X - m_s A_X \\ F_Y - m_s A_Y \end{Bmatrix} = -\begin{bmatrix} H_{XX} & H_{XY} \\ H_{YX} & H_{YY} \end{bmatrix} \begin{Bmatrix} D_X \\ D_Y \end{Bmatrix} \tag{8}$$

where **F** and **A** are complex force and acceleration vectors expressed in the frequency domain, and the dynamic stiffness coefficient matrix defines the seal reaction forces. There are four unknowns $\mathbf{H}_{xx}$, $\mathbf{H}_{xy}$, $\mathbf{H}_{yx}$, and $\mathbf{H}_{yy}$.

To solve for the four unknowns the stator is shaken in orthogonal, X and Y directions. By shaking in two orthogonal directions four independent equations are obtained with four unknowns given by equation 9.

$$\begin{bmatrix} F_{XX} - m_s A_{XX} & F_{XX} - m_s A_{XX} \\ F_{XX} - m_s A_{XX} & F_{XX} - m_s A_{XX} \end{bmatrix} = -\begin{bmatrix} H_{XX} & H_{XY} \\ H_{YX} & H_{YY} \end{bmatrix} \begin{bmatrix} D_{XX} & D_{XY} \\ D_{YX} & D_{YY} \end{bmatrix} \tag{9}$$

Equation 9 is valid for small motion about a centered position, and has been verified by previous tests. Also the assumption is made that k_{xy} is equal to $-k_{yx}$; the data supports this assumption. The stiffness and damping terms are found directly from the impedances.

$$K(\Omega) = \text{Re}(H_{ii}(\Omega)) \tag{10}$$

$$k(\Omega) = \text{Re}(H_{ij}(\Omega)) \tag{11}$$

$$C(\Omega) = \frac{\text{Im}(H_{ii}(\Omega))}{\Omega} \tag{12}$$

$$c(\Omega) = \frac{\text{Im}(H_{ij}(\Omega))}{\Omega} \tag{13}$$

Test seals

The tests for this thesis were conducted using a pair of variable hole depth hole-pattern seals. The hole depth decreased from the inlet to the exit of the seal. The hole depth decrease follows equation 14

$$H_d = H_{d,in} + \frac{H_{d,ex} - H_{d,in}}{\sqrt{L}} \sqrt{Z} \, ,$$ (14)

where Z is the axial position within the seal and downstream of the inlet. In equation 14, H_d is the hole depth, $H_{d,in}$ is the inlet hole depth, $H_{d,ex}$ is the exit hole depth, and L is the seal's length. The design for these seals was $H_{d,in}$ = 5.067 mm (0.1995 in), $H_{d,ex}$ = 1.689 mm (0.0665 in), and L = 81.610 mm (3.213 in.). The seals followed the trend for decreasing hole depth. However, the centered hole depth was machined 5.842 mm (0.23 in.) deeper than designed. The extra depth is mainly due to the tip of the drill bit being triangular and not square. The seals were machined out of 6061 aluminum with a constant hole diameter of 3.175 mm (0.125 inches).

The test seals' inner diameter measurements are presented in Table 1. The inner bore diameter of the seals was measured using a three-point gauge that is accurate to 0.00254 mm (0.0001 in). Each seal was measured in three locations, rotating 60 degrees between each measurement, at both the inlet of the seals and the outlet of the seal. As can be seen in Table 1, the seals were matched very well.

Table 1 Seal diameter dimensions

Seal 1				
Angle	Inlet		Outlet	
0	114.729 mm	(4.5169 in)	114.729 mm	(4.5169 in)
60	114.727 mm	(4.5168 in)	114.732 mm	(4.5170 in)
120	114.729 mm	(4.5169 in)	114.729 mm	(4.5169 in)
Average:	114.728 mm	(4.5169 in)	114.730 mm	(4.5169 in)

Seal 2				
Angle	Inlet		Outlet	
0	114.727 mm	(4.5168 in)	114.727 mm	(4.5168 in)
60	114.732 mm	(4.5170 in)	114.724 mm	(4.5167 in)
120	114.727 mm	(4.5168 in)	114.729 mm	(4.5169 in)
Average:	114.729 mm	(4.5169in)	114.727 mm	(4.5168 in)

Gamma is a way to describe how close together the holes are. Gamma is the ratio of the area of the holes to the area of the inner surface of the seal. The seals tested have a gamma of 0.69; therefore 69% of the inner surface area is taken up by holes. The seals are 85.725 mm (3.375 in) long and as shown in Table 1, the diameter of the seals is an average of 114.729 mm (4.5169 in), therefore these seals have a L/D ratio of 0.75. Figure 4 shows the important dimensions of the test seal.
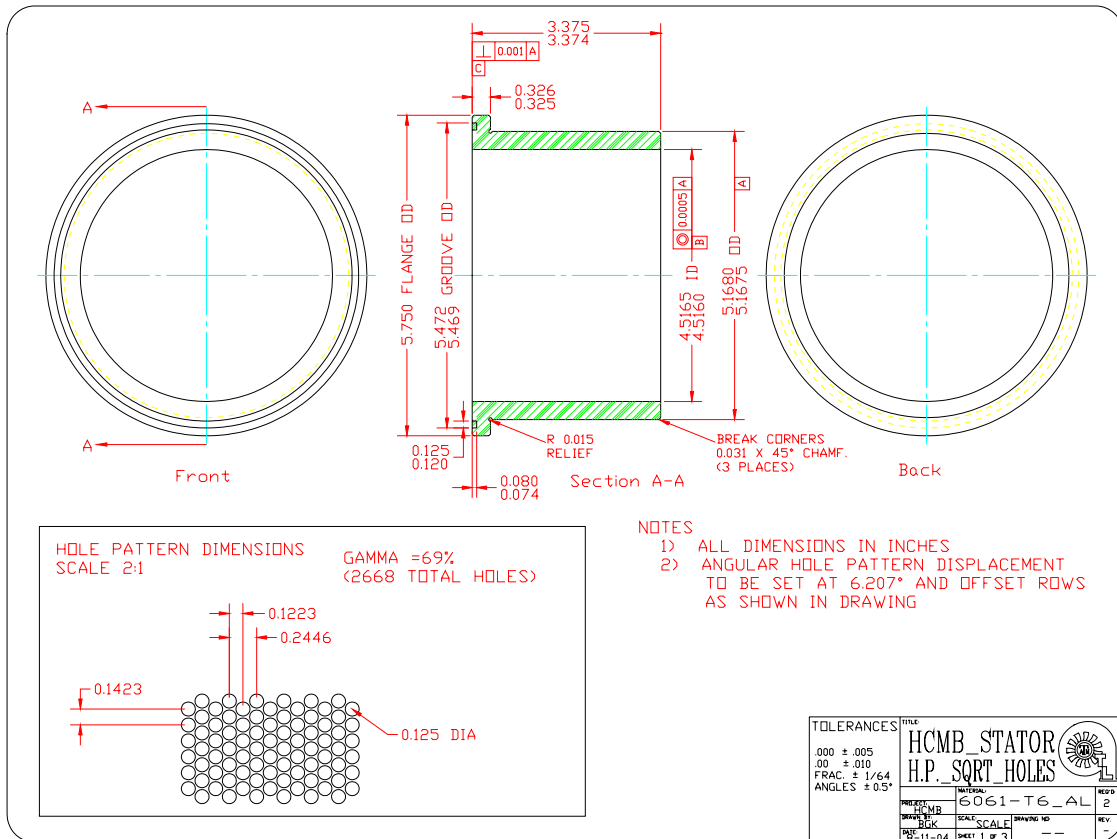
Fig. 4 Drawing of the test seals

Fluid preswirl

Circumferential fluid flow causes cross-coupled stiffness and damping terms. Some seals are more sensitive to fluid rotation and therefore produce larger cross-coupled terms given the same fluid swirl conditions [11]. Some of the test matrix conditions for the seals were chosen to explore how the seals respond to various inlet swirl conditions. Figure 5 shows a cross-section of the different preswirl rings [11].
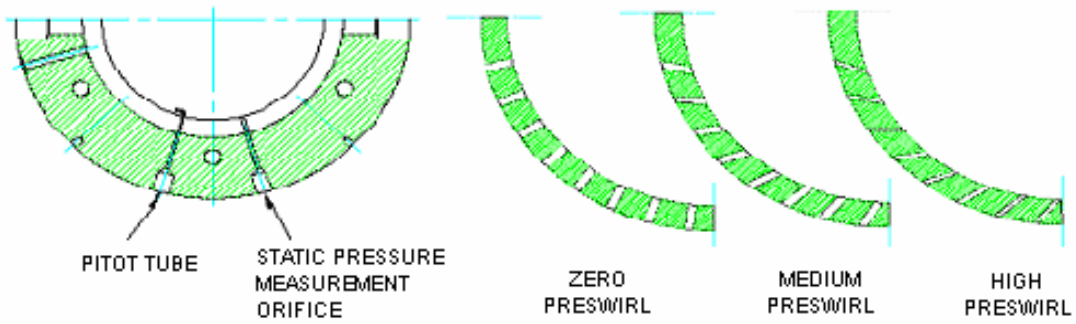
Fig. 5 Cross-section view of the preswirl rings

Fluid preswirl is defined as the fluid's circumferential velocity divided by the rotor's surface speed, equation 15.

$$\text{Ratio}_{\text{pre-swirl}} = \frac{V_t \cdot 60}{\pi \cdot N \cdot D_r} \tag{15}$$
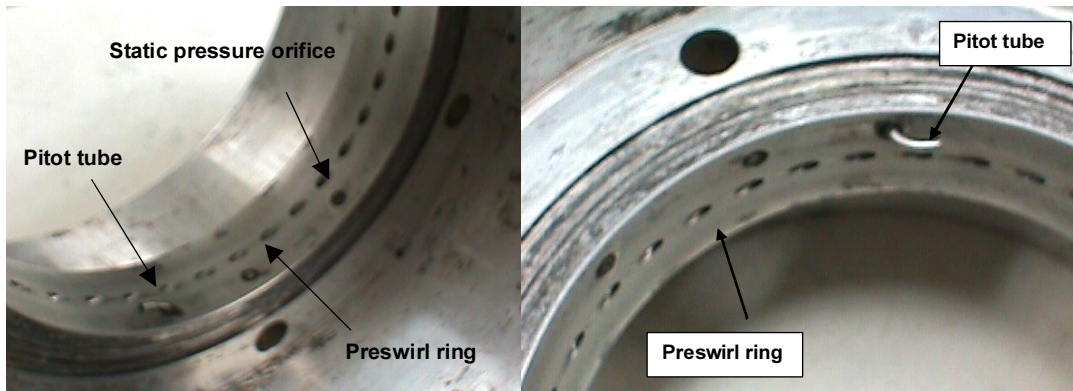
Fig. 6 Preswirl ring and preswirl measurement

A pre-swirl ratio of 1.0 means that the fluid enters the seal with a speed equal to the surface velocity of the rotor, and a value of 0.5 means that the fluid is rotating at half of

the rotor's surface speed. Also, a negative preswirl ratio value would indicate that the fluid is rotating against the direction of rotation of the rotor.

This test rig measures the fluid circumferential velocity using a pitot tube located at the inlet annulus; it measures the fluid swirl immediately before the fluid enters the test seals. The pitot tube can be seen in Fig. 6. The fluid circumferential velocity is calculated based on the pressure differential between the static and stagnation pressures measured in the inlet annulus. Figure 6 shows the stator inlet annulus, and the pre-swirl ring is visible. The inlet annulus is also shown in the stator diagram in Fig. 3 Section B-B.

The preswirl ring in the inlet annulus directs the air circumferentially [11]. The high-pressure air is fed into the inlet annulus and then flows through the preswirl ring before entering the test seals. Three levels of preswirl rings were tested, and they are called, zero, medium, and high. The zero preswirl ring has holes that are radial, injecting the air radially onto the rotor. The medium pre-swirl ring is designed to give the incoming air a preswirl ratio of approximately 0.5, for the medium rotor speed of 15,200 RPM. The high preswirl ring is designed to produce a preswirl ratio of approximately 1.0, again with a rotor speed of 15,200 RPM. Figure 5 shows a cross-section view of the three preswirl rings and another view of the pitot tube and static pressure measurement orifice [11].

Leakage flow

All annular seals allow a certain amount of leakage to occur [11]. Leakage depends on many factors, but the main factors in determining how much mass flow a given annular gas seal will allow in a giving situation are, the pressure drop across the seal, the radial clearance between the rotor and the seal, the length of the seal, and the relative roughness of the seal and rotor surfaces [11].

The test rig measures the volumetric flow rate of air that flows through the rig by a turbine style flow meter up stream of the test seals. The flow meter is located between the inlet control valve and the inlet annulus of the test stator, and measures the total flow through both seals. Since the seals are physically as close to identical as

possible, and the pressure drop across both seals is measured and found to be approximately the same, the flow is assumed to be split evenly between each seal.

The temperature and pressure of the air passing through the flow meter are also measured and used to convert from the volumetric flow rate to the mass flow rate [11]. As the test is running, the volumetric flow rate, the temperature, and the pressure of the air are recorded five times before a shake test is run. These five samples are recorded while the test rig is operating in a steady state condition. The five data points are then averaged and the average value is what has been reported [11].

Test conditions

The seals were tested in a variety of conditions, four pressure ratios, three preswirls, and three rotor speeds with a total of 36 different test conditions. The test matrix is presented in Table 2. The inlet pressure changed from 41.37 bar (600 psi), to 34.47 bar (500 psi), to 27.58 bar (400 psi) for the three different inlet preswirl conditions. There was also a test run with an inlet pressure of 55.16 bar (800 psi) for zero preswirl, all rotor speeds, and 50 percent pressure ratio. As noted previously, the rig can be used to test seals with a supply pressure up to 70 bars (1015 psi). However, the current seals had static stability problems at higher supply pressures and lower pressure ratios. Specifically, the stator shifted into contact with the rotor. This was because of a seal instability that worsened with increased inlet preswirl. The maximum allowable pressure was tested for each inlet preswirl. The different inlet pressures are listed in Table 2. The temperature of the incoming air was recorded, to make corrections for air density. Relative humidity of the incoming air is not controlled. The relative humidity of the air was not measured.

There was a rub during testing with zero inlet preswirl, a rotor speed of 20,200 RPM, and 30 percent pressure ratio. Therefore, there is no data for this test condition. There was no visible damage to the seals. They were measured in the inlet, exit and center, in the same manner as mentioned earlier, and found to still be concentric. However, the diameter did increase by approximately 0.02032 mm (0.0008 in.).

Table 2 Test matrix

Pre-Swirl	Rotor Speed	Radial Seal Clearance	Inlet Pressure	Pressure Ratio
(-)	(N)	(mm)	(bar)	(-)
Zero	10,200	0.20	55.16	0.5
	15,200	0.20	55.16	0.5
	20,200	0.20	55.16	0.5
Zero	10,200	0.20	41.37	0.30, 0.40, 0.50
	15,200	0.20	41.37	0.30, 0.40, 0.50
	20,200	0.20	41.37	0.30, 0.40, 0.50
Medium	10,200	0.20	34.47	0.30, 0.40, 0.50
	15,200	0.20	34.47	0.30, 0.40, 0.50
	20,200	0.20	34.47	0.30, 0.40, 0.50
High	10,200	0.20	27.58	0.30, 0.40, 0.50
	15,200	0.20	27.58	0.30, 0.40, 0.50
	20,200	0.20	27.58	0.30, 0.40, 0.50

EXPERIMENTAL RESULTS

Baseline data

To account for the stiffness and damping that are not produced by the test seals, baseline data are measured. The baseline data are obtained by assembling the test rig without seals in the test stator. The stator is pressurized, and with the rotor spinning, the stator is shaken and data recorded. This step is taken to measure the forces that result from the exit labyrinth seals and the stiffness and damping of the stator assembly. The rotordynamic coefficients are obtained by subtracting the baseline real and imaginary impedances from the corresponding real and imaginary impedances produced with the test seals installed.

Test data uncertainty

There is some uncertainty with any measurement [11]. With these experiments, there is uncertainty in the measurements of force, acceleration, pressure, temperature, and rotor speed. Kurtin et al. [14] performed uncertainty analysis for the static coefficients of the test rig. The uncertainties are presented in Table 3.

Table 3 Static parameter's uncertainties

Shaft Speed	Pressure	Flow Rate	Eccentricity Ratio
(N)	(P)	$(\dot{Q})$	(e)
10 RPM	3.747 kPa	0.177 L/min	0.005

To obtain an uncertainty value for the impedances, a single dynamic test was repeated ten times. The uncertainty of the impedances was found in this manner for each test. During testing the 15,200 RPM rotor speed test was repeated ten times. The data were then reduced to calculate the stiffness and damping terms. The standard

deviation of each term at the discrete frequencies is then calculated. The standard deviation of the term is plotted as uncertainty bars on the data graphs [11].

Uncertainty data were taken in the same manner for the baseline data. All of the data that are reported in this thesis combine the baseline and test uncertainties. Equation 16 shows how the uncertainties are combined.

$$U_{total} = \sqrt{U_{Baseline}^2 + U_{Test\_data}^2} \qquad (16)$$

Non-dimensional and normalized rotordynamic coefficients

Seal data are non-dimensionalized so comparisons can be made to seals that have a larger diameter, different clearance, or length. Non-dimensionalizing also collapses the data to a more condensed form.

The non-dimensionalization used for the direct and cross-coupled stiffness can be seen in equation 17. The normalization used for direct and cross-coupled damping is shown in equation 18.

$$K^* = K\frac{C_r}{L \cdot 2 \cdot R \cdot \Delta P} \qquad\qquad k^* = k\frac{C_r}{L \cdot 2 \cdot R \cdot \Delta P} \qquad (17)$$

$$C^* = C\frac{C_r}{L \cdot 2 \cdot R \cdot \Delta P} \qquad\qquad c^* = c\frac{C_r}{L \cdot 2 \cdot R \cdot \Delta P} \qquad (18)$$

In equations 17 and 18, L is the length of the seal, R is the radius of the seal, ΔP is the pressure differential, and C_r is the radial clearance of the seal. The normalization for damping produces units of seconds.

The non-dimensionalization used for leakage is shown in equation 19.

$$\varphi = \frac{\dot{m}}{\pi \cdot D \cdot C_r} \left(\sqrt{\frac{R_c T_{in}}{2 \cdot \Delta P \cdot P_{in}}} \right) \qquad (19)$$

In the above equation $\dot{m}$ is the mass flow rate, D is the diameter of the seal, C_r is the radial clearance of the seal, R_c is the ideal gas constant, T_{in} is the inlet temperature, ΔP is the differential pressure, and P_{in} is the inlet pressure.

Fig. 7 illustrates the effect of a 13.19 bar (200 psi) change in inlet pressure on non-dimensional and normalized rotordynamic coefficients. The data were taken for two inlet pressures (55.16 bar and 41.37 bar) with zero inlet preswirl, 50 percent pressure ratio, and a rotor speed of 20,200 RPM. The normalized direct stiffness, direct damping, effective stiffness and effective damping are virtually identical. There is a small change in the normalized cross-coupled coefficients. The comparison is the same for all rotor speeds. Figure 7 illustrates the effectiveness of comparing rotordynamic coefficients using non-dimensional and normalized coefficients for a 13.19 bar difference in inlet pressure. This is an encouraging finding because when comparing different inlet preswirls there will be a maximum inlet pressure difference of 13.19 bar.
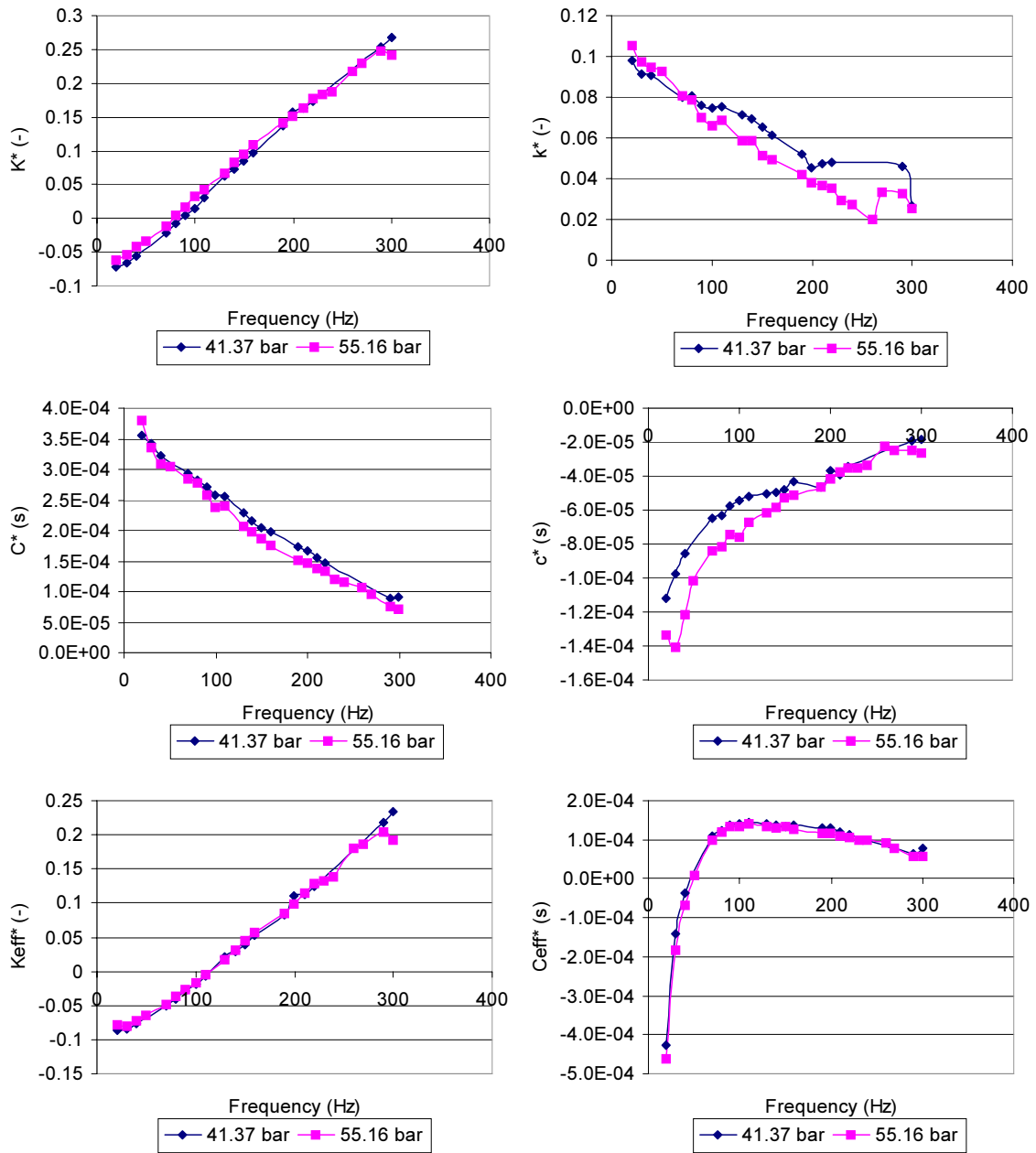
Fig. 7 Non-dimensional coefficients versus excitation frequencies for different inlet
pressures with zero preswirl, PR = 50%, ω = 20,200 RPM

DISCUSSION OF RESULTS FOR VARIABLE HOLE DEPTH HOLE-PATTERN SEALS

The matrix used for testing was designed to discover how the rotordynamic characteristics and leakage of the seals react to changes in pressure ratio, inlet preswirl, and rotor speed. The results presented comparing different preswirls will be non-dimensionalized for stiffness and normalized for damping because of the different inlet pressures used at different inlet preswirl conditions.

Direct and cross-coupled stiffness

This section considers the effect of the different test conditions on direct and cross-coupled stiffness. The direct and cross-coupled stiffness comes from the real part of the impedance, as shown in equations 10 and 11. These seals exhibited a negative stiffness at lower frequencies for all test cases, which is not expected for hole-pattern seals. This may be an indication that some sort of friction factor jump phenomenon is occurring, Ha and Childs [7]. To date, it is believed that three seals at Texas A&M Turbomachinery Laboratory have exhibited this behavior. However, there has been no published work to explain why or when this behavior occurs.

Figure 8 is a good illustration of how the pressure ratio affects direct and cross coupled stiffness. The data presented in Fig. 8 are the average of the direct and cross-coupled stiffness in the X and Y directions. All data presented will be the average of the coefficients in the X and Y directions unless otherwise noted. Figure 8 shows that pressure ratio does not have a strong influence on either direct or cross-coupled stiffness.
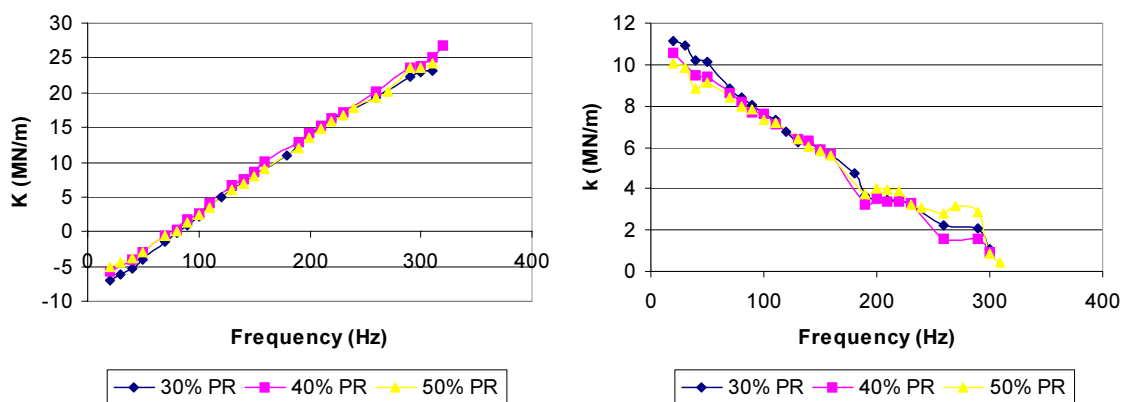
Fig. 8 Direct and cross-coupled stiffness versus excitation frequency for all pressure ratios, with a medium inlet preswirl, ω = 20,200 RPM and P_i = 34.47 bar

Figure 9 demonstrates the influence of the preswirl on non-dimensional direct and cross-coupled stiffness.
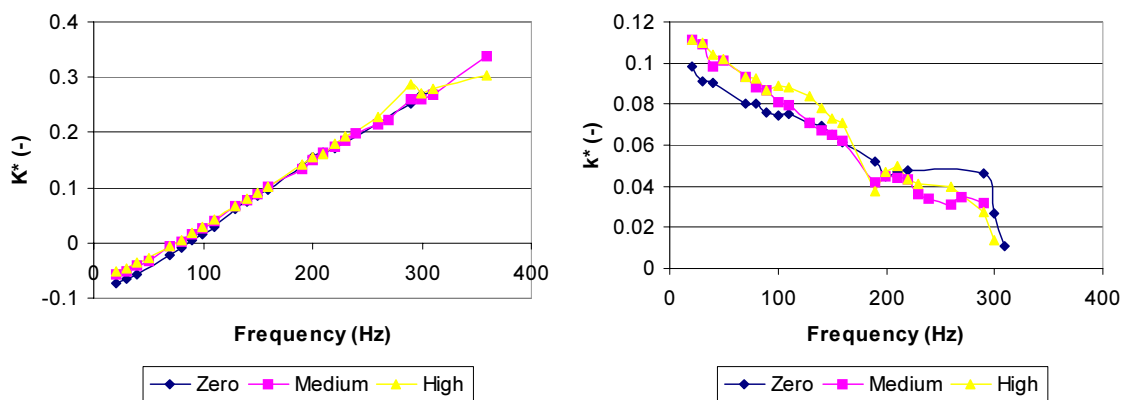
Fig. 9 Non-dimensional direct and cross-coupled stiffness versus excitation frequency for all preswirls, PR = 50%, ω = 20,200 RPM and P_i = 41.37 bar, 34.47 bar, 27.57 bar

The inlet pressure is different for each inlet preswirl, see Table 2. The data illustrate that non-dimensional direct stiffness is not influenced by the inlet preswirl. There is a slight increase in non-dimensional cross-coupled stiffness at lower excitation

frequencies; with preswirl having no influence at higher excitation frequencies. However, there is little difference between medium and high inlet preswirls. This outcome is more pronounced in most tests cases.

The effect of speed on direct and cross-coupled stiffness is illustrated in Fig. 10. Speed does not affect direct stiffness, but does have an effect on cross-coupled stiffness. The cross-coupled stiffness increases with speed. This result is expected since rotor speed increases fluid circumferential velocities.
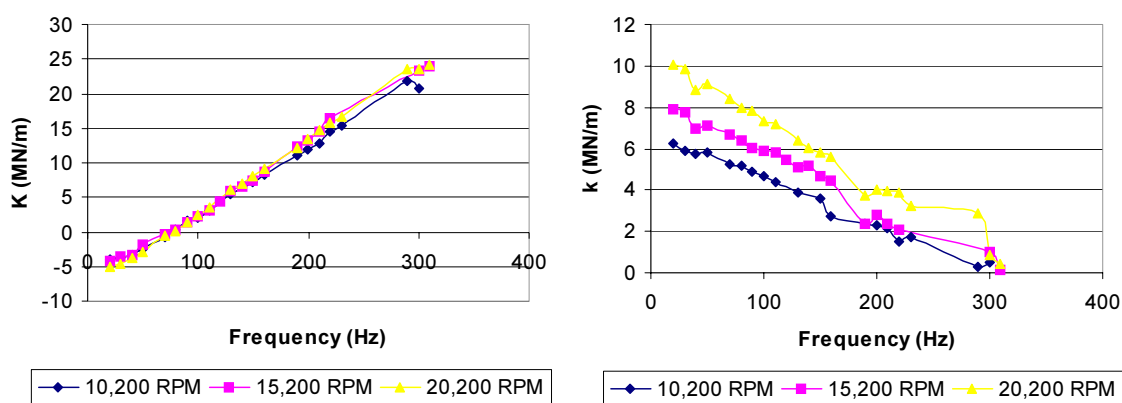
Fig. 10 Direct and cross-coupled stiffness versus excitation frequency for all speeds, with a medium inlet preswirl, PR = 50% and P_i = 34.47 bar

Direct and cross-coupled damping

This section examines the effect of the different test conditions on direct and cross-coupled damping. The direct and cross-coupled damping comes from the imaginary part of the impedance, as shown in equations 12 and 13.

Figure 11 illustrates how the pressure ratio affects normalized direct and cross-coupled damping. The normalized direct damping increases with an increase in pressure ratio for all excitation frequencies. The normalized cross-coupled damping is not strongly influenced by pressure ratio. The magnitude of cross-coupled damping is slightly greater for a pressure ratio of 50 percent, and virtually identical for pressure ratios of 30 and 40 percent. As mentioned earlier, ΔP is used in the normalization of

the results. Therefore, the normalized data indicate that the cross-coupled damping is linearly influenced by pressure ratio, while pressure ratio has a stronger than linear influence on direct damping.
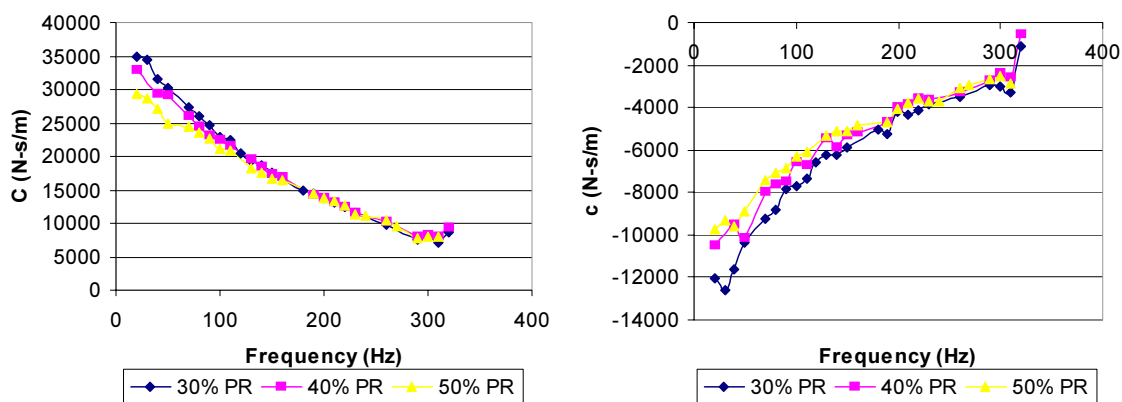
Fig. 11 Direct and cross-coupled damping versus excitation frequency for all pressure ratios, with medium inlet preswirl, ω = 20,200 RPM and P_i = 34.47 bar

The influence of fluid preswirl on the normalized direct and cross-coupled damping is demonstrated in Fig. 12. The inlet pressure is different for each inlet preswirl, see Table 1. For a 50 percent pressure ratio preswirl has a small effect on the normalized direct damping at lower frequencies, causing the normalized direct damping to increase with a decrease in preswirl. For pressure ratios of 30 and 40 percent, preswirl does not influence direct damping. Normalized cross-coupled damping is influenced by preswirl. Note that the greatest magnitude of normalized cross-coupled damping occurs with medium inlet preswirl, and the least occurs with zero inlet preswirl. It would be expected that the greatest magnitude of cross-coupled damping would occur at the highest inlet preswirl due to an increase in fluid tangential velocity. This may be caused by the normalization and the different inlet pressure at each preswirl condition.
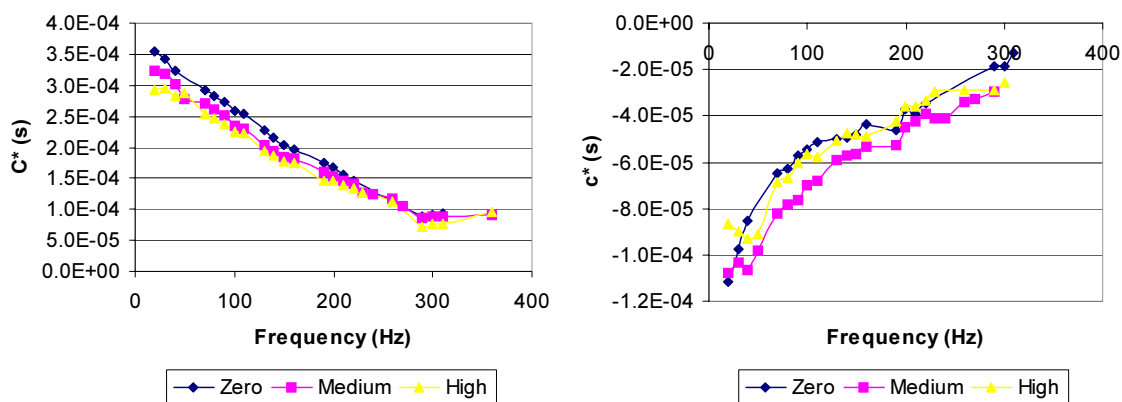
Fig. 12 Normalized direct and cross-coupled damping versus excitation frequency for all inlet preswirls, PR = 50%, ω = 20,200 RPM and P_i = 41.37 bar, 34.47 bar, 27.57 bar

The effect of speed on direct and cross-coupled damping is illustrated in Fig. 13. Speed does not influence direct damping but does influence cross-coupled damping. The magnitude of the cross-coupled damping increases with an increase in speed, particularly at lower excitation frequencies. This is again expected, because an increase in rotor speed increases circumferential velocity.
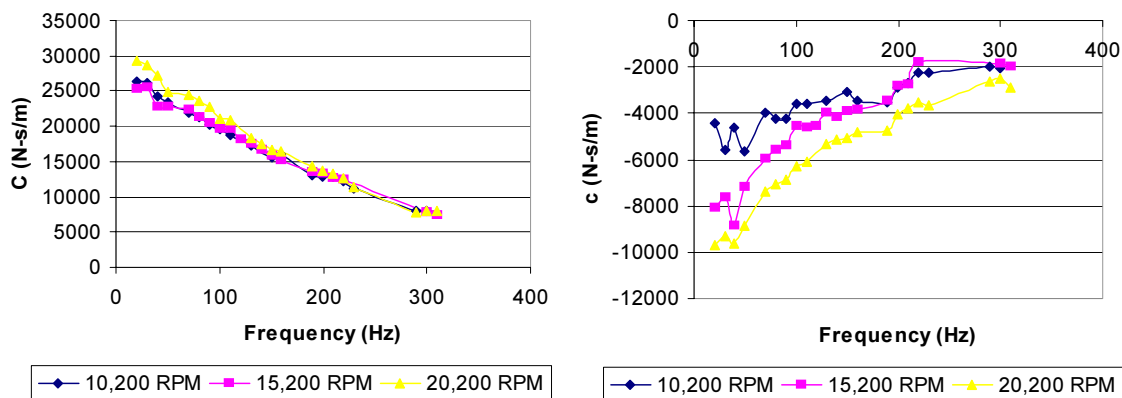
Fig. 13 Direct and cross-coupled damping versus excitation frequency for all speeds, with medium inlet preswirl, PR = 50% and P_i = 34.47 bar

Effective stiffness

Effective stiffness is the effective centering force of the system. The formula for effective stiffness is given in equation 5. The effect of pressure ratio, inlet preswirl, and rotor speed on effective stiffness is explored in this section.

Figure 14 is a good illustration of the effect of pressure ratio on effective stiffness. Pressure ratio does not influence effective stiffness.

Fig. 14 Effective stiffness versus excitation frequency for all pressure ratios, with medium inlet preswirl, ω = 20,200 RPM and P_i = 34.47 bar

The influence of preswirl on non-dimensional effective stiffness is show in Fig. 15. Recall that there is a different inlet pressure for each inlet preswirl, see Table 2. Normalized effective stiffness is not influenced by preswirl.
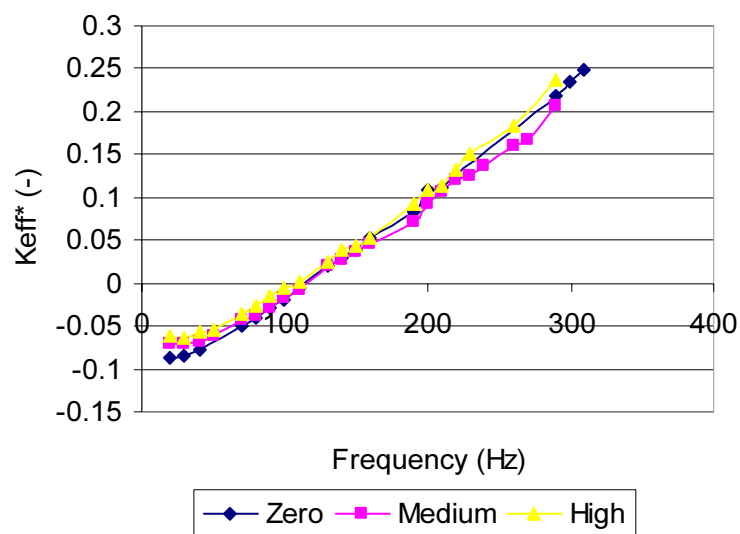
Fig. 15 Non-dimensional effective stiffness versus excitation frequency for all inlet preswirls, PR = 50%, ω = 20,200 RPM and P_i = 41.37 bar, 34.47 bar, 27.57 bar

Figure 16 illustrates the effect of speed on effective stiffness. Effective stiffness is not significantly influenced by rotor speed.
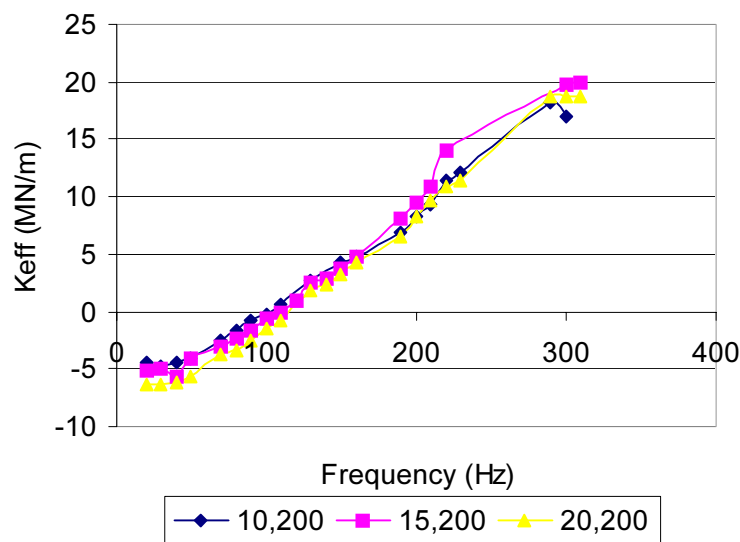
Fig. 16 Effective stiffness versus excitation frequency for all speeds, with medium inlet preswirl, PR = 50 % and P_i = 34.47 bar

Effective damping

Effective damping is one of the best indicators in determining the stability of a roughened stator annular gas seal. Effective damping is defined in equation 6. This section will present the effect of pressure ratio, inlet preswirl, and rotor speed on effective damping.

Figure 17 illustrates the effect of pressure ratio on effective damping. Effective damping is not influenced by pressure ratio.

Fig. 17 Effective damping versus excitation frequency for all pressure ratios, with medium inlet preswirl, ω = 20,200 RPM and P_i = 34.47 bar

Figure 18 shows effective damping for the three preswirls tested, each having a different inlet pressure, see Table 2. An increase in preswirl causes the normalized effective damping to decrease at lower frequencies, and the effective damping cross-over frequency to slightly increase. This outcome is more pronounced for most test conditions. This illustrates the desirability of swirl brakes with this seal.
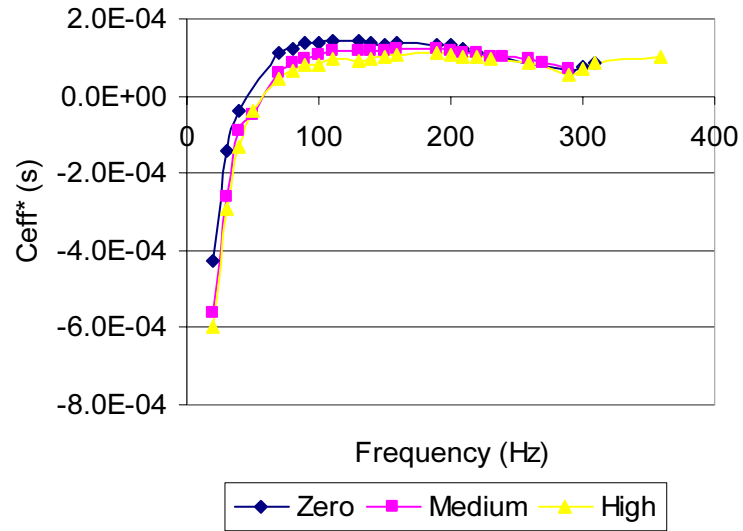
Fig. 18 Normalized effective damping versus excitation frequency for all preswirls, PR =
50%, ω = 20,200 RPM and P_i = 41.37 bar, 34.47 bar, 27.57 bar

The influence of speed on effective damping is shown in Fig. 19. The cross-over frequency of the effective damping increases with speed. At lower excitation frequencies, there is also a decrease in effective damping with an increase in speed.
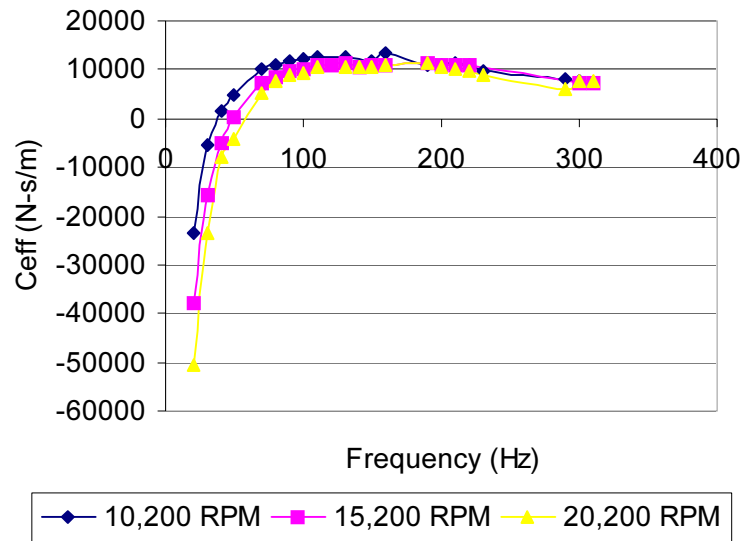
Fig. 19 Effective damping versus excitation frequency for all speeds, with medium inlet preswirl, PR = 50% and P_i = 34.47 bar

Seal leakage

Figure 20 shows leakage versus preswirl for different pressure ratios. The data show that preswirl has very little effect on leakage. It can also be seen that pressure ratio has little effect on the leakage. The data presented are the non-dimensional leakage for a rotor speed of 10,200 RPM. There is not a significant change in leakage at different speeds.
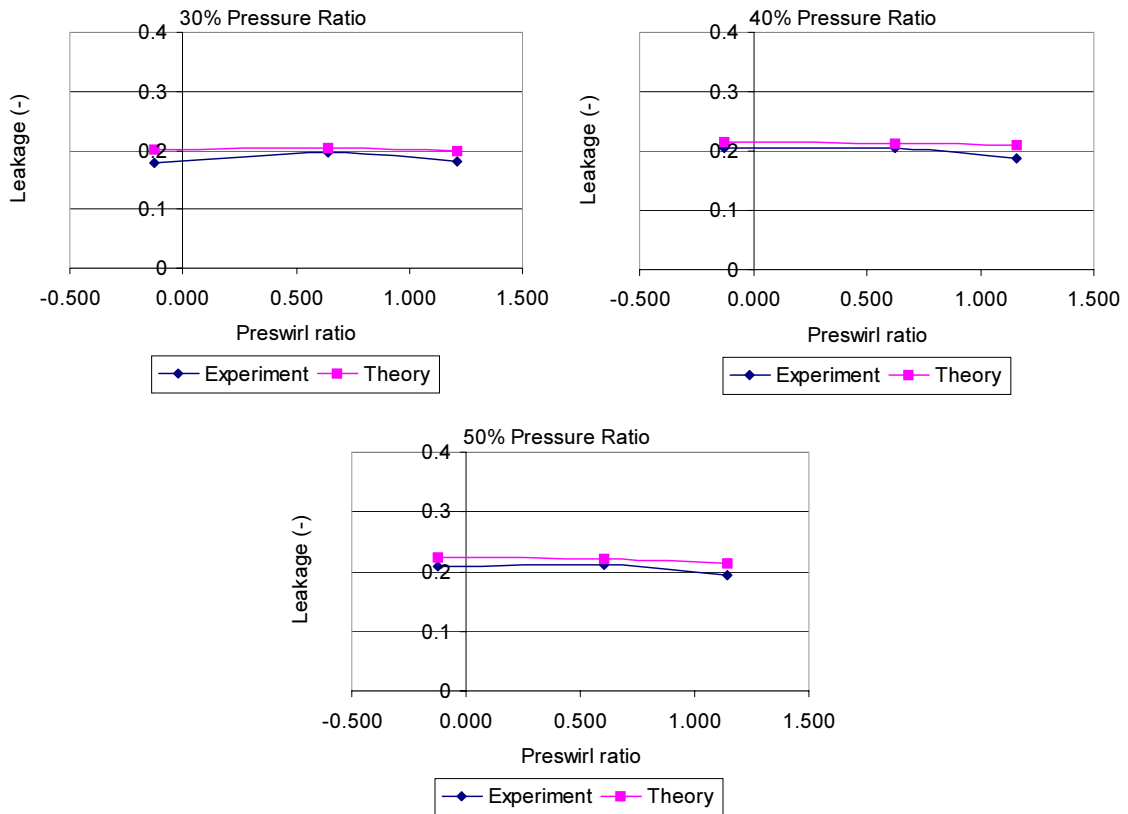
Fig. 20 Non-dimensional leakage versus inlet preswirl for ω=10,200 RPM

Figure 20 shows that ISOTSEAL does an excellent job of predicting seal leakage. ISOTSEAL is based on a bulk flow model, and uses a Blasius friction factor model shown in equation 20.

$$f_f = n\,\mathrm{Re}^m \qquad\qquad (20)$$

The values used for the Blasius friction factor model were n_{rotor} = 0.0568, m_{rotor} = -0.217, n_{stator} = 0.0785, and n_{stator} = -0.1011.

Exact test conditions

Table 4 shows inlet and exit temperature and pressure, rotor speed and exact inlet preswirl data for all tests.

Table 4 Test Conditions

Inlet Preswirl Condition	P_i (bar)	P_e (bar)	ω (RPM)	T_i (K)	T_e (K)	Exact Preswirl (-)
Zero	56.78	26.67	10200	287.20	281.86	-0.108
	57.25	26.48	15200	287.71	286.41	-0.038
	55.58	25.32	20200	288.11	291.23	0.065
	40.76	11.36	10200	287.21	284.49	-0.128
	41.88	11.49	15200	287.34	287.26	-0.066
	42.38	11.27	20200	287.98	293.09	0.054
	42.02	16.80	10200	285.82	281.92	-0.126
	42.90	16.91	15200	286.04	285.69	-0.060
	42.44	16.49	20200	287.06	291.64	0.054
	42.55	20.39	10200	288.23	284.28	-0.125
	43.45	20.49	15200	288.62	287.53	-0.063
	40.96	19.11	20200	289.64	288.00	-0.044
Medium	35.23	10.63	10200	281.67	279.14	0.638
	35.90	10.67	15200	281.66	282.52	0.422
	35.68	10.32	20200	282.10	289.61	0.306
	33.79	13.29	10200	280.95	280.01	0.627
	34.37	13.37	15200	281.05	281.96	0.414
	36.40	13.92	20200	281.39	289.86	0.298
	34.57	16.42	10200	280.85	279.45	0.606
	35.41	16.66	15200	281.07	284.37	0.397
	36.57	17.05	20200	281.31	290.38	0.287
High	27.58	8.01	10200	282.70	281.34	1.212
	28.14	8.09	15200	282.72	283.08	0.801
	28.71	8.21	20200	282.98	285.78	0.589
	27.46	10.97	10200	283.57	280.90	1.160
	27.99	11.10	15200	283.53	284.88	0.767
	29.01	11.50	20200	283.81	290.35	0.565
	27.32	12.20	10200	282.52	281.19	1.143
	27.93	12.36	15200	282.49	282.07	0.751
	29.33	13.11	20200	283.32	290.92	0.550

COMPARISON BETWEEN CONSTANT HOLE DEPTH AND VARIABLE HOLE DEPTH HOLE-PATTERN SEALS

One of the main goals of this testing was to compare the characteristics of variable hole depth (VHD) hole-pattern seals to the characteristics of constant hole depth (CHD) hole-pattern seals. The constant hole depth seals used for comparison are from Wade [11]. Non-dimensional stiffness coefficients and leakage, as well as normalized damping coefficients are used to compare the seals. This was done because the seals were not tested under the exact same conditions. The data taken for the constant hole depth seals is labeled CHD, and the label for the variable hole depth seal data is VHD. The data presented is for the zero and high inlet preswirl condition, a pressure ratio of approximately 30 percent and 50 percent, and a rotor speed of 10,200 RPM and 20,200 RPM. The pressure ratio for the CHD seals was 27 percent and 47 percent, and for the VHD seals the pressure ratio was 30 percent and 50 percent. The label of "30%" and "50%" was used for simplicity. Also, the supply pressure for the CHD seals was 70 bar (1015 psi) for all tests. The supply pressure for the VHD seals was 55.16 bar (800 psi) for zero preswirl with 50 percent pressure ratio, 41.37 bar (600 psi) for zero preswirl with 30 percent pressure ratio, and 27.58 bar (400 psi) for high preswirl.

Figure 21 shows the non-dimensional direct and cross-coupled stiffness for both CHD and VHD seals. The direct stiffness for VHD seals is smaller than that of CHD seals at lower excitation frequencies, then becomes greater at higher excitation frequencies. This outcome was the case for all test conditions. The point at which the two seals direct stiffnesses are equal is between 150 Hz and 220 Hz. The cross coupled stiffness are either very similar or lower for the VHD seals.

The normalized direct and cross-coupled damping for both CHD and VHD hole-pattern seals is shown in Fig. 22. For all cases, the direct damping is greater for the VHD seal. The difference in direct damping is larger at lower excitation frequencies,
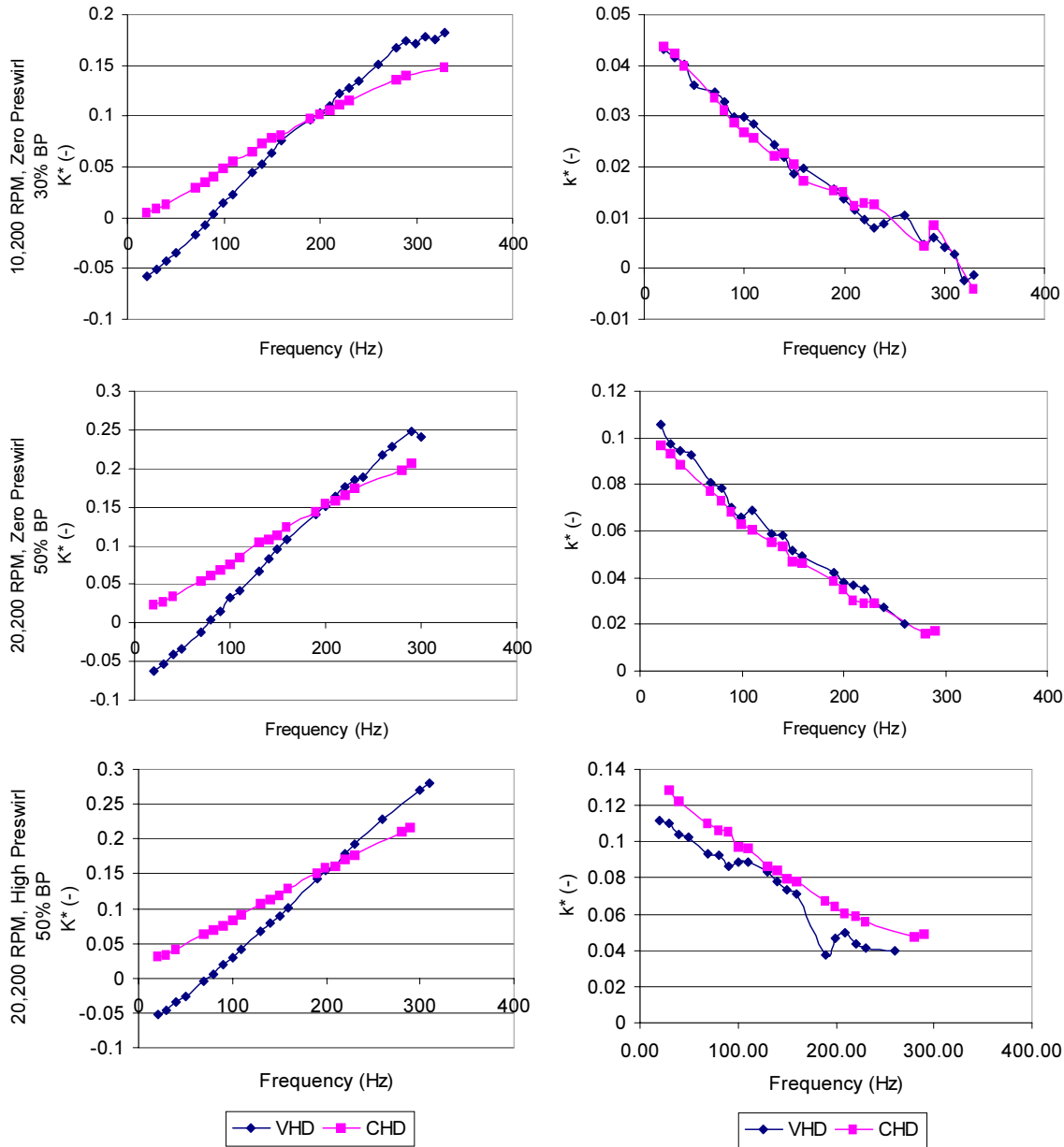
Fig. 21 Non-dimensional direct and cross-coupled stiffness for CHD and VHD hole-pattern seals

and decreases as the excitation frequency increases. From Fig. 22, it may appear that rotor speed has an influence on cross-coupled damping. This is not the case. The cross-coupled damping is most influenced by pressure ratio, as well as inlet preswirl.

As these two parameters increase, the difference between VHD and CHD hole-pattern seals increases. In every case where there was a significant difference, the VHD seals had a lower magnitude of cross-coupled damping.

Figure 23 shows the non-dimensional effective stiffness and normalized effective damping for VHD and CHD hole-pattern seals. The effective damping for VHD seals is always greater than CHD seals. Also, the cross-over frequency for VHD seals is always less than CHD seals.   The difference in cross-over frequency was normally between 25 Hz and 40 Hz, with the smallest difference being 13 Hz in one instance. This translates into an average decrease in cross-over frequency of 40 percent. The effective stiffness of the VHD seals is lower at lower frequencies and higher at higher frequencies. This is the case for all test conditions. The VHD seals have negative stiffness at lower frequencies, while CHD seals do not.

Figure 24 compares the non-dimensionalized leakage coefficients at zero inlet preswirl for variable hole depth and constant hole depth seals. For all speeds and pressure ratios, variable hole depth seals have approximately 10 percent less non-dimensional leakage.
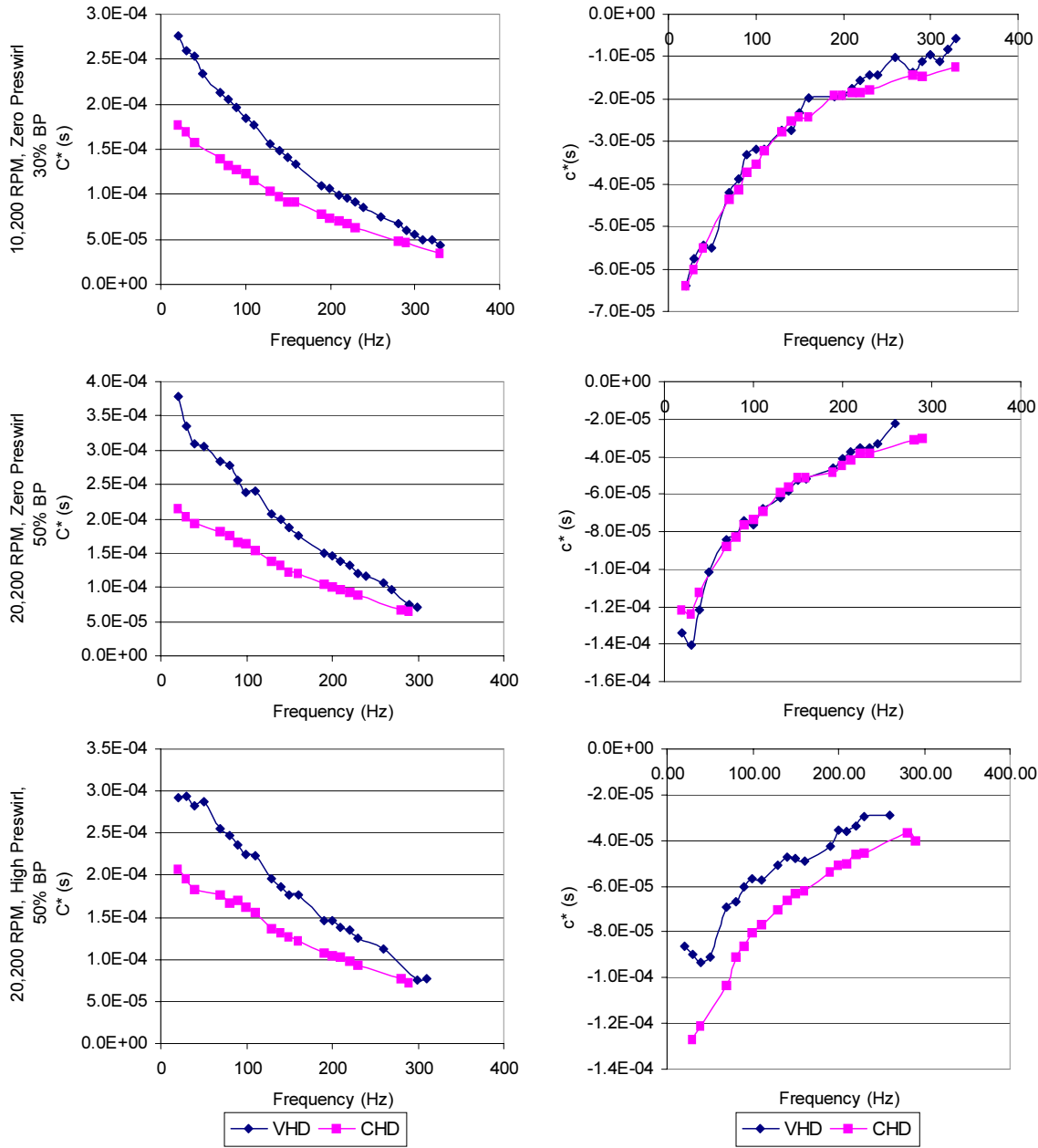
Fig. 22 Normalized direct and cross-coupled damping for VHD and CHD hole-pattern seals
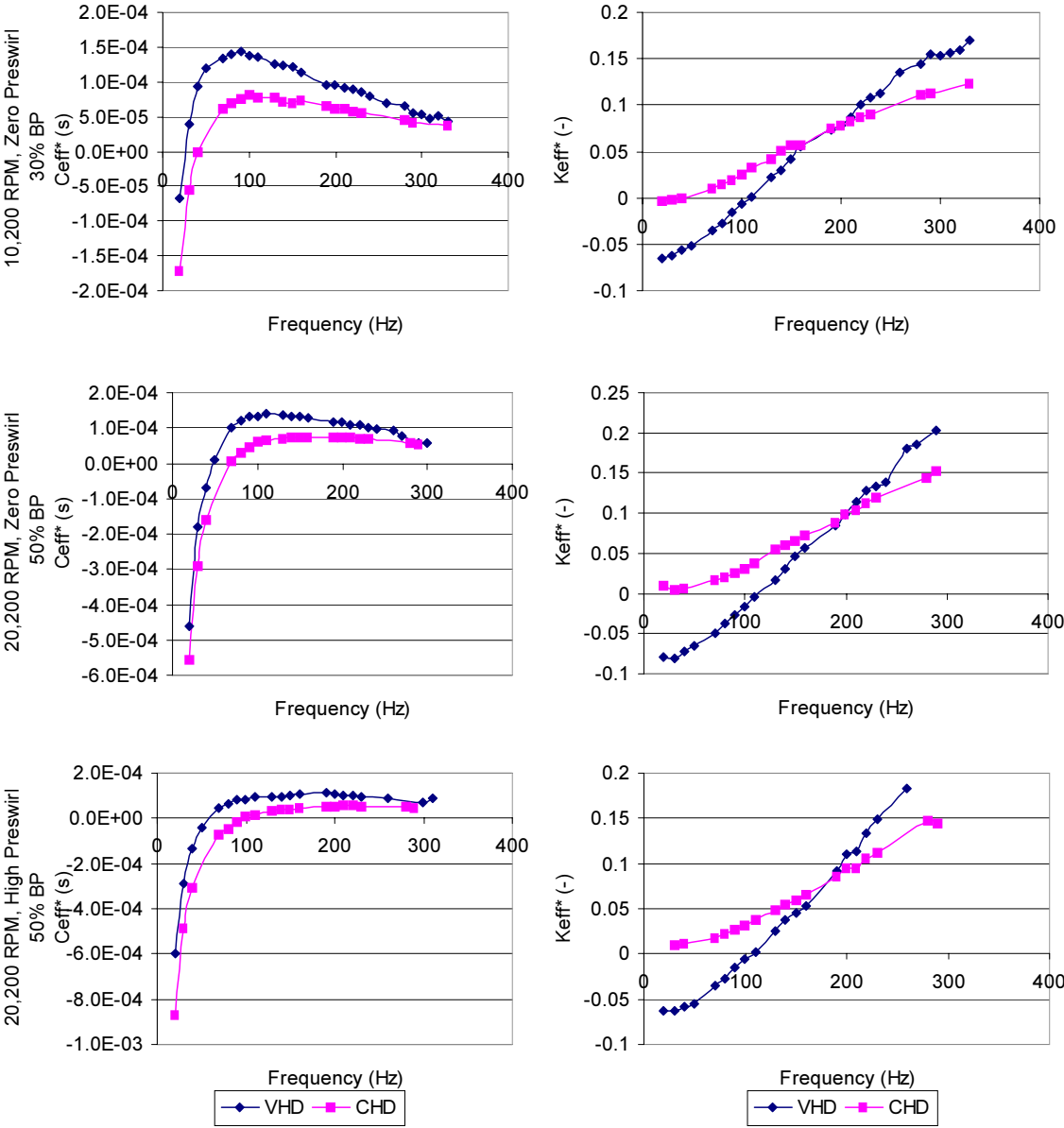
Fig. 23 Normalized effective damping and non-dimensional effective stiffness for CHD and VHD hole-pattern seals
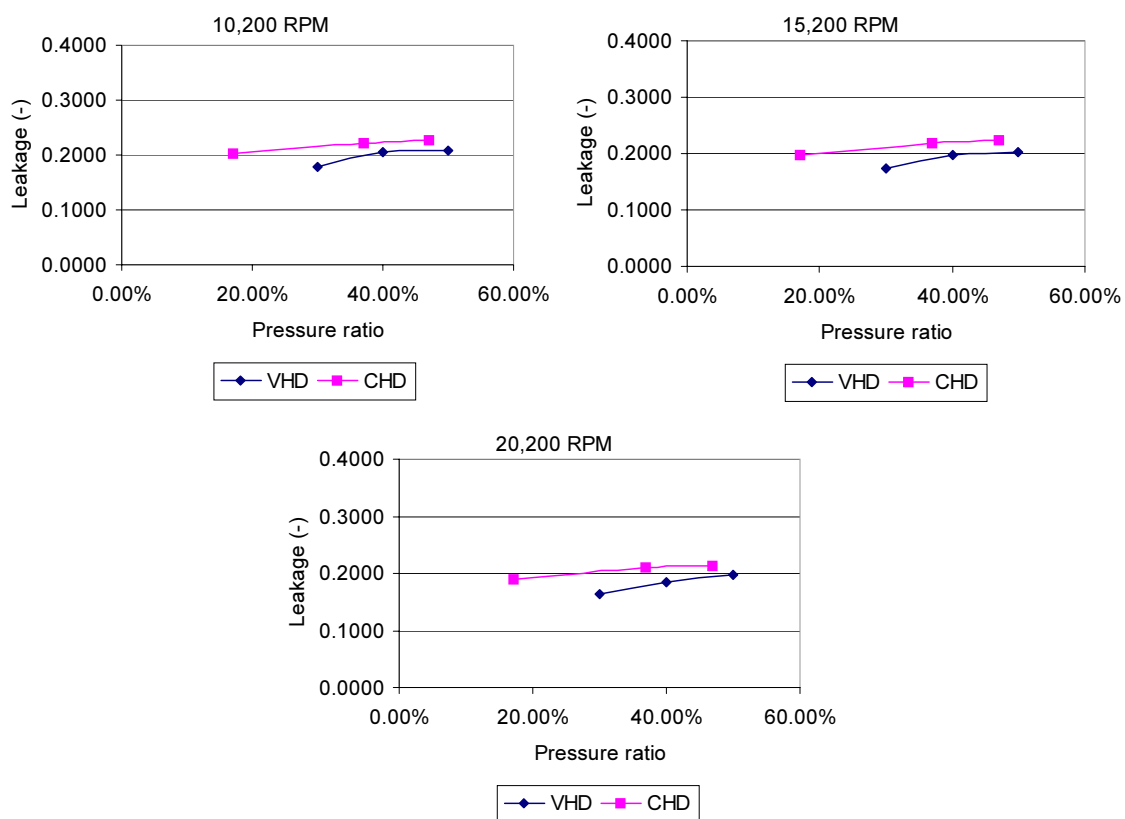
Fig. 24 Non-dimensional leakage coefficients for VHD and CHD seals versus pressure ratio, for different speeds with zero inlet preswirl

EXPERIMENT VERSUS THEORETICAL PREDICTIONS

This section will compare the experimental results with those predicted by ISOTSEAL 2. This section will not be non-dimensionalized or normalized, because the comparison is between ISOTSEAL 2 and the experimental data, not between separate sets of experimental data. The experimental results contain uncertainty bars that result from the dynamic uncertainty described earlier. The error bars represent one standard deviation.

Direct and cross-coupled stiffness

Figure 25 presents direct and cross-coupled stiffness versus excitation frequency for all pressure ratios at 20,200 RPM and medium inlet preswirl. The data points have uncertainty bars and the theory is a solid line. ISOTSEAL 2 over-predicts the direct stiffness at lower frequencies and under-predicts the direct stiffness at higher frequencies for all pressure ratios. This seal configuration has almost a linear relation between stiffness and excitation frequency. In hole-pattern seals previously tested, there was a polynomial trend. There is a negative stiffness at lower frequencies at every pressure ratio, but it is only predicted for 30% pressure ratio. As mentioned earlier, this negative stiffness suggests that there is some sort of friction factor jump occurring within these seals, Ha and Childs [7]. The trend of the cross-coupled stiffness is well predicted for all pressure ratios, while the magnitude is slightly under-predicted.

Figure 26 shows the direct and cross-coupled stiffness coefficients versus excitation frequency at each inlet preswirl condition tested. The data in Fig. 26 were recorded with a rotor speed of 20,200 RPM, and a pressure ratio of 50 percent. For all inlet preswirl conditions, ISOTSEAL 2 over-predicts the direct stiffness at lower excitation frequencies, and under-predicts the direct stiffness at higher excitation frequencies. The pressure ratio has little effect on the accuracy of the theory for direct stiffness. For cross-coupled stiffness the theory becomes more accurate as the inlet preswirl increases. The zero preswirl case is largely under-predicted, while the medium preswirl results are only slightly under-predicted. ISOTSEAL 2 does a good job of predicting the high inlet preswirl condition.
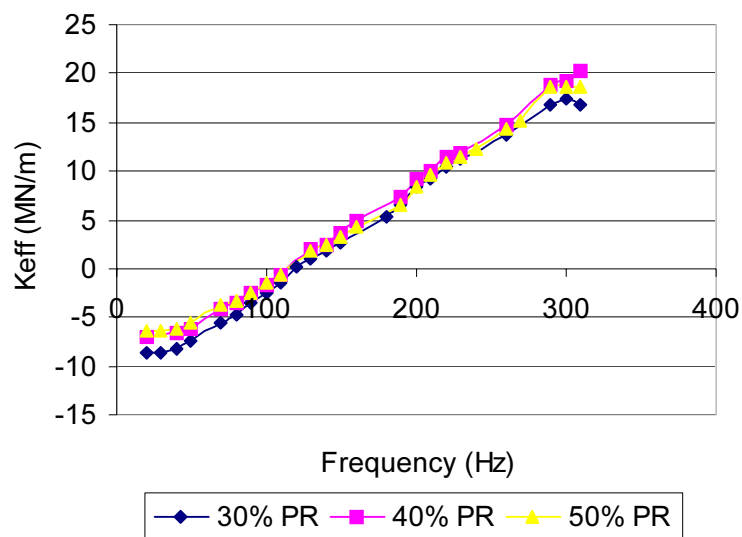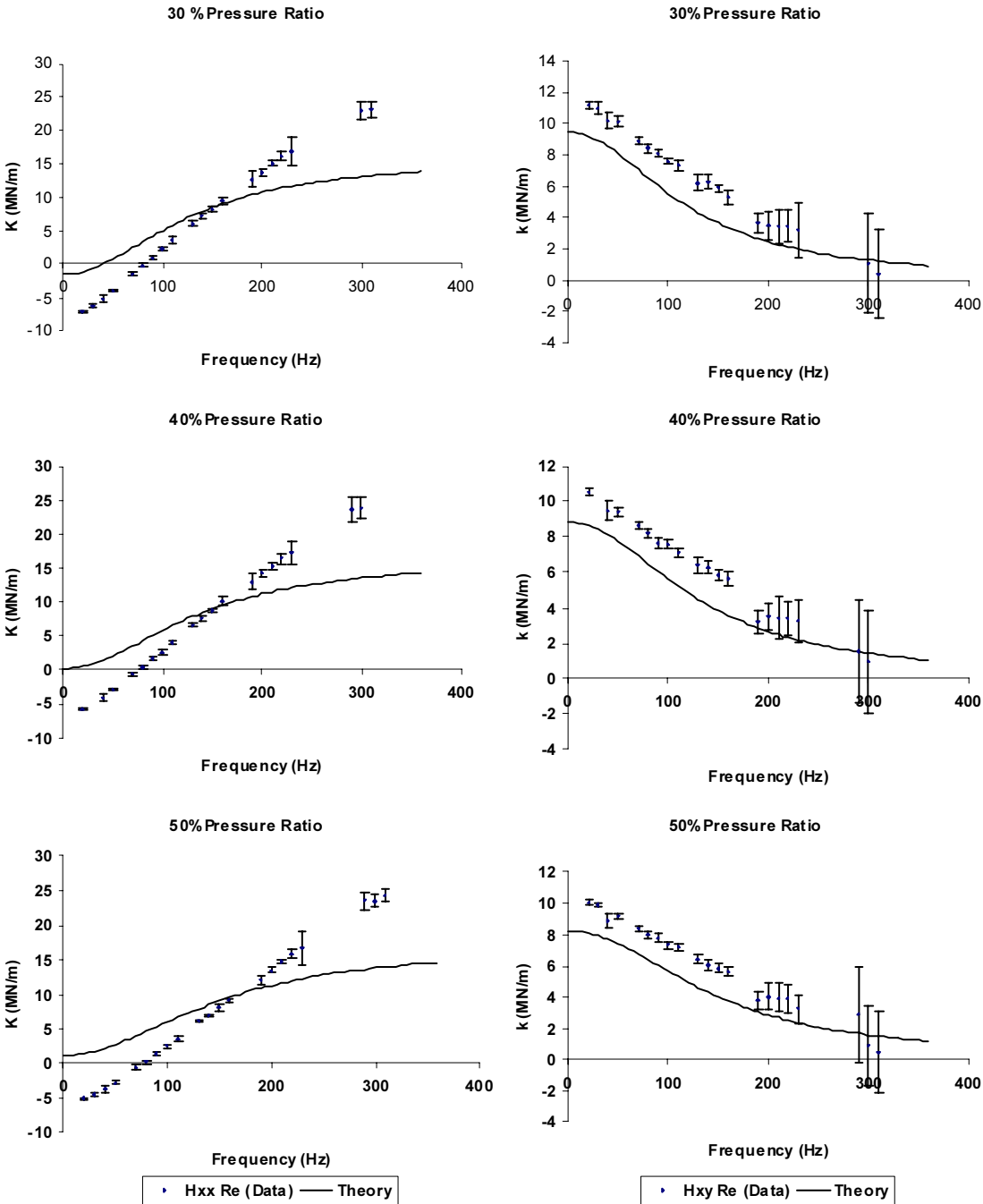
Fig. 25 Direct and cross-coupled stiffness versus excitation frequency for different pressure ratios, with medium inlet preswirl, ω = 20,200 RPM and P_i = 34.47 bar
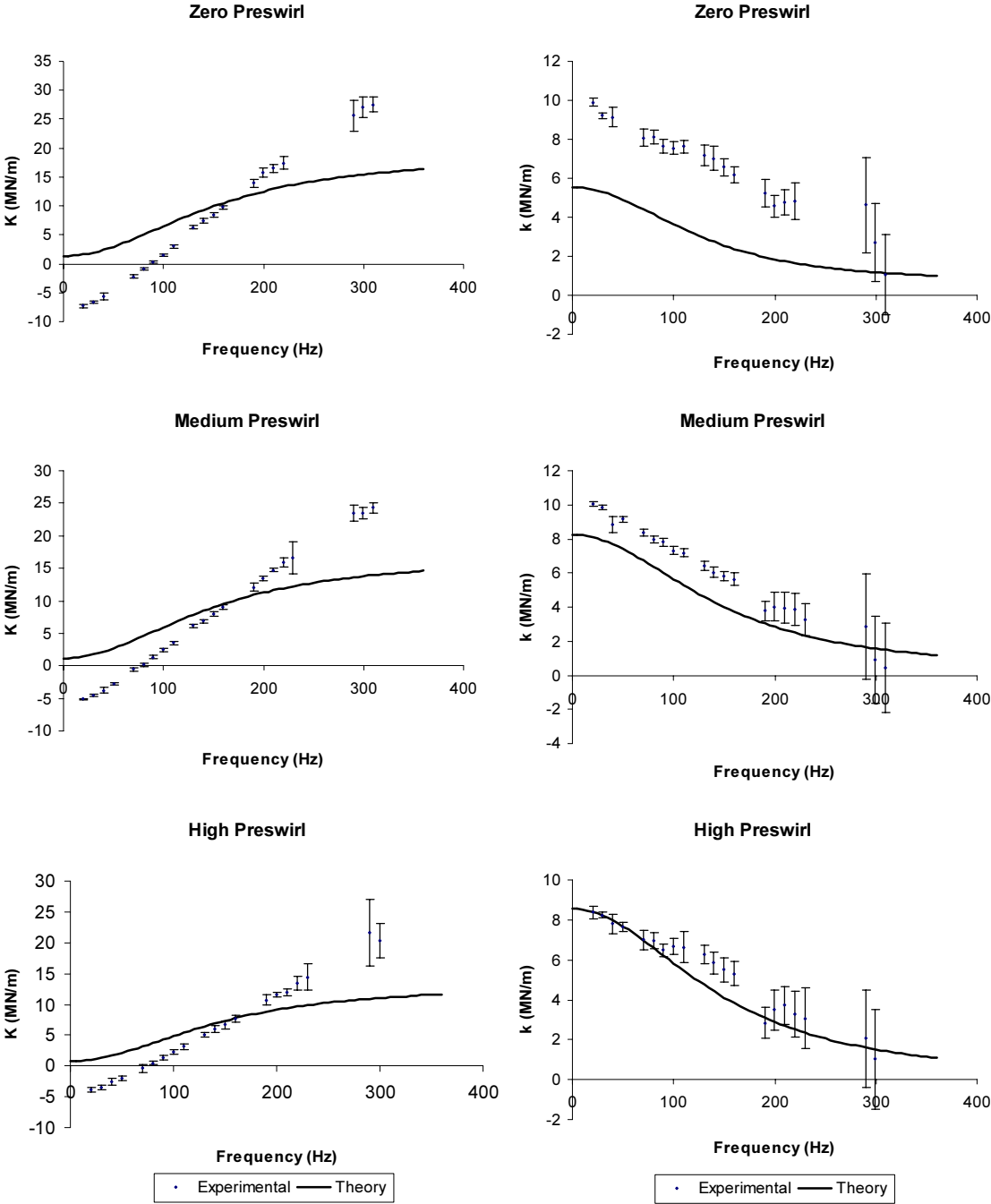
Fig. 26 Direct and cross-coupled stiffness versus excitation frequency for different inlet preswirl conditions, ω = 20,200 RPM, PR = 50% and P_i = 41.37 bar, 34.47 bar, 27.57 bar

Figure 27 shows the direct stiffness versus excitation frequency for all speeds tested. The data were measured for a medium inlet preswirl, and a pressure ratio of 50 percent. Again, direct stiffness is over-predicted at lower excitation frequencies and under-predicted at higher excitation frequencies. Cross-coupled stiffness is slightly under-predicted at all rotor speeds. Rotor speed has little effect on the accuracy of the theory for direct and cross-coupled stiffness.

Direct and cross-coupled damping

Figure 28 shows direct and cross-coupled damping versus excitation frequency for all pressure ratios tested. The data were taken with a medium inlet preswirl and a rotor speed of 20,200 RPM. The theory under-predicts direct damping for all pressure ratios, becoming more accurate at higher excitation frequencies. The accuracy of the theory is not influenced by pressure ratio. ISOTSEAL 2 does a very good job of predicting cross-coupled damping at every pressure ratio.

The direct and cross-coupled damping for different preswirls are presented in Fig. 29. The data were recorded with a pressure ratio of 50% and a rotor speed of 20,200 RPM. The damping is under-predicted in all cases, with the accuracy of the prediction increasing as the excitation frequency increases. This outcome is not affected by the inlet preswirl. The prediction for the cross-coupled damping is much more accurate. For zero preswirl, the magnitude of the cross-coupled damping is under-predicted, becoming more accurate at high excitation frequencies. The cross-coupled damping is well predicted for the medium preswirl condition. For the high preswirl condition, the magnitude of the cross-coupled damping is over-predicted, becoming more accurate at higher excitation frequencies.

10,200 RPM

10,200 RPM

15,200 RPM

15,200 RPM

20,200 RPM

20,200 RPM
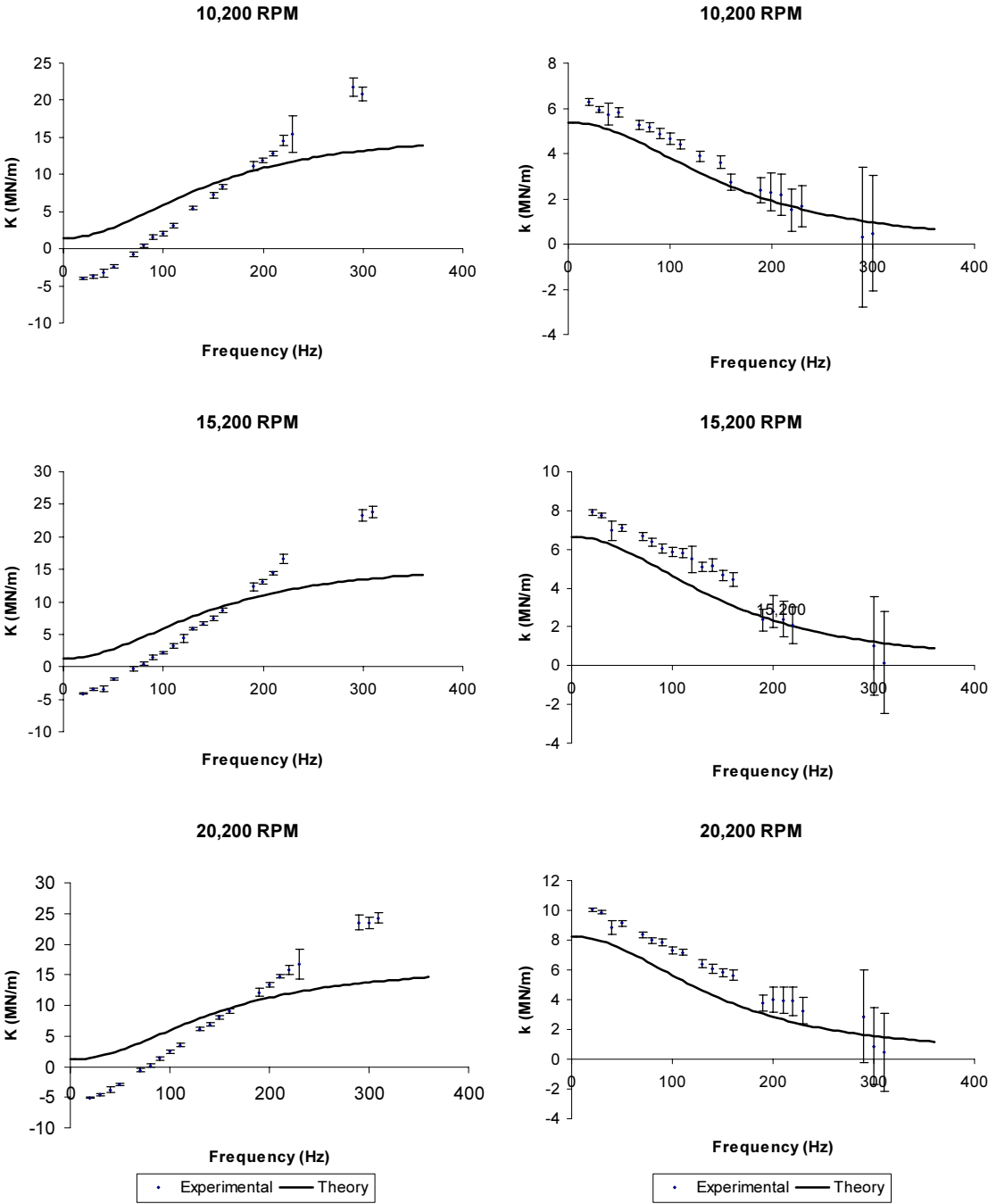
Fig. 27 Direct and cross-coupled stiffness versus excitation frequency for different rotor speeds, with medium preswirl, PR = 50%, and P_i = 34.47 bar

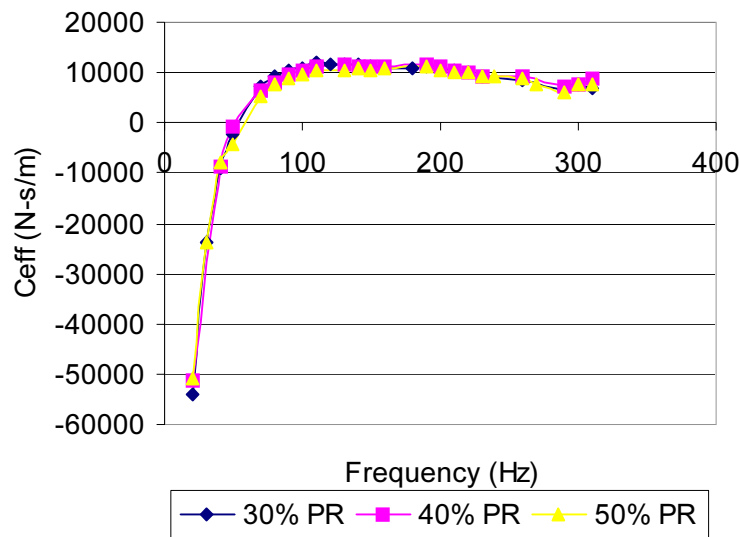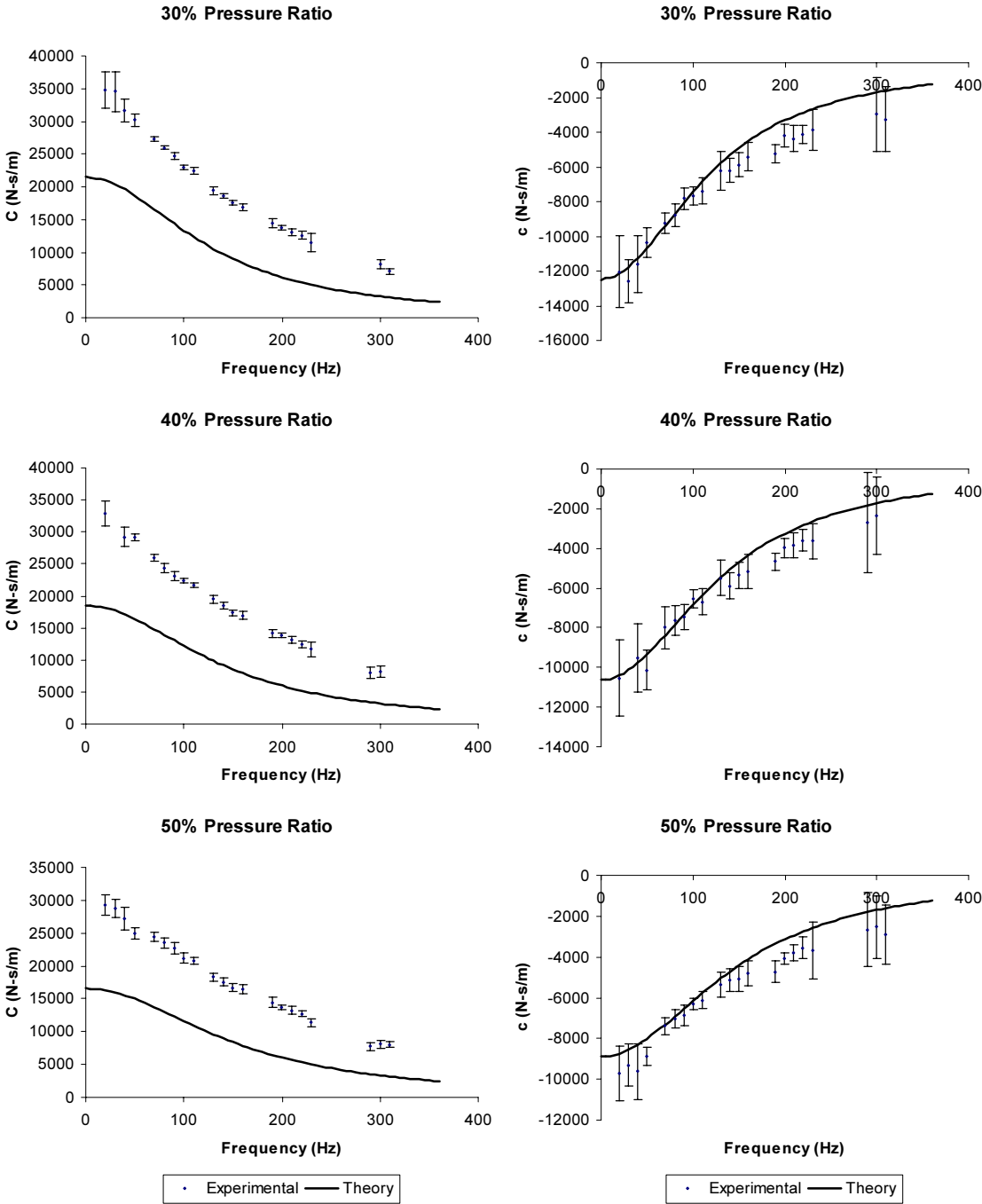Fig. 28 Direct and cross-coupled damping versus excitation frequency for different pressure ratios, with medium inlet preswirl, ω = 20,200 RPM and P_i = 34.47 bar
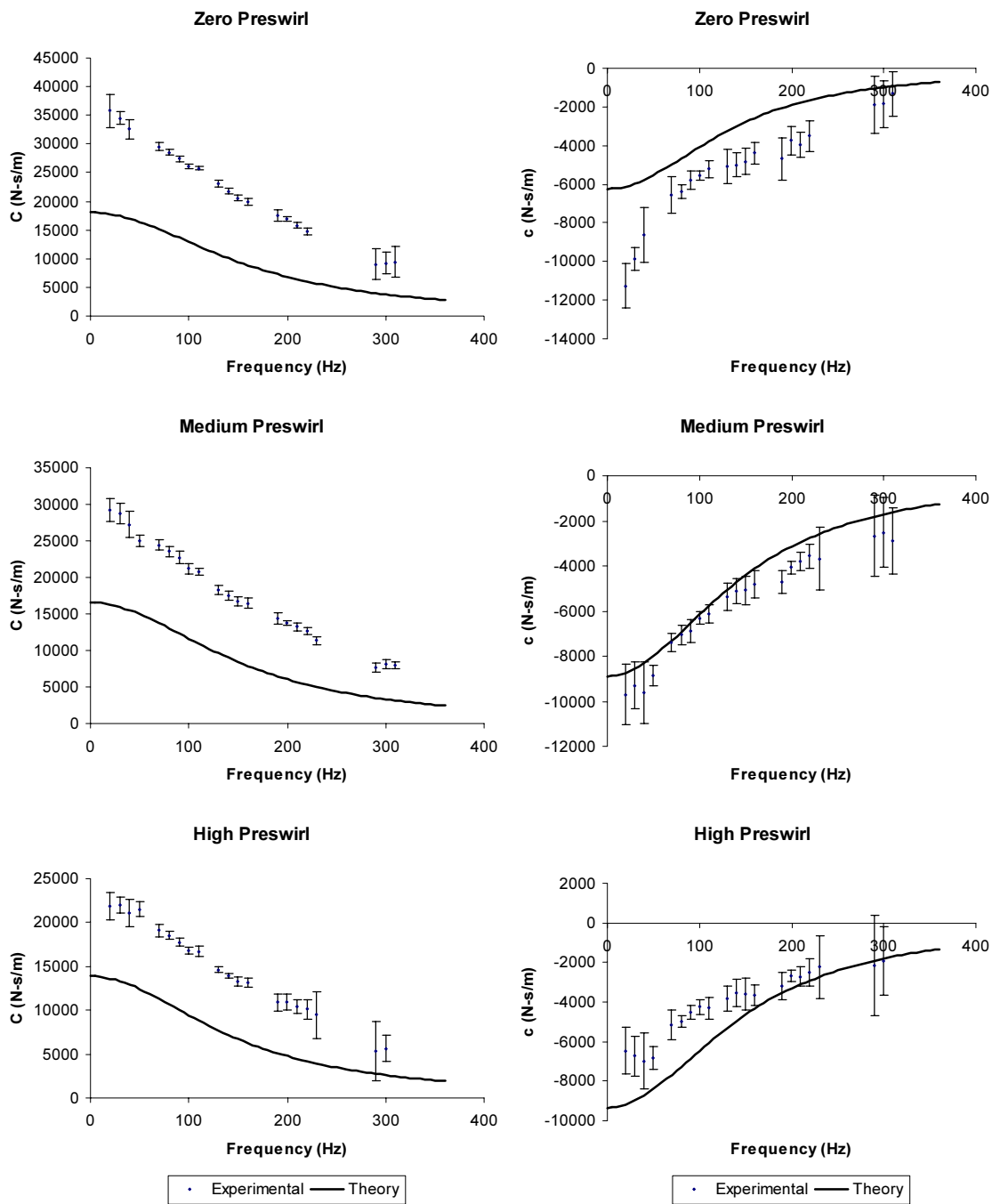
Fig. 29 Direct and cross-coupled damping versus excitation frequency for different preswirl ratios, PR = 50%, ω = 20,200 RPM and P_i = 41.37 bar, 34.47 bar, 27.57 bar

Figure 30 shows the direct and cross-coupled damping versus excitation frequency for all rotor speeds tested. The data were obtained with medium inlet preswirl and a pressure ratio of 50 percent. The direct damping is under-predicted at all speeds, with the prediction improving as the excitation frequency increases. The prediction for the cross-coupled damping is good. The error bars are higher than desired for the 10,200 RPM case. Usually, to decrease the uncertainty of the coefficients the magnitude of the stator shake is increased. This was not possible because of the negative stiffness displayed by these seals. The large error bars are also largely due to the small cross-coupled damping displayed at this rotor speed.

Effective damping and effective stiffness

Figure 31 shows the influence of pressure ratio on effective stiffness and effective damping. The data were taken with the medium inlet preswirl and a rotor speed of 20,200 RPM. The effective stiffness is over-predicted at lower excitation frequencies and under-predicted at higher excitation frequencies for all pressure ratios. The effective damping is under-predicted, but the effective damping cross-over frequency is very well predicted, for all pressure ratios.

Figure 32 shows effective stiffness and effective damping at all inlet preswirls tested. The data were taken with a pressure ratio of 50% and a rotor speed of 20,200 RPM. Again, the effective stiffness is over-predicted at lower frequencies and under-predicted at higher frequencies. The predictions are more accurate at higher preswirl ratios, especially for lower excitation frequencies. The effective damping is under predicted for all preswirl conditions, becoming more accurate at higher preswirls. Again, the effective damping cross-over frequency is well predicted.
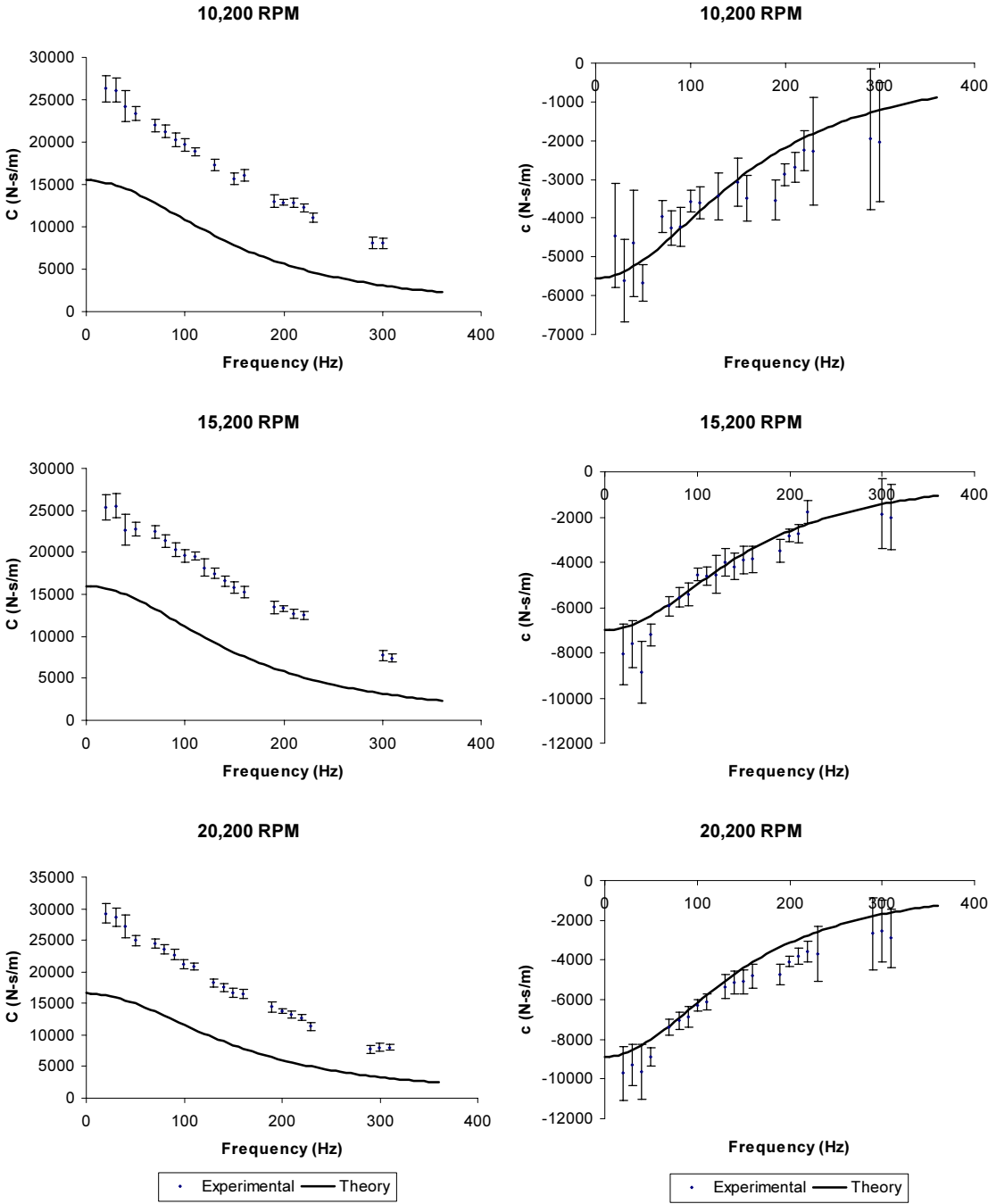
Fig. 30 Direct and cross-coupled damping versus excitation frequency for different rotor speeds, with medium inlet preswirl, PR = 50% and Pi = 34.47 bar
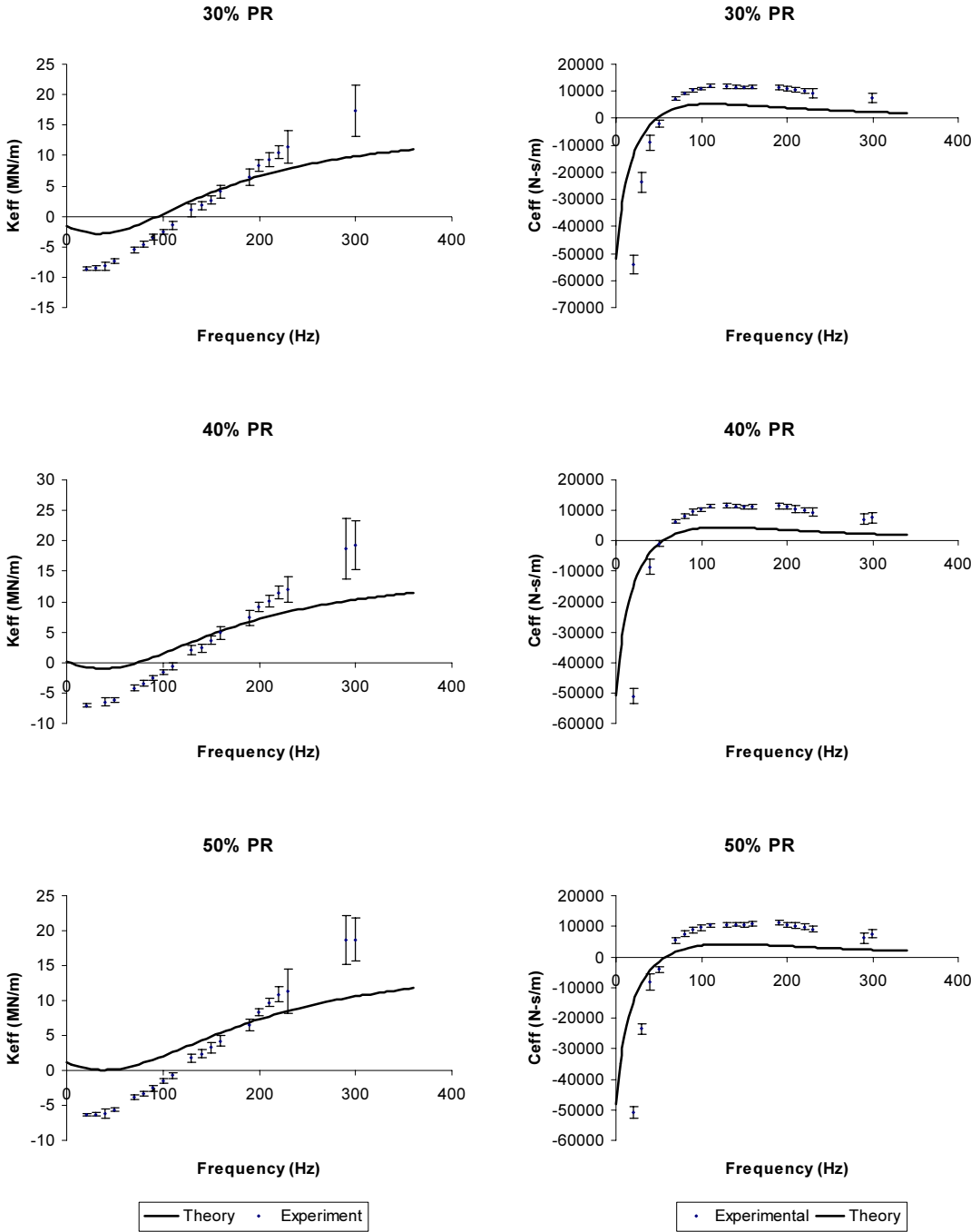
Fig. 31 Effective stiffness and effective damping versus excitation frequency for different pressure ratios, with medium inlet preswirl, ω = 20,200 RPM and P_i = 34.47 bar
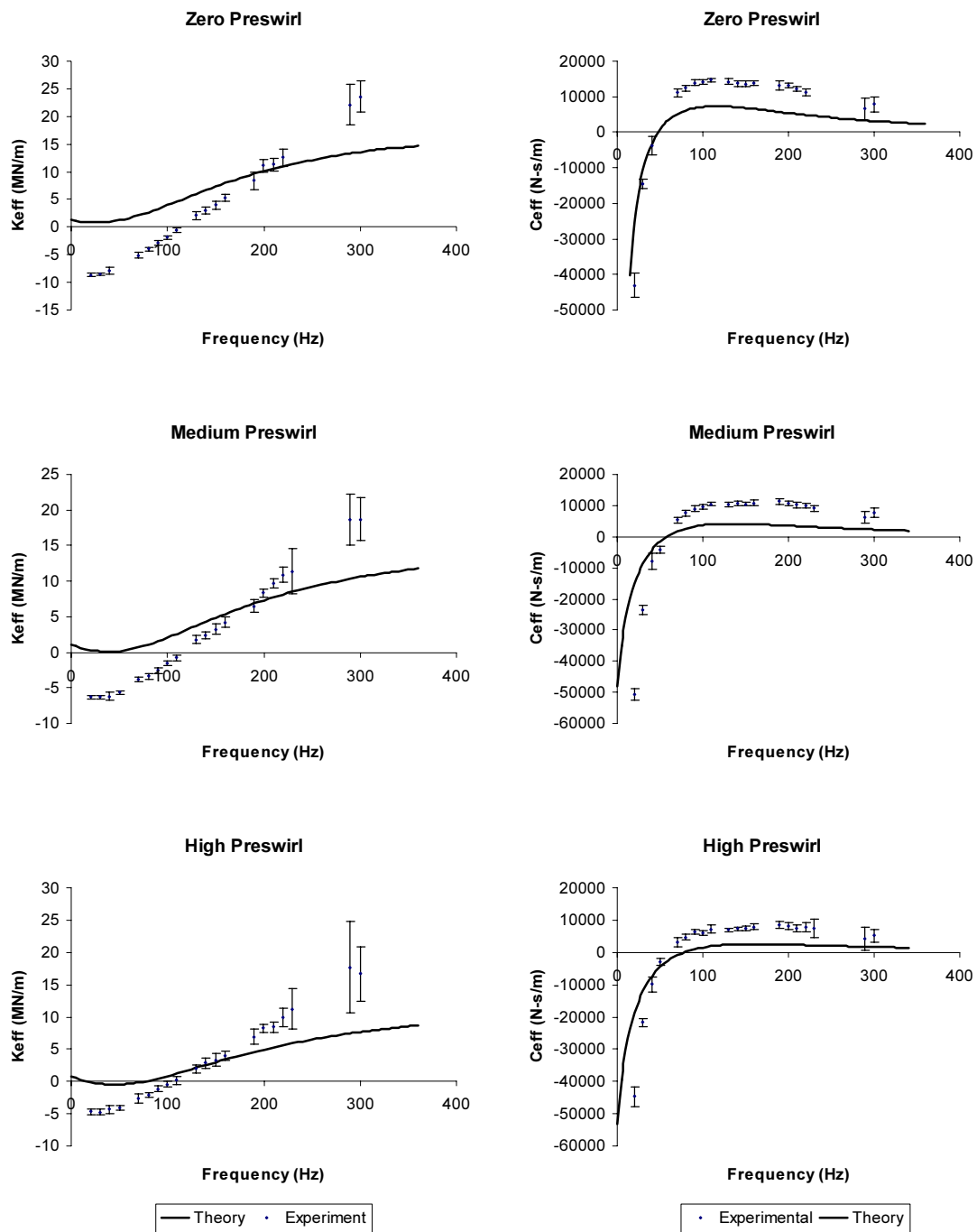
Fig. 32 Effective stiffness and effective damping versus excitation frequency for different preswirl ratios, PR = 50%, ω = 20,200 RPM and P_i = 41.37 bar, 34.47 bar, 27.57 bar

Figure 33 illustrates the influence of rotor speed on the predictions for effective stiffness and effective damping. Again, the effective stiffness is over-predicted at lower frequencies and under-predicted at higher frequencies. The effective damping is again under-predicted, with the effective damping cross-over frequency being very well predicted. The accuracy of predictions for neither effective damping, nor effective stiffness is influenced by speed. The data were taken with the medium preswirl condition, and a pressure ratio of 50 percent.

Seal leakage

Figure 34 shows the influence of pressure ratio on the experimental leakage, as well as the predicted seal leakage from ISOTSEAL 2. The leakage has been non-dimensionalized. The data are from a rotor speed of 10,200 RPM and all inlet preswirl conditions. The leakage slightly increases with an increase in pressure ratio. ISOTSEAL does an excellent job of predicting leakage at all pressure ratios and inlet preswirls.
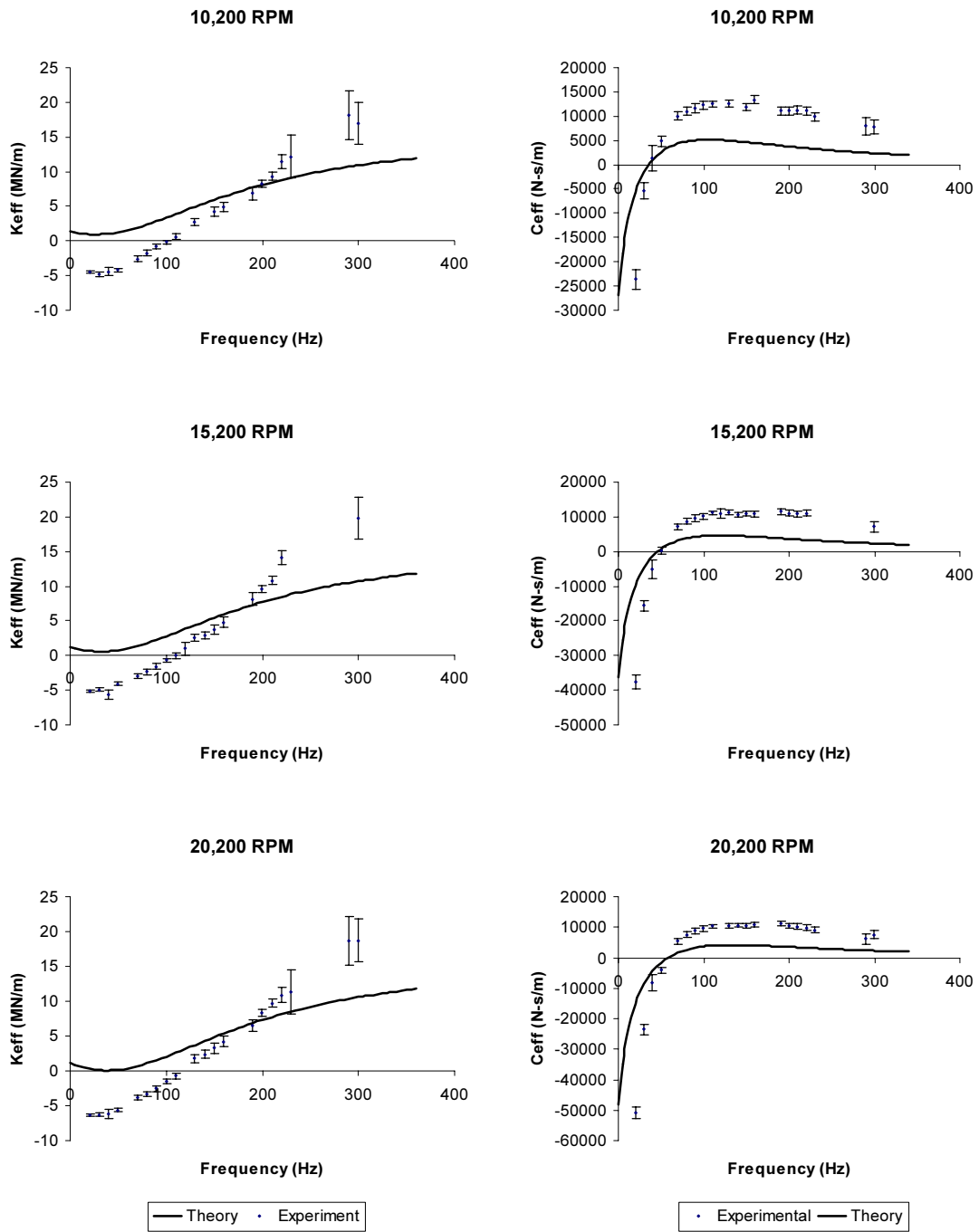
Fig. 33 Effective stiffness and effective damping versus excitation frequency for different rotor speeds, with medium inlet preswirl, PR = 50% and P_i = 34.47 bar
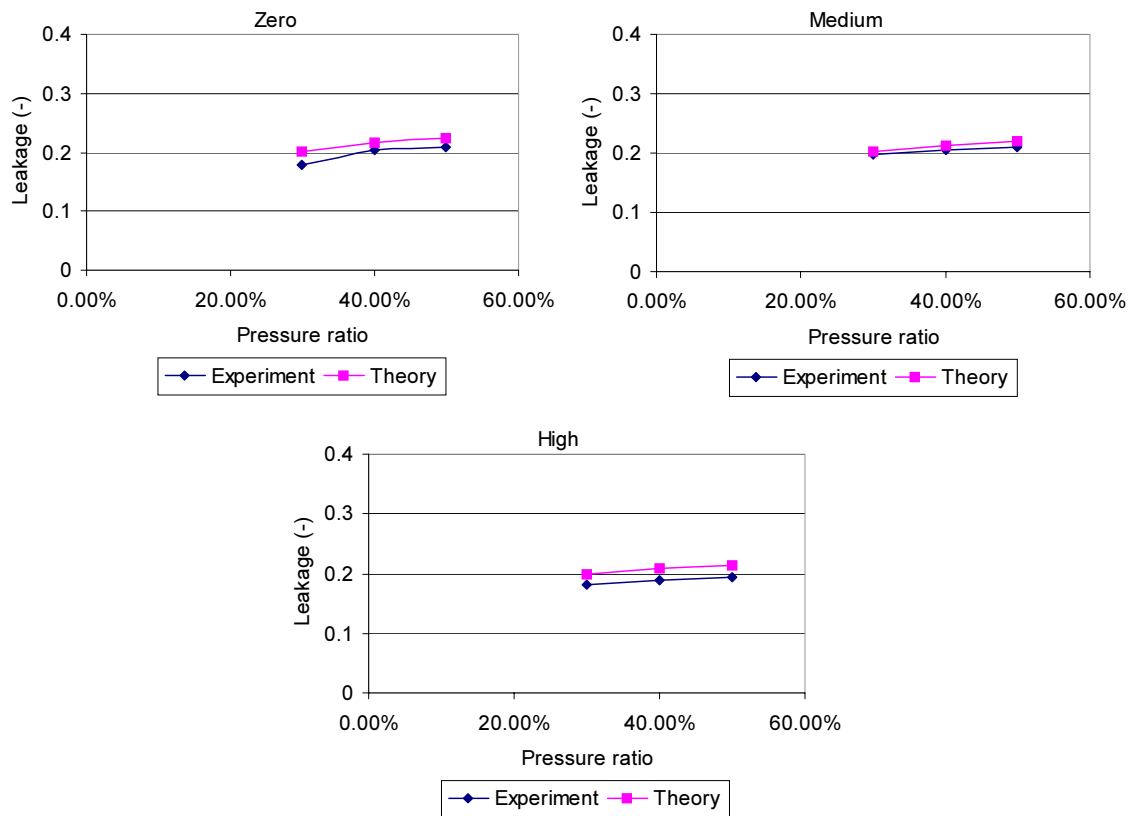
Fig. 34 Non-dimensional leakage versus pressure ratio for all preswirl conditions

SUMMARY AND CONCLUSIONS

This research had the following objectives: (1) test variable hole depth hole-pattern seals, and see how the rotordynamic characteristics and leakage compare to predictions by ISOTSEAL 2, and (2) compare the results from the variable hole depth hole-pattern seals to constant hole depth hole-pattern seals. The testing parameters varied to determine the characteristics of the seals were: pressure ratio, inlet preswirl, and rotor speed. The supply pressure was also varied due to the seal instability previously mentioned.

The three pressure ratios tested did not significantly influence rotordynamic characteristics.

Normalized results had to be used to compare inlet preswirls. The normalized results indicate that inlet fluid preswirl increased the cross-coupled stiffness. As would be expected, this caused the effective damping to decrease with an increase in preswirl, and the effective damping cross-over frequency to increase.

Both stiffness and damping cross-coupled coefficients increase with speed. This was expected because an increase in rotor speed increases circumferential velocity, which is known to increase cross-coupled forces.

The experimental results were compared to theoretical predictions by ISOTSEAL 2. Cross-coupled stiffness and cross-coupled damping were both reasonably predicted. Direct stiffness was poorly predicted. Direct stiffness is over-predicted at lower excitation frequencies and under-predicted at higher frequencies. This was also the case for effective stiffness. Effective damping was slightly under-predicted, but ISOTSEAL 2 did a good job predicting the effective damping cross-over frequency. Seal leakage is well predicted by ISOTSEAL 2.

The seal characteristics were compared to those for a constant hole depth hole-pattern seal. The variable hole-depth seal had a higher direct damping. The cross-coupled stiffness and cross-coupled damping coefficients were either very similar, or lower for the variable hole depth seals. The direct stiffness for the variable hole depth seal was lower at lower excitation frequencies, and higher at higher excitation frequencies. The effective stiffness behaved in the same manner. The variable hole depth seals displayed a negative direct and effective stiffness, which the constant hole

depth seals did not. The effective damping was much larger in the variable hole depth seals, and the effective damping cross-over frequency was drastically lower. The difference in cross-over frequency was normally in the range of 20 Hz to 40 Hz, or around 40 percent.

REFERENCES

1. Yu, Z., and Childs, D., 1998, "A Comparison of Experimental Rotordynamic Coefficients and Leakage Characteristics between Hole-Pattern Gas Damper Seals and a Honeycomb Seal," Journal of Engineering for Gas Turbines and Power, **120**, pp. 778-783.

2. Childs, D., and Moyer, D., 1985, "Vibration Characteristics of the HPOTP (High Pressure Oxygen Turbopump) of the SSME (Space Shuttle Main Engine)," ASME Trans., Journal of Engineering for Gas Turbine and Power, **107**, pp. 152-159.

3. Shin, Y., 2005, "Modifications to a Two-Control-Volume, Frequency Dependent, Transfer-Function Analysis of Hole-Pattern Gas Annular Seals," MS Thesis, Department of Mechanical Engineering. Texas A&M University, College Station.

4. Nelson, C. C., 1984, "Analysis for Leakage and Rotordynamic Coefficients of Surface Roughened Tapered Annular Gas Seals," Journal of Engineering for Gas Turbines and Power," **106**, pp. 927-934.

5. Childs, D., Elrod, D., and Hale, K., 1989, "Annular Honeycomb Seals: Test Results for Leakage and Rotordynamic Coefficients; Comparison to Labyrinth and Smooth Configurations," ASME Journal of Tribology, **111**, pp.293-301.

6. Kleynahns, G., and Childs, D., 1997, "The Acoustic Influence of Cell Depth on the Rotordynamic Coefficients of a High-Pressure Honeycomb Annular Gas Seal, Measurements Versus Predictions," ASME Paper 2022-TRIB-207.

7. Ha, T., and Childs, D., 1994, "Annular Honeycomb-Stator Turbulent Gas Seal Analysis Using New Friction-Factor Model Based on Flat Plate Tests," ASME Journal of Tribology, 116, pp. 352-360.

8. Dawson, M., 2000, "A Comparison of the Static and Dynamic Characteristics of Straight-Bore and Convergent Tapered-Bore Honeycomb Annular Gas Seals," MS Thesis, Department of Mechanical Engineering. Texas A&M University, College Station.

9. Holt, C., 2001, "Rotordynamic Evaluation of Frequency Dependent Impedances of Hole-Pattern Gas Damper Seals," MS Thesis, Department of Mechanical Engineering. Texas A&M University, College Station.

10. Weatherwax, M., 2001, "A Study of the Effects of Eccentricity on Honeycomb Annular Gas Seals," MS Thesis, Department of Mechanical Engineering. Texas A&M University, College Station.

11. Wade, J., 2001, "Test Versus Predictions for Rotordynamic Coefficients and Leakage Rates of Hole-Pattern Gas Seals at Two Clearances in Choked and Unchoked Conditions, " MS Thesis, Department of Mechanical Engineering. Texas A&M University, College Station.

12. Childs, D., Hale, K., 1994, "A Test Apparatus and Facility to Identify the Rotordynamic Coefficients of High-Speed Hydrostatic Bearings," ASME Journal of Tribology, **116**, pp. 337-334.

13. Dawson, M., Childs, D., Holt, C., and Phillips, S., 2002, "Theory Versus Experiments for the Dynamic Impedances of Annular Gas Seals: Part 1 – Test Facility and Apparatus," Journal of Engineering for Gas Turbines and Power, **124**, pp. 958-963.

14. Kurtin, K. A., Childs, D. W., San Andres, L. A., and Hale, R. K., 1993, "Experimental Versus Theoretical Characteristics of a High-Speed Hybrid (Combination Hydrostatic and Hydrodynamic) Bearing," ASME Journal of Tribology, **115**, pp. 160-169.

APPENDIX A

The following examples show how to convert normalized damping to damping, and non-dimensional leakage to leakage.

The equation used to normalize damping is equation 18 in the text. Equation A.1 is the conversion from normalized damping to damping.

$$C = C^* \frac{L \cdot 2 \cdot R \cdot \Delta P}{C_r} \qquad \text{A.1}$$

Below is a sample calculation using equation A.1. In the sample calculation diameter is used in place of two times the radius.

$$C = 6*10^{-5}(s)*\frac{0.0858(m)*0.1147(m)*4.17(MN/m^2)}{0.00213(m)} = 0.001156\left(MN-s/m\right)$$

$$= 1156.00\left(N-s/m\right)$$

The equation used to non-dimensionalize leakage is equation 19 in the text. Equation A.2 is the conversion used to go from non-dimensional leakage to leakage.

$$\dot{m} = \phi \cdot \pi \cdot D \cdot C_r \cdot \left(\sqrt{\frac{2 \cdot \Delta P \cdot P_{in}}{R_c T_{in}}}\right) \qquad \text{A.2}$$

A sample calculation is presented below using equation A.2.

$$\dot{m} = 0.1796*\pi*114.727(mm)*0.2131(mm)*\sqrt{\frac{2*2.9395(MN/m^2)*4.1756(MN/m^2)}{287(Nm/kgK)*287.21(K)}}$$

$$= 0.1796 * \pi * 114.727(mm) * 0.2131(mm) *$$

$$\sqrt{\frac{2 * 2.9395(M\cancel{N}/m^2) * 4.1756(M(kg\cancel{m}/s^2)/m^{\cancel{2}})}{287(\cancel{N}m/kgK) * 287.21(K)}}$$

$$= 0.1796 * \pi * 114.727(\cancel{mm}) * 0.2131(\cancel{mm}) * 0.01725\left(\frac{kg}{\cancel{m^2}s}\right) * \cancel{1000000}$$

$$= 0.238(kg/s)$$

APPENDIX B

The measured impedances at different conditions are given in the following tables.

Table 5 Zero preswirl, PR = 30%, ω = 10,200

				Test Data								Uncertainties			
f	Rzxx	Izxx	Rzxy	Izxy	Rzyx	Izyx	Rzyy	Izyy	Rzxx	Izxx	Rzxy	Izxy	Rzyx	Izyx	Rzyy	Izyy
20	-8.08	4.84	5.88	-1.09	-6.23	1.16	-8.03	4.88	0.201	0.127	0.097	0.185	0.161	0.163	0.145	0.114
30	-7.28	6.91	5.68	-1.53	-5.97	1.52	-7.14	6.78	0.059	0.090	0.103	0.077	0.128	0.113	0.148	0.116
40	-6.18	8.82	5.35	-1.83	-5.94	2.01	-5.98	9.05	0.364	0.325	0.098	0.093	0.288	0.288	0.120	0.152
50	-4.95	10.59	4.97	-2.13	-5.16	2.72	-4.59	10.02	0.179	0.220	0.194	0.130	0.111	0.155	0.170	0.143
70	-2.44	13.38	4.83	-2.59	-4.92	2.60	-2.41	12.94	0.223	0.208	0.209	0.187	0.136	0.195	0.315	0.267
80	-1.03	14.36	4.54	-2.70	-4.69	2.79	-1.16	14.54	0.180	0.213	0.214	0.206	0.140	0.202	0.198	0.208
90	0.42	15.33	4.06	-2.61	-4.30	2.66	0.42	15.83	0.144	0.258	0.161	0.229	0.123	0.156	0.130	0.287
100	1.84	16.19	4.06	-3.24	-4.34	2.37	2.11	16.43	0.228	0.264	0.178	0.167	0.212	0.196	0.173	0.327
110	3.32	17.35	3.99	-3.27	-4.01	2.89	3.22	17.12	0.193	0.274	0.243	0.172	0.147	0.177	0.130	0.340
130	6.11	18.23	3.40	-3.18	-3.41	3.10	6.39	17.53	0.195	0.232	0.187	0.124	0.256	0.208	0.184	0.199
140	7.60	18.64	3.06	-3.53	-3.11	3.26	7.31	17.90	0.233	0.241	0.133	0.211	0.133	0.107	0.260	0.239
150	8.92	18.49	2.51	-3.38	-2.69	2.74	8.95	18.83	0.125	0.295	0.123	0.131	0.099	0.174	0.260	0.166
160	9.84	18.77	2.81	-2.07	-2.77	3.46	11.39	18.81	0.153	0.191	0.200	0.159	0.137	0.135	0.224	0.270
190	13.34	18.24	2.18	-3.38	-2.20	3.11	13.78	18.46	0.212	0.323	0.177	0.132	0.233	0.192	0.244	0.257
200	14.22	19.05	2.14	-3.60	-1.68	3.18	14.63	18.34	0.202	0.314	0.185	0.163	0.262	0.269	0.169	0.249
210	15.22	18.52	1.84	-3.38	-1.38	3.09	15.81	18.41	0.177	0.256	0.178	0.163	0.149	0.307	0.198	0.210
220	16.97	19.31	1.54	-3.37	-1.17	2.69	17.33	18.07	0.290	0.353	0.195	0.162	0.228	0.415	0.251	0.254
230	18.28	19.08	0.80	-3.50	-1.42	2.25	17.71	18.08	0.342	0.252	0.346	0.227	0.310	0.565	0.233	0.272
290	24.13	15.89	-0.63	-1.82	-2.38	3.80	24.81	14.59	0.305	0.303	0.351	0.439	0.431	0.335	0.382	0.331
320	24.31	15.36	-0.44	0.15	0.22	4.89	25.11	12.52	0.467	0.384	0.219	0.323	0.358	0.447	0.325	0.330

Table 6 Zero preswirl, PR = 30%, ω = 15,200

				Test Data								Uncertainties			
f	Rzxx	Izxx	Rzxy	Izxy	Rzyx	Izyx	Rzyy	Izyy	Rzxx	Izxx	Rzxy	Izxy	Rzyx	Izyx	Rzyy	Izyy
20	-8.35	5.19	9.18	-2.20	-9.66	2.25	-8.24	5.33	0.201	0.127	0.097	0.185	0.161	0.163	0.145	0.114
30	-7.80	7.50	8.58	-2.46	-8.97	2.70	-7.51	7.38	0.059	0.090	0.103	0.077	0.128	0.113	0.148	0.116
40	-5.82	7.66	8.25	-3.01	-8.51	4.31	-6.50	9.48	0.364	0.325	0.098	0.093	0.288	0.288	0.120	0.152
50	-5.26	11.53	7.81	-3.14	-7.94	3.44	-5.00	11.23	0.179	0.220	0.194	0.130	0.111	0.155	0.170	0.143
70	-2.72	14.60	6.90	-3.47	-7.30	4.01	-2.38	14.54	0.223	0.208	0.209	0.187	0.136	0.195	0.315	0.267
80	-1.02	15.91	6.94	-3.81	-6.90	4.28	-0.87	15.73	0.180	0.213	0.214	0.206	0.140	0.202	0.198	0.208
90	0.76	16.88	6.27	-4.66	-6.33	4.13	0.70	17.01	0.144	0.258	0.161	0.229	0.123	0.156	0.130	0.287
100	1.85	17.46	5.80	-4.30	-6.40	4.28	2.23	17.83	0.228	0.264	0.178	0.167	0.212	0.196	0.173	0.327
110	3.48	18.70	5.32	-4.46	-5.82	4.48	3.87	18.13	0.193	0.274	0.243	0.172	0.147	0.177	0.130	0.340
130	6.77	19.49	4.83	-5.08	-4.40	5.35	7.06	18.76	0.195	0.232	0.187	0.124	0.256	0.208	0.184	0.199
140	8.53	19.58	4.13	-5.03	-4.70	4.77	8.27	19.23	0.233	0.241	0.133	0.211	0.133	0.107	0.260	0.239
150	9.04	19.81	4.20	-4.77	-4.19	4.63	9.82	19.30	0.125	0.295	0.123	0.131	0.099	0.174	0.260	0.166
160	11.20	19.74	3.50	-4.64	-4.13	4.95	11.37	19.70	0.153	0.191	0.200	0.159	0.137	0.135	0.224	0.270
190	14.71	20.51	2.60	-5.24	-2.04	5.35	15.12	19.55	0.212	0.323	0.177	0.132	0.233	0.192	0.244	0.257
200	15.80	21.63	2.59	-4.79	-1.10	4.79	16.07	19.51	0.202	0.314	0.185	0.163	0.262	0.269	0.169	0.249
210	16.48	20.62	1.54	-4.69	-1.29	5.28	17.21	19.96	0.177	0.256	0.178	0.163	0.149	0.307	0.198	0.210
220	17.16	21.32	1.00	-5.28	0.04	5.37	18.20	20.27	0.290	0.353	0.195	0.162	0.228	0.415	0.251	0.254
230	16.35	22.39	1.32	-7.39	1.26	7.54	16.73	19.01	0.342	0.252	0.346	0.227	0.310	0.565	0.233	0.272
290	23.19	19.40	-4.74	-4.80	1.05	6.16	25.52	19.32	0.305	0.303	0.351	0.439	0.431	0.335	0.382	0.331
300	26.02	18.15	-2.93	-2.36	0.09	6.08	25.87	17.16	0.594	0.759	0.409	0.596	0.756	0.931	0.663	0.780

Table 7 Zero preswirl, PR = 40%, ω = 10,200

f	Test Data								Uncertainties							
	Rzxx	Izxx	Rzxy	Izxy	Rzyx	Izyx	Rzyy	Izyy	Rzxx	Izxx	Rzxy	Izxy	Rzyx	Izyx	Rzyy	Izyy
20	-6.64	4.18	5.43	-0.71	-5.05	0.93	-5.41	3.75	0.225	0.142	0.171	0.274	0.191	0.182	0.204	0.234
30	-6.36	5.76	5.25	-1.08	-4.98	1.36	-4.90	5.60	0.089	0.106	0.148	0.095	0.137	0.101	0.109	0.108
40	-5.37	7.54	5.05	-1.28	-4.89	1.36	-4.73	7.04	0.369	0.333	0.153	0.166	0.295	0.288	0.143	0.115
50	-4.03	9.19	4.62	-1.64	-5.10	2.23	-4.00	8.48	0.171	0.180	0.167	0.094	0.157	0.128	0.175	0.217
70	-2.10	11.96	4.54	-1.92	-4.23	1.80	-2.13	12.09	0.168	0.238	0.288	0.233	0.190	0.145	0.280	0.373
80	-1.06	13.04	4.02	-1.85	-4.24	2.46	-0.36	13.23	0.225	0.285	0.246	0.163	0.176	0.137	0.155	0.223
90	0.20	14.31	4.29	-2.46	-3.63	2.62	0.81	14.13	0.195	0.337	0.263	0.211	0.162	0.181	0.232	0.259
100	1.27	15.27	4.43	-2.15	-3.57	2.23	1.86	15.16	0.180	0.290	0.270	0.269	0.194	0.166	0.280	0.256
110	2.48	16.19	3.47	-1.92	-3.55	2.37	3.36	16.47	0.205	0.215	0.259	0.446	0.166	0.151	0.415	0.522
120	3.61	17.31	3.64	-2.47	-3.49	2.43	3.33	16.23	0.242	0.312	0.505	0.536	0.539	0.544	0.723	1.195
130	5.95	18.08	4.39	-3.76	-3.20	1.57	4.00	16.83	0.342	0.395	0.399	0.464	0.211	0.155	0.399	0.316
140	7.03	17.71	3.09	-2.45	-3.35	2.09	7.18	18.04	0.178	0.377	0.441	0.426	0.254	0.275	0.536	0.532
150	7.98	17.47	2.72	0.38	-3.51	2.10	10.70	19.03	0.304	0.397	0.397	0.197	0.226	0.242	0.390	0.476
160	9.40	18.84	8.43	-0.10	-2.61	2.29	11.70	13.06	0.284	0.336	0.496	0.279	0.191	0.172	0.422	0.406
190	11.91	20.15	5.51	-0.91	-0.93	3.31	15.92	16.17	0.397	0.499	0.505	0.304	0.394	0.162	0.454	0.431
200	13.19	20.48	2.99	-0.95	-1.24	3.25	14.94	18.74	0.382	0.542	0.373	0.456	0.419	0.299	0.706	0.327
210	14.23	20.64	3.12	-2.64	-1.05	3.17	14.71	18.85	0.427	0.530	0.427	0.557	0.485	0.391	0.474	0.603
220	17.66	20.80	2.62	-3.45	-0.74	1.93	15.33	19.06	0.568	0.791	0.618	0.641	0.738	0.525	0.722	0.882
230	18.07	19.06	2.32	-1.69	-1.78	1.68	16.84	18.37	1.666	1.521	1.339	1.296	1.517	1.504	1.311	1.539
290	25.21	19.16	0.29	-2.24	-1.37	2.55	23.69	18.41	1.133	1.183	1.335	3.404	1.265	0.900	3.012	1.198
320	23.88	17.80	0.01	-0.65	-1.42	4.11	22.98	16.48	0.868	0.934	0.956	1.058	0.920	0.557	1.312	0.747

Table 8 Zero preswirl, PR = 40%, ω = 15,200

f	Test Data								Uncertainties							
	Rzxx	Izxx	Rzxy	Izxy	Rzyx	Izyx	Rzyy	Izyy	Rzxx	Izxx	Rzxy	Izxy	Rzyx	Izyx	Rzyy	Izyy
20	-7.99	4.64	7.73	-1.30	-7.67	1.35	-6.40	3.91	0.225	0.142	0.171	0.274	0.191	0.182	0.204	0.234
30	-6.73	6.40	7.62	-1.53	-7.22	1.81	-6.19	6.33	0.089	0.106	0.148	0.095	0.137	0.101	0.109	0.108
40	-6.60	7.39	7.48	-2.05	-6.22	2.65	-5.74	8.08	0.369	0.333	0.153	0.166	0.295	0.288	0.143	0.115
50	-4.24	9.66	7.06	-2.19	-7.14	2.07	-4.52	9.69	0.171	0.180	0.167	0.094	0.157	0.128	0.175	0.217
70	-2.44	12.90	6.23	-2.70	-6.51	2.74	-2.54	13.02	0.168	0.238	0.288	0.233	0.190	0.145	0.280	0.373
80	-1.25	14.50	6.38	-2.69	-6.20	2.80	-0.81	14.07	0.225	0.285	0.246	0.163	0.176	0.137	0.155	0.223
90	0.52	15.28	6.09	-3.52	-6.00	2.74	0.15	15.34	0.195	0.337	0.263	0.211	0.162	0.181	0.232	0.259
100	1.58	16.34	5.81	-2.70	-5.56	3.08	1.57	16.34	0.180	0.290	0.270	0.269	0.194	0.166	0.280	0.256
110	3.07	17.19	5.44	-4.20	-5.32	3.27	2.40	16.61	0.205	0.215	0.259	0.446	0.166	0.151	0.415	0.522
130	6.25	18.79	4.63	-2.57	-5.20	3.34	5.85	18.69	0.342	0.395	0.399	0.464	0.211	0.155	0.399	0.316
140	6.84	19.41	5.66	-2.97	-4.98	3.93	8.01	19.02	0.178	0.377	0.441	0.426	0.254	0.275	0.536	0.532
150	8.16	19.50	4.71	-3.49	-4.21	3.22	8.67	18.91	0.304	0.397	0.397	0.197	0.226	0.242	0.390	0.476
160	9.41	19.91	3.83	-3.06	-4.34	3.59	9.00	20.22	0.284	0.336	0.496	0.279	0.191	0.172	0.422	0.406
190	14.32	20.45	3.58	-3.76	-2.41	3.16	14.10	21.14	0.397	0.499	0.505	0.304	0.394	0.162	0.454	0.431
200	16.30	21.02	2.76	-2.98	-2.60	2.80	15.95	20.96	0.382	0.542	0.373	0.456	0.419	0.299	0.706	0.327
210	17.42	20.81	2.25	-2.94	-1.87	2.93	17.00	21.48	0.427	0.530	0.427	0.557	0.485	0.391	0.474	0.603
220	20.46	21.52	1.12	-0.69	-2.45	0.40	20.47	22.51	0.568	0.791	0.618	0.641	0.738	0.525	0.722	0.882
230	23.05	22.96	-5.48	-3.34	-0.38	-1.79	18.63	29.18	1.666	1.521	1.339	1.296	1.517	1.504	1.311	1.539
290	27.45	20.35	-3.48	-0.75	-1.69	0.86	27.08	23.43	1.133	1.183	1.335	3.404	1.265	0.900	3.012	1.198
320	27.88	15.94	-1.06	-0.68	-3.77	3.81	25.00	17.26	0.868	0.934	0.956	1.058	0.920	0.557	1.312	0.747

Table 9 Zero preswirl, PR = 40%, ω = 20,200

f	Test Data								Uncertainties							
	Rzxx	Izxx	Rzxy	Izxy	Rzyx	Izyx	Rzyy	Izyy	Rzxx	Izxx	Rzxy	Izxy	Rzyx	Izyx	Rzyy	Izyy
20	-8.01	4.66	10.12	-1.81	-10.77	1.27	-8.29	4.97	0.225	0.142	0.171	0.274	0.191	0.182	0.204	0.234
30	-7.45	6.63	9.29	-2.07	-10.05	2.06	-7.50	7.12	0.089	0.106	0.148	0.095	0.137	0.101	0.109	0.108
40	-6.57	8.54	9.27	-2.38	-9.63	2.69	-6.47	9.01	0.369	0.333	0.153	0.166	0.295	0.288	0.143	0.115
70	-2.87	12.99	7.65	-3.11	-8.97	3.25	-2.46	14.02	0.168	0.238	0.288	0.233	0.190	0.145	0.280	0.373
80	-1.63	15.10	8.21	-3.62	-8.28	3.97	-0.80	15.16	0.225	0.285	0.246	0.163	0.176	0.137	0.155	0.223
90	0.36	15.64	7.82	-4.15	-8.17	3.74	-0.16	16.29	0.195	0.337	0.263	0.211	0.162	0.181	0.232	0.259
100	1.24	16.42	7.16	-4.03	-8.17	4.01	1.36	17.81	0.180	0.290	0.270	0.269	0.194	0.166	0.280	0.256
110	2.67	17.44	7.08	-4.66	-7.20	4.57	3.66	17.95	0.205	0.215	0.259	0.446	0.166	0.151	0.415	0.522
130	6.12	18.66	6.75	-4.60	-7.22	4.26	5.38	19.20	0.342	0.395	0.399	0.464	0.211	0.155	0.399	0.316
140	6.66	18.97	5.88	-4.07	-6.67	4.90	7.40	19.46	0.178	0.377	0.441	0.426	0.254	0.275	0.536	0.532
150	8.35	19.02	5.96	-4.81	-6.63	5.31	9.27	20.45	0.304	0.397	0.397	0.197	0.226	0.242	0.390	0.476
160	9.51	20.18	5.40	-4.48	-5.71	5.17	9.65	20.06	0.284	0.336	0.496	0.279	0.191	0.172	0.422	0.406
190	13.39	20.19	4.89	-6.03	-5.14	5.33	14.35	21.32	0.397	0.499	0.505	0.304	0.394	0.162	0.454	0.431
200	15.05	20.93	4.37	-5.41	-5.04	5.10	15.66	20.50	0.382	0.542	0.373	0.456	0.419	0.299	0.706	0.327
210	16.29	20.40	4.43	-5.18	-4.52	5.46	16.62	20.79	0.427	0.530	0.427	0.557	0.485	0.391	0.474	0.603
220	17.29	21.23	4.06	-5.67	-4.10	4.76	17.75	20.27	0.568	0.791	0.618	0.641	0.738	0.525	0.722	0.882
230	19.16	20.76	3.99	-5.57	-4.24	5.07	19.09	19.95	1.666	1.521	1.339	1.296	1.517	1.504	1.311	1.539
290	24.32	19.23	1.80	-2.57	-2.77	5.22	26.95	17.49	1.133	1.183	1.335	3.404	1.265	0.900	3.012	1.198
300	24.53	20.16	2.18	-0.98	-3.36	5.88	25.74	15.30	1.088	0.916	2.097	1.775	1.262	0.631	1.383	2.240

Table 10 Zero preswirl, PR = 50%, ω = 10,200

f	Test Data								Uncertainties							
	Rzxx	Izxx	Rzxy	Izxy	Rzyx	Izyx	Rzyy	Izyy	Rzxx	Izxx	Rzxy	Izxy	Rzyx	Izyx	Rzyy	Izyy
20	-6.64	3.67	4.80	-0.46	-4.69	0.60	-5.01	3.83	0.224	0.141	0.389	0.131	0.175	0.150	0.110	0.144
30	-5.55	5.75	5.17	-0.62	-4.60	0.87	-4.77	5.47	0.176	0.092	0.125	0.095	0.150	0.122	0.113	0.152
40	-4.91	6.85	5.06	-0.90	-4.41	1.31	-4.05	6.96	0.378	0.336	0.186	0.143	0.284	0.291	0.166	0.150
50	-3.91	9.02	4.87	-1.25	-4.42	1.24	-3.30	7.78	0.212	0.208	0.176	0.108	0.119	0.116	0.197	0.121
70	-1.96	11.49	4.70	-1.37	-3.73	1.16	-1.39	11.36	0.273	0.307	0.301	0.552	0.181	0.141	0.308	0.411
80	-0.79	12.83	4.08	-1.72	-3.70	1.87	-0.53	12.57	0.139	0.258	0.220	0.134	0.258	0.181	0.191	0.255
90	0.76	14.10	3.99	-1.72	-3.15	1.96	0.88	13.67	0.194	0.367	0.286	0.286	0.228	0.173	0.197	0.247
100	1.22	14.83	4.23	-1.72	-3.87	2.14	2.04	14.51	0.193	0.307	0.201	0.137	0.207	0.110	0.233	0.288
110	2.23	15.87	3.65	-1.80	-3.47	2.45	3.17	16.18	0.169	0.318	0.221	0.261	0.170	0.204	0.306	0.265
130	5.53	17.72	4.29	-2.57	-2.89	2.59	4.82	16.92	0.189	0.447	0.521	0.362	0.378	0.224	0.353	0.625
140	6.62	17.63	3.18	-2.12	-3.40	2.52	6.34	18.31	0.168	0.418	0.399	0.189	0.317	0.146	0.510	0.661
150	7.57	17.19	2.34	-0.78	-3.52	2.88	9.04	19.42	0.350	0.506	0.371	0.407	0.218	0.404	0.342	0.284
160	9.22	18.23	8.76	0.94	-3.50	2.04	12.04	13.20	0.203	0.388	0.388	0.151	0.206	0.208	0.218	0.287	0.355
190	13.40	19.72	5.99	-3.14	-1.83	2.10	13.57	16.86	0.265	0.584	0.631	0.315	0.224	0.303	0.651	0.533
200	14.14	20.84	3.10	-2.88	-1.50	1.93	12.68	19.09	0.426	0.556	0.455	0.459	0.341	0.462	0.749	0.526
210	15.70	19.89	2.62	-2.44	-1.24	2.26	14.59	20.33	0.611	0.654	0.472	0.483	0.473	0.438	0.675	0.373
220	16.78	20.68	2.81	-2.36	-1.47	2.20	15.98	19.57	1.096	0.814	0.886	0.865	0.666	0.748	1.122	1.011
230	17.55	20.71	2.71	-2.04	-1.42	2.29	17.05	19.57	2.713	1.610	2.503	1.210	1.603	2.787	1.672	2.794
290	24.24	19.02	0.29	-2.46	-2.01	2.23	22.43	17.93	1.156	1.252	2.738	2.414	1.275	1.047	2.640	2.586
300	25.65	19.04	0.34	-0.63	-1.50	3.32	22.05	17.86	1.032	1.059	1.186	1.607	0.990	0.914	1.887	1.126

Table 11 Zero preswirl, PR = 50%, ω = 15,200

f	Test Data								Uncertainties							
	Rzxx	Izxx	Rzxy	Izxy	Rzyx	Izyx	Rzyy	Izyy	Rzxx	Izxx	Rzxy	Izxy	Rzyx	Izyx	Rzyy	Izyy
20	-7.26	4.45	8.07	-1.06	-6.54	0.92	-6.37	4.23	0.224	0.141	0.389	0.131	0.175	0.150	0.110	0.144
30	-6.26	5.82	7.02	-1.22	-6.67	1.15	-5.72	6.24	0.176	0.092	0.125	0.095	0.150	0.122	0.113	0.152
40	-9.01	5.29	6.81	-1.82	-4.70	2.44	-5.03	7.86	0.378	0.336	0.186	0.143	0.284	0.291	0.166	0.150
50	-4.19	9.45	7.07	-1.59	-6.29	1.60	-4.12	9.33	0.212	0.208	0.176	0.108	0.119	0.116	0.197	0.121
70	-2.58	12.40	6.53	-1.32	-5.57	1.73	-2.63	11.51	0.273	0.307	0.301	0.552	0.181	0.141	0.308	0.411
80	-1.07	14.21	6.35	-2.40	-5.98	2.24	-0.95	13.75	0.139	0.258	0.220	0.134	0.258	0.181	0.191	0.255
90	0.57	14.99	6.46	-2.42	-5.79	2.38	0.80	14.76	0.194	0.367	0.286	0.286	0.228	0.173	0.197	0.247
100	1.55	15.66	5.60	-2.32	-5.50	2.43	1.75	15.68	0.193	0.307	0.201	0.137	0.207	0.110	0.233	0.288
110	2.95	16.80	5.84	-3.65	-4.99	2.63	2.50	17.10	0.169	0.318	0.221	0.261	0.170	0.204	0.306	0.265
130	5.97	18.56	5.49	-2.42	-5.35	2.96	6.36	18.62	0.189	0.447	0.521	0.362	0.378	0.224	0.353	0.625
140	6.94	18.19	4.85	-3.12	-5.30	2.95	7.15	19.88	0.168	0.418	0.399	0.189	0.317	0.146	0.510	0.661
150	8.28	19.09	4.61	-3.32	-4.62	2.56	7.96	19.09	0.350	0.506	0.371	0.407	0.218	0.404	0.342	0.284
160	9.33	19.30	4.49	-2.91	-4.77	3.29	9.66	19.79	0.203	0.388	0.151	0.206	0.208	0.218	0.287	0.355
190	14.56	20.46	3.88	-3.74	-3.44	2.33	14.02	20.40	0.265	0.584	0.631	0.315	0.224	0.303	0.651	0.533
200	16.66	21.08	3.21	-1.82	-3.54	1.75	16.74	20.84	0.426	0.556	0.455	0.459	0.341	0.462	0.749	0.526
210	17.64	21.06	3.53	-1.93	-3.39	1.79	17.27	21.37	0.611	0.654	0.472	0.483	0.473	0.438	0.675	0.373
220	20.80	20.42	2.86	0.67	-4.22	-0.92	20.19	22.24	1.096	0.814	0.886	0.865	0.666	0.748	1.122	1.011
230	30.13	22.70	-7.04	3.13	-2.41	-9.71	25.58	31.34	2.713	1.610	2.503	1.210	1.603	2.787	1.672	2.794
290	30.04	19.43	-3.49	11.37	-3.84	-1.94	39.99	22.49	1.156	1.252	2.738	2.414	1.275	1.047	2.640	2.586
300	26.90	19.85	-4.35	5.54	-2.10	2.27	32.61	19.75	1.032	1.059	1.186	1.607	0.990	0.914	1.887	1.126

Table 12 Zero preswirl, PR = 50%, ω = 20,200

f	Test Data								Uncertainties							
	Rzxx	Izxx	Rzxy	Izxy	Rzyx	Izyx	Rzyy	Izyy	Rzxx	Izxx	Rzxy	Izxy	Rzyx	Izyx	Rzyy	Izyy
20	-6.42	4.98	5.79	-1.07	-6.31	1.13	-6.39	5.02	0.224	0.141	0.389	0.131	0.175	0.150	0.110	0.144
30	-5.55	7.14	5.59	-1.51	-6.08	1.51	-5.48	6.96	0.176	0.092	0.125	0.095	0.150	0.122	0.113	0.152
40	-4.54	9.09	5.16	-1.84	-5.93	1.94	-4.35	9.26	0.378	0.336	0.186	0.143	0.284	0.291	0.166	0.150
70	-0.87	13.88	4.74	-2.46	-4.93	2.57	-0.67	13.42	0.273	0.307	0.301	0.552	0.181	0.141	0.308	0.411
80	0.65	14.93	4.40	-2.50	-4.73	2.75	0.62	14.96	0.139	0.258	0.220	0.134	0.258	0.181	0.191	0.255
90	2.02	15.97	3.89	-2.42	-4.36	2.64	2.12	16.27	0.194	0.367	0.286	0.286	0.228	0.173	0.197	0.247
100	3.51	16.91	3.83	-2.96	-4.35	2.31	3.78	17.03	0.193	0.307	0.201	0.137	0.207	0.110	0.233	0.288
110	5.05	18.23	3.77	-2.84	-4.02	2.83	4.92	17.74	0.169	0.318	0.221	0.261	0.170	0.204	0.306	0.265
130	7.93	19.24	3.26	-2.48	-3.45	2.97	8.19	18.32	0.189	0.447	0.521	0.362	0.378	0.224	0.353	0.625
140	9.35	19.83	3.12	-2.66	-3.00	3.10	9.03	18.71	0.168	0.418	0.399	0.189	0.317	0.146	0.510	0.661
150	10.85	19.72	2.80	-2.41	-2.65	2.46	10.67	19.78	0.350	0.506	0.371	0.407	0.218	0.404	0.342	0.284
160	11.83	20.19	3.26	-0.99	-2.55	3.15	13.37	19.92	0.203	0.388	0.151	0.206	0.208	0.218	0.287	0.355
190	15.62	20.61	3.44	-2.91	-2.09	2.24	15.46	20.07	0.265	0.584	0.631	0.315	0.224	0.303	0.651	0.533
200	16.84	20.92	2.80	-3.21	-1.89	2.41	16.88	20.08	0.426	0.556	0.455	0.459	0.341	0.462	0.749	0.526
210	17.47	20.80	2.68	-3.01	-1.29	2.18	17.99	20.20	0.611	0.654	0.472	0.483	0.473	0.438	0.675	0.373
220	19.40	21.57	2.43	-3.06	-1.20	1.47	19.45	20.00	1.096	0.814	0.886	0.865	0.666	0.748	1.122	1.011
230	20.72	21.72	1.81	-3.32	-1.58	0.70	20.06	20.31	2.713	1.610	2.503	1.210	1.603	2.787	1.672	2.794
290	26.75	21.26	0.01	-1.41	-2.82	1.45	27.46	17.44	1.156	1.252	2.738	2.414	1.275	1.047	2.640	2.586
300	28.19	22.10	0.17	-1.53	-2.29	0.59	26.49	16.78	1.032	1.059	1.186	1.607	0.990	0.914	1.887	1.126

Table 13 Medium preswirl, PR = 30%, ω = 10,200

	Test Data								Uncertainties							
f	Rzxx	Izxx	Rzxy	Izxy	Rzyx	Izyx	Rzyy	Izyy	Rzxx	Izxx	Rzxy	Izxy	Rzyx	Izyx	Rzyy	Izyy
20	-4.95	3.45	6.66	-0.91	-7.25	0.87	-5.74	4.05	0.190	0.246	0.127	0.120	0.169	0.152	0.138	0.132
30	-5.05	5.23	6.50	-1.31	-6.78	1.69	-5.01	5.74	0.257	0.150	0.114	0.271	0.192	0.174	0.115	0.156
40	-4.34	6.60	6.50	-1.64	-6.80	2.40	-3.97	7.34	0.391	0.349	0.199	0.232	0.302	0.287	0.172	0.195
50	-3.22	8.22	5.88	-1.52	-6.44	2.32	-3.34	8.54	0.167	0.144	0.152	0.143	0.167	0.120	0.180	0.257
70	-1.16	10.88	6.36	-2.05	-5.58	2.45	-1.04	11.18	0.092	0.141	0.172	0.112	0.100	0.185	0.299	0.178
80	-0.35	11.41	5.52	-2.29	-5.50	3.07	0.33	11.96	0.099	0.173	0.172	0.171	0.153	0.174	0.251	0.225
90	0.53	12.54	5.47	-2.15	-5.02	3.02	1.16	12.89	0.075	0.139	0.289	0.154	0.161	0.174	0.271	0.217
100	1.89	13.11	5.32	-2.58	-5.06	2.86	1.98	13.64	0.102	0.115	0.193	0.146	0.129	0.194	0.162	0.160
110	3.02	14.13	4.95	-2.75	-4.63	3.20	3.40	14.02	0.151	0.253	0.298	0.301	0.115	0.181	0.324	0.340
130	5.90	14.88	4.51	-3.01	-4.03	3.45	5.75	15.07	0.160	0.221	0.312	0.267	0.232	0.209	0.502	0.270
140	6.26	15.12	3.98	-2.77	-4.02	3.59	7.22	15.50	0.154	0.164	0.203	0.216	0.172	0.267	0.350	0.141
150	7.36	15.49	3.91	-3.08	-3.45	3.30	8.27	15.92	0.119	0.213	0.161	0.164	0.154	0.210	0.273	0.193
160	8.29	16.14	4.53	-3.37	-3.32	4.18	9.35	15.50	0.119	0.154	0.266	0.240	0.101	0.152	0.355	0.328
190	11.03	15.75	1.47	-3.37	-2.86	4.43	12.99	16.26	0.344	0.344	0.468	0.576	0.284	0.237	0.746	0.360
200	12.03	16.90	1.84	-2.17	-2.17	4.42	13.45	15.69	0.266	0.276	0.291	0.492	0.290	0.263	0.496	0.327
210	12.83	16.87	2.11	-2.23	-2.12	4.86	14.06	15.93	0.163	0.413	0.436	0.654	0.319	0.308	0.419	0.458
220	14.28	17.49	2.10	-2.54	-2.24	4.40	14.98	16.16	0.470	0.748	0.808	0.666	0.544	0.549	0.486	0.854
230	15.94	17.07	1.61	-1.90	-2.10	4.64	16.46	15.64	1.325	1.805	1.380	1.527	1.716	1.397	1.387	1.340
290	20.52	14.30	0.84	0.51	-1.08	7.76	20.94	12.61	0.885	1.946	1.315	3.108	1.379	0.958	2.456	1.253
300	21.06	14.90	1.26	0.40	-1.08	8.06	20.66	14.04	0.454	1.133	1.008	1.278	0.772	0.578	1.417	0.790

Table 14 Medium preswirl, PR = 30%, ω = 15,200

	Test Data								Uncertainties							
f	Rzxx	Izxx	Rzxy	Izxy	Rzyx	Izyx	Rzyy	Izyy	Rzxx	Izxx	Rzxy	Izxy	Rzyx	Izyx	Rzyy	Izyy
20	-6.42	4.15	9.06	-0.76	-9.40	1.25	-6.35	4.12	0.190	0.246	0.127	0.120	0.169	0.152	0.138	0.132
30	-4.42	5.82	8.20	-2.54	-9.03	2.06	-5.45	6.19	0.257	0.150	0.114	0.271	0.192	0.174	0.115	0.156
40	-5.14	6.00	8.00	-2.07	-7.94	3.00	-4.40	7.84	0.391	0.349	0.199	0.232	0.302	0.287	0.172	0.195
50	-3.43	8.69	7.92	-2.22	-8.11	2.77	-3.27	9.07	0.167	0.144	0.152	0.143	0.167	0.120	0.180	0.257
70	-1.08	11.14	7.30	-3.10	-7.38	3.32	-1.04	11.44	0.092	0.141	0.172	0.112	0.100	0.185	0.299	0.178
80	-0.23	12.37	7.24	-3.08	-7.18	3.93	0.43	12.70	0.099	0.173	0.172	0.171	0.153	0.174	0.251	0.225
90	0.92	13.33	7.46	-3.45	-6.25	3.58	1.40	13.14	0.075	0.139	0.289	0.154	0.161	0.174	0.271	0.217
100	2.02	13.67	6.17	-3.42	-6.25	3.59	2.23	13.84	0.102	0.115	0.193	0.146	0.129	0.194	0.162	0.160
110	3.03	14.63	6.18	-3.74	-6.14	3.99	3.28	15.16	0.151	0.253	0.298	0.301	0.115	0.181	0.324	0.340
130	6.21	15.56	5.82	-3.87	-5.10	4.26	6.29	15.24	0.160	0.221	0.312	0.267	0.232	0.209	0.502	0.270
140	6.90	15.90	5.22	-3.85	-4.76	3.91	7.06	15.47	0.154	0.164	0.203	0.216	0.172	0.267	0.350	0.141
150	7.74	15.88	4.95	-4.00	-4.56	4.50	8.45	15.94	0.119	0.213	0.161	0.164	0.154	0.210	0.273	0.193
160	8.88	16.47	4.82	-4.02	-4.45	5.00	9.86	16.24	0.119	0.154	0.266	0.240	0.101	0.152	0.355	0.328
190	11.90	16.25	1.36	-3.99	-3.42	4.54	14.06	16.92	0.344	0.344	0.468	0.576	0.284	0.237	0.746	0.360
200	13.82	17.43	2.46	-3.07	-3.11	4.36	14.24	16.61	0.266	0.276	0.291	0.492	0.290	0.263	0.496	0.327
210	15.14	17.69	2.54	-2.08	-2.89	4.29	15.54	16.73	0.163	0.413	0.436	0.654	0.319	0.308	0.419	0.458
220	17.63	17.73	2.06	-1.42	-2.98	3.67	17.43	16.78	0.470	0.748	0.808	0.666	0.544	0.549	0.486	0.854
230	21.90	19.24	-2.74	0.34	0.17	1.22	19.57	21.01	1.325	1.805	1.380	1.527	1.716	1.397	1.387	1.340
290	0.88	1.95	1.32	3.11	1.38	0.96	2.46	1.25	0.885	1.946	1.315	3.108	1.379	0.958	2.456	1.253
300	23.48	16.42	1.49	3.07	0.29	8.07	24.82	14.04	0.454	1.133	1.008	1.278	0.772	0.578	1.417	0.790

Table 15 Medium preswirl, PR = 30%, ω = 20,200

f	Test Data								Uncertainties							
	Rzxx	Izxx	Rzxy	Izxy	Rzyx	Izyx	Rzyy	Izyy	Rzxx	Izxx	Rzxy	Izxy	Rzyx	Izyx	Rzyy	Izyy
20	-7.09	4.51	11.04	-1.41	-11.29	1.61	-7.09	4.23	0.190	0.246	0.127	0.120	0.169	0.152	0.138	0.132
30	-6.13	6.60	10.90	-2.39	-11.00	2.36	-6.23	6.41	0.257	0.150	0.114	0.271	0.192	0.174	0.115	0.156
40	-5.07	7.93	10.07	-2.94	-10.32	2.89	-5.47	7.96	0.391	0.349	0.199	0.232	0.302	0.287	0.172	0.195
50	-3.53	9.22	10.04	-3.24	-10.22	3.27	-4.61	9.72	0.167	0.144	0.152	0.143	0.167	0.120	0.180	0.257
70	-1.44	11.81	8.72	-4.04	-8.98	4.10	-1.44	12.20	0.092	0.141	0.172	0.112	0.100	0.185	0.299	0.178
80	-0.43	12.96	8.41	-4.16	-8.39	4.67	-0.03	13.15	0.099	0.173	0.172	0.171	0.153	0.174	0.251	0.225
90	0.68	13.72	7.98	-4.29	-8.15	4.56	1.24	14.24	0.075	0.139	0.289	0.154	0.161	0.174	0.271	0.217
100	2.19	14.44	7.72	-4.82	-7.44	4.81	2.33	14.40	0.102	0.115	0.193	0.146	0.129	0.194	0.162	0.160
110	3.43	15.12	7.16	-5.04	-7.47	5.16	3.79	15.87	0.151	0.253	0.298	0.301	0.115	0.181	0.324	0.340
130	6.02	15.65	6.15	-4.92	-6.29	5.28	6.15	16.00	0.160	0.221	0.312	0.267	0.232	0.209	0.502	0.270
140	7.31	16.29	6.25	-5.51	-6.26	5.39	7.10	16.44	0.154	0.164	0.203	0.216	0.172	0.267	0.350	0.141
150	7.94	16.18	5.70	-5.53	-6.05	5.55	8.53	16.86	0.119	0.213	0.161	0.164	0.154	0.210	0.273	0.193
160	9.18	16.99	5.21	-4.91	-5.41	5.98	9.81	16.77	0.119	0.154	0.266	0.240	0.101	0.152	0.355	0.328
190	11.99	17.06	3.00	-5.85	-4.32	6.67	13.41	17.26	0.344	0.344	0.468	0.576	0.284	0.237	0.746	0.360
200	13.07	17.83	3.43	-4.11	-3.56	6.43	14.26	16.81	0.266	0.276	0.291	0.492	0.290	0.263	0.496	0.327
210	14.89	17.99	3.68	-4.64	-3.21	6.86	15.20	16.47	0.163	0.413	0.436	0.654	0.319	0.308	0.419	0.458
220	16.21	17.77	3.06	-4.76	-3.88	6.64	16.15	16.85	0.470	0.748	0.808	0.666	0.544	0.549	0.486	0.854
230	17.20	16.88	2.70	-3.98	-3.73	7.21	16.64	16.29	1.325	1.805	1.380	1.527	1.716	1.397	1.387	1.340
290	0.88	1.95	1.32	3.11	1.38	0.96	2.46	1.25	0.885	1.946	1.315	3.108	1.379	0.958	2.456	1.253
300	23.35	15.19	1.20	-1.85	-0.97	9.36	22.52	15.68	0.454	1.133	1.008	1.278	0.772	0.578	1.417	0.790
310	22.18	12.27	-1.09	-1.28	-1.97	11.46	24.13	15.20	0.733	0.785	0.826	1.119	0.470	0.852	0.925	0.914

Table 16 Medium preswirl, PR = 40%, ω = 10,200

f	Test Data								Uncertainties							
	Rzxx	Izxx	Rzxy	Izxy	Rzyx	Izyx	Rzyy	Izyy	Rzxx	Izxx	Rzxy	Izxy	Rzyx	Izyx	Rzyy	Izyy
20	-4.34	3.38	6.45	-0.58	-6.75	0.77	-4.70	3.71	0.133	0.136	0.127	0.110	0.076	0.093	0.145	0.112
40	-3.30	6.23	5.96	-0.77	-6.23	1.92	-3.17	6.78	0.356	0.356	0.210	0.202	0.296	0.280	0.172	0.150
50	-2.18	7.48	5.59	-1.34	-6.01	2.28	-1.97	8.06	0.180	0.139	0.166	0.147	0.128	0.128	0.191	0.159
70	-0.53	9.83	5.54	-1.50	-5.21	2.28	-0.76	10.30	0.152	0.156	0.239	0.203	0.094	0.164	0.178	0.118
80	0.45	10.72	5.32	-1.84	-5.19	2.59	0.38	11.35	0.162	0.184	0.258	0.163	0.186	0.122	0.190	0.259
90	0.96	11.45	5.37	-1.36	-4.72	2.92	1.91	12.12	0.121	0.197	0.187	0.197	0.176	0.223	0.295	0.379
100	2.28	12.31	4.78	-2.57	-4.41	2.50	2.43	12.43	0.121	0.200	0.088	0.071	0.139	0.114	0.231	0.214
110	3.35	13.15	5.06	-2.53	-4.07	2.69	4.02	13.51	0.177	0.172	0.183	0.296	0.205	0.130	0.216	0.284
130	5.98	13.90	4.49	-3.44	-3.30	2.96	5.33	13.75	0.179	0.226	0.220	0.256	0.189	0.210	0.267	0.327
140	6.30	14.66	4.16	-2.33	-3.53	3.39	7.42	14.85	0.136	0.176	0.227	0.218	0.128	0.189	0.272	0.242
150	6.75	14.51	4.47	-1.22	-2.84	4.22	9.68	14.66	0.113	0.208	0.144	0.152	0.203	0.232	0.226	0.265
160	7.29	13.81	6.32	-2.59	-4.43	4.11	8.67	12.44	0.175	0.236	0.230	0.308	0.183	0.185	0.301	0.325
190	10.83	14.02	3.40	-2.81	-3.08	4.36	13.48	13.98	0.238	0.437	0.481	0.498	0.144	0.242	0.442	0.538
200	11.44	15.49	2.09	-1.35	-3.21	4.13	13.25	15.44	0.162	0.525	0.374	0.332	0.247	0.305	0.493	0.441
210	12.40	15.71	2.73	-2.21	-2.81	4.66	13.83	15.27	0.368	0.474	0.443	0.365	0.378	0.284	0.350	0.373
220	14.21	17.24	2.24	-2.52	-1.80	4.12	15.22	15.33	0.605	0.425	0.639	0.762	0.457	0.506	0.614	0.599
230	16.01	16.54	1.96	-1.58	-2.04	4.07	16.31	15.15	1.252	0.867	1.262	1.160	0.668	1.111	1.132	1.105
290	20.01	14.23	0.46	0.01	-0.73	7.52	21.21	13.05	0.826	1.323	1.819	2.145	1.282	0.753	1.842	1.783
300	19.86	14.42	0.60	0.75	-1.20	8.68	21.24	12.68	0.990	0.880	1.472	0.920	1.152	1.171	1.580	0.987

Table 17 Medium preswirl, PR = 40%, ω = 15,200

f	Test Data								Uncertainties							
	Rzxx	Izxx	Rzxy	Izxy	Rzyx	Izyx	Rzyy	Izyy	Rzxx	Izxx	Rzxy	Izxy	Rzyx	Izyx	Rzyy	Izyy
20	-4.64	3.64	8.34	-0.79	-8.50	1.18	-4.43	3.72	0.133	0.136	0.127	0.110	0.076	0.093	0.145	0.112
40	-2.39	4.59	7.69	-1.82	-7.58	3.24	-3.64	7.08	0.356	0.356	0.210	0.202	0.296	0.280	0.172	0.150
50	-2.25	7.87	7.28	-1.96	-7.09	2.42	-2.17	8.25	0.180	0.139	0.166	0.147	0.128	0.128	0.191	0.159
70	-0.36	10.12	6.56	-2.17	-6.48	3.09	-0.20	10.47	0.152	0.156	0.239	0.203	0.094	0.164	0.178	0.118
80	0.48	11.47	7.01	-2.79	-6.27	3.51	0.93	11.72	0.162	0.184	0.258	0.163	0.186	0.122	0.190	0.259
90	1.83	12.21	6.69	-3.06	-5.68	3.16	1.29	12.09	0.121	0.197	0.187	0.197	0.176	0.223	0.295	0.379
100	2.60	12.64	6.27	-3.09	-5.56	3.46	3.04	12.92	0.121	0.200	0.088	0.071	0.139	0.114	0.231	0.214
110	3.54	13.66	5.84	-3.44	-5.55	3.92	3.98	14.16	0.177	0.172	0.183	0.296	0.205	0.130	0.216	0.284
130	6.03	14.36	5.48	-2.77	-4.34	3.64	6.58	14.22	0.179	0.226	0.220	0.256	0.189	0.210	0.267	0.327
140	7.19	14.88	5.25	-3.85	-4.77	4.11	7.27	14.88	0.136	0.176	0.227	0.218	0.128	0.189	0.272	0.242
150	8.01	14.63	4.41	-3.79	-4.67	3.97	8.18	15.62	0.113	0.208	0.144	0.152	0.203	0.232	0.226	0.265
160	8.83	16.02	4.87	-3.47	-3.81	4.49	10.29	15.06	0.175	0.236	0.230	0.308	0.183	0.185	0.301	0.325
190	11.96	15.30	2.07	-3.28	-2.96	4.51	14.76	15.74	0.238	0.437	0.481	0.498	0.144	0.242	0.442	0.538
200	13.56	16.09	2.55	-2.40	-3.01	3.68	14.66	15.10	0.162	0.525	0.374	0.332	0.247	0.305	0.493	0.441
210	15.00	16.63	3.01	-2.26	-2.98	3.72	15.29	14.83	0.368	0.474	0.443	0.365	0.378	0.284	0.350	0.373
220	17.11	17.39	2.32	-2.13	-2.98	3.73	16.85	15.83	0.605	0.425	0.639	0.762	0.457	0.506	0.614	0.599
230	24.07	15.44	1.15	1.91	-2.97	-1.66	21.27	16.27	1.252	0.867	1.262	1.160	0.668	1.111	1.132	1.105
290	25.42	12.18	3.77	6.07	-3.16	3.83	27.52	10.05	0.826	1.323	1.819	2.145	1.282	0.753	1.842	1.783
300	24.88	14.66	3.94	1.45	0.55	5.87	25.21	10.29	0.990	0.880	1.472	0.920	1.152	1.171	1.580	0.987

Table 18 Medium preswirl, PR = 40%, ω = 20,200

f	Test Data								Uncertainties							
	Rzxx	Izxx	Rzxy	Izxy	Rzyx	Izyx	Rzyy	Izyy	Rzxx	Izxx	Rzxy	Izxy	Rzyx	Izyx	Rzyy	Izyy
20	-5.68	4.07	10.66	-1.38	-10.42	1.27	-5.79	4.18	0.133	0.136	0.127	0.110	0.076	0.093	0.145	0.112
30	-4.90	5.90	10.41	-1.87	-10.30	2.35	-4.81	5.94	0.679	0.909	0.237	0.731	1.865	0.996	1.044	0.826
40	-3.44	7.00	9.35	-2.56	-9.65	2.22	-4.75	7.68	0.356	0.356	0.210	0.202	0.296	0.280	0.172	0.150
50	-2.60	8.92	9.40	-3.35	-9.47	3.02	-3.33	9.40	0.180	0.139	0.166	0.147	0.128	0.128	0.191	0.159
70	-0.84	11.49	9.00	-3.19	-8.29	3.84	-0.52	11.37	0.152	0.156	0.239	0.203	0.094	0.164	0.178	0.118
80	0.24	12.30	8.48	-3.61	-7.96	4.03	0.48	12.23	0.162	0.184	0.258	0.163	0.186	0.122	0.190	0.259
90	1.61	13.03	7.94	-4.12	-7.36	4.31	1.75	13.05	0.121	0.197	0.187	0.197	0.176	0.223	0.295	0.379
100	2.55	14.00	7.90	-4.06	-7.28	4.15	2.48	14.12	0.121	0.200	0.088	0.071	0.139	0.114	0.231	0.214
110	3.82	14.98	7.58	-4.43	-6.64	4.82	4.23	14.93	0.177	0.172	0.183	0.296	0.205	0.130	0.216	0.284
130	6.41	16.12	6.88	-3.91	-5.88	5.05	6.78	15.68	0.179	0.226	0.220	0.256	0.189	0.210	0.267	0.327
140	7.56	15.91	6.29	-5.14	-6.31	5.22	7.60	16.54	0.136	0.176	0.227	0.218	0.128	0.189	0.272	0.242
150	8.37	16.09	6.11	-4.87	-5.61	5.20	8.97	16.61	0.113	0.208	0.144	0.152	0.203	0.232	0.226	0.265
160	9.53	16.93	5.88	-4.53	-5.43	5.81	10.58	17.14	0.175	0.236	0.230	0.308	0.183	0.185	0.301	0.325
190	11.99	16.82	2.29	-5.15	-4.16	6.00	13.86	16.95	0.238	0.437	0.481	0.498	0.144	0.242	0.442	0.538
200	13.31	18.04	3.20	-3.85	-3.78	6.16	15.06	16.82	0.162	0.525	0.374	0.332	0.247	0.305	0.493	0.441
210	14.63	18.13	3.64	-3.78	-3.18	6.40	15.76	16.50	0.368	0.474	0.443	0.365	0.378	0.284	0.350	0.373
220	16.21	17.65	3.02	-3.81	-3.70	6.10	16.62	16.82	0.605	0.425	0.639	0.762	0.457	0.506	0.614	0.599
230	17.27	17.13	2.70	-4.16	-3.87	6.31	17.13	16.53	1.252	0.867	1.262	1.160	0.668	1.111	1.132	1.105
290	22.73	14.39	0.77	-0.81	-2.34	9.01	24.63	14.66	0.826	1.323	1.819	2.145	1.282	0.753	1.842	1.783
300	22.96	14.43	0.11	0.20	-1.77	9.15	24.55	16.41	0.990	0.880	1.472	0.920	1.152	1.171	1.580	0.987

Table 19 Medium preswirl, PR = 50%, ω = 10,200

f	Rzxx	Izxx	Rzxy	Izxy	Rzyx	Izyx	Rzyy	Izyy	Rzxx	Izxx	Rzxy	Izxy	Rzyx	Izyx	Rzyy	Izyy
			Test Data									Uncertainties				
20	-3.62	3.13	6.09	-0.41	-6.46	0.71	-4.26	3.48	0.105	0.098	0.141	0.087	0.144	0.189	0.092	0.114
30	-3.69	4.79	5.81	-0.88	-6.04	1.23	-3.79	5.05	0.130	0.075	0.133	0.107	0.210	0.199	0.166	0.142
40	-3.22	5.87	5.79	-0.83	-5.69	1.50	-3.35	6.29	0.359	0.325	0.168	0.123	0.311	0.284	0.229	0.121
50	-2.19	7.39	5.42	-1.27	-6.24	2.29	-2.58	7.29	0.148	0.170	0.193	0.094	0.104	0.172	0.194	0.136
70	-0.76	9.58	5.40	-1.43	-5.11	2.04	-0.86	9.72	0.102	0.134	0.176	0.154	0.107	0.072	0.152	0.165
80	0.28	10.48	5.38	-1.78	-4.94	2.49	0.56	10.88	0.131	0.132	0.166	0.151	0.101	0.107	0.169	0.142
90	1.47	11.23	5.27	-2.15	-4.46	2.62	1.73	11.63	0.121	0.110	0.168	0.219	0.114	0.237	0.301	0.268
100	1.93	12.37	5.09	-2.00	-4.24	2.47	2.15	12.33	0.156	0.134	0.112	0.109	0.117	0.128	0.172	0.168
110	2.68	12.70	4.86	-2.25	-3.96	2.72	3.47	13.36	0.116	0.100	0.143	0.195	0.115	0.168	0.261	0.208
130	5.11	13.75	4.02	-2.74	-3.73	2.87	5.86	14.47	0.080	0.196	0.204	0.196	0.179	0.206	0.274	0.237
140	6.64	14.66	4.67	-2.90	-3.51	2.83	6.43	14.67	0.150	0.196	0.236	0.128	0.124	0.126	0.122	0.176
150	7.15	14.52	3.81	-2.97	-3.40	2.82	7.24	15.02	0.146	0.199	0.152	0.137	0.172	0.167	0.289	0.231
160	8.13	16.07	2.94	-3.24	-2.51	3.76	8.57	16.23	0.178	0.191	0.223	0.204	0.095	0.102	0.167	0.223
190	10.09	15.76	2.53	-3.92	-2.20	4.52	12.05	15.30	0.189	0.321	0.214	0.250	0.309	0.356	0.369	0.313
200	11.16	17.15	2.46	-2.88	-2.11	4.34	12.61	15.16	0.256	0.431	0.173	0.424	0.390	0.223	0.356	0.219
210	12.58	17.53	2.41	-2.54	-1.94	4.55	13.08	16.45	0.270	0.342	0.272	0.316	0.343	0.236	0.263	0.421
220	14.55	17.77	1.40	-2.25	-1.61	3.98	14.53	16.02	0.505	0.582	0.552	0.540	0.490	0.562	0.622	0.668
230	15.97	16.46	1.42	-2.22	-1.97	4.34	14.95	15.51	1.275	0.957	0.770	1.328	0.738	1.406	1.292	0.691
290	21.69	15.24	-0.47	0.26	-1.07	7.39	21.76	14.29	1.232	1.314	0.919	1.678	1.233	0.935	1.186	1.133
300	21.98	15.79	0.50	0.99	-0.46	8.69	19.74	14.58	0.854	0.655	1.163	0.940	0.842	0.606	0.931	0.751

Table 20 Medium preswirl, PR = 50%, ω = 15,200

f	Rzxx	Izxx	Rzxy	Izxy	Rzyx	Izyx	Rzyy	Izyy	Rzxx	Izxx	Rzxy	Izxy	Rzyx	Izyx	Rzyy	Izyy
			Test Data									Uncertainties				
20	-4.29	3.02	8.09	-0.87	-7.74	1.15	-4.00	3.35	0.105	0.098	0.141	0.087	0.144	0.189	0.092	0.114
30	-3.36	4.72	7.86	-1.46	-7.63	1.40	-3.62	4.90	0.130	0.075	0.133	0.107	0.210	0.199	0.166	0.142
40	-3.96	4.90	7.64	-1.75	-6.29	2.69	-2.86	6.50	0.359	0.325	0.168	0.123	0.311	0.284	0.229	0.121
50	-1.81	7.05	7.11	-2.19	-7.14	2.34	-1.89	7.28	0.148	0.170	0.193	0.094	0.104	0.172	0.194	0.136
70	-0.52	9.85	7.15	-2.60	-6.19	2.62	-0.19	9.86	0.102	0.134	0.176	0.154	0.107	0.072	0.152	0.165
80	-0.02	10.59	6.63	-2.57	-6.14	3.02	0.87	10.89	0.131	0.132	0.166	0.151	0.101	0.107	0.169	0.142
90	1.23	11.42	6.56	-2.87	-5.56	3.23	1.70	11.58	0.121	0.110	0.168	0.219	0.114	0.237	0.301	0.268
100	1.85	12.58	6.43	-2.84	-5.31	2.85	2.48	12.04	0.156	0.134	0.112	0.109	0.117	0.128	0.172	0.168
110	2.91	13.32	6.20	-3.28	-5.41	3.07	3.47	13.66	0.116	0.100	0.143	0.195	0.115	0.168	0.261	0.208
130	5.48	14.35	5.66	-3.14	-4.51	3.37	6.20	14.19	0.080	0.196	0.204	0.196	0.179	0.206	0.274	0.237
140	6.39	14.65	5.67	-3.78	-4.70	3.56	6.78	14.51	0.150	0.196	0.236	0.128	0.124	0.126	0.122	0.176
150	7.07	14.52	4.97	-3.61	-4.35	3.74	7.86	15.35	0.146	0.199	0.152	0.137	0.172	0.167	0.289	0.231
160	8.19	15.54	4.82	-3.72	-4.06	4.05	9.19	15.16	0.178	0.191	0.223	0.204	0.095	0.102	0.167	0.223
190	11.53	16.17	2.31	-4.55	-2.42	3.78	13.09	15.97	0.189	0.321	0.214	0.250	0.309	0.356	0.369	0.313
200	12.98	17.72	2.96	-3.52	-2.64	3.55	13.26	15.71	0.256	0.431	0.173	0.424	0.390	0.223	0.356	0.219
210	14.69	17.72	2.67	-3.36	-2.11	3.85	14.15	15.82	0.270	0.342	0.272	0.316	0.343	0.236	0.263	0.421
220	17.20	17.46	1.52	-2.26	-2.64	2.66	15.86	17.07	0.505	0.582	0.552	0.540	0.490	0.562	0.622	0.668
300	23.28	15.77	1.84	-0.14	-0.18	6.85	23.35	13.44	0.854	0.655	1.163	0.940	0.842	0.606	0.931	0.751
310	23.92	14.48	0.75	0.39	0.43	8.17	23.82	14.18	0.670	0.835	1.047	0.683	0.546	0.945	0.765	0.615

Table 21 Medium preswirl, PR = 50%, ω = 20,200

f	Test Data								Uncertainties							
	Rzxx	Izxx	Rzxy	Izxy	Rzyx	Izyx	Rzyy	Izyy	Rzxx	Izxx	Rzxy	Izxy	Rzyx	Izyx	Rzyy	Izyy
20	-5.04	3.54	10.17	-1.25	-9.92	1.19	-5.18	3.82	0.105	0.098	0.141	0.087	0.144	0.189	0.092	0.114
30	-4.42	5.09	9.81	-1.66	-9.91	1.84	-4.66	5.73	0.130	0.075	0.133	0.107	0.210	0.199	0.166	0.142
40	-3.77	6.57	8.95	-2.06	-8.76	2.78	-3.75	7.09	0.359	0.325	0.168	0.123	0.311	0.284	0.229	0.121
50	-2.44	7.77	9.51	-2.68	-8.79	2.89	-3.25	7.91	0.148	0.170	0.193	0.094	0.104	0.172	0.194	0.136
70	-0.72	10.74	8.58	-3.22	-8.18	3.27	-0.42	10.74	0.102	0.134	0.176	0.154	0.107	0.072	0.152	0.165
80	0.07	11.64	8.08	-3.44	-7.89	3.64	0.21	11.99	0.131	0.132	0.166	0.151	0.101	0.107	0.169	0.142
90	1.62	12.63	7.94	-4.29	-7.69	3.47	1.02	13.02	0.121	0.110	0.168	0.219	0.114	0.237	0.301	0.268
100	2.54	13.07	7.46	-3.96	-7.18	3.97	2.38	13.54	0.156	0.134	0.112	0.109	0.117	0.128	0.172	0.168
110	3.16	14.15	7.45	-4.20	-6.92	4.24	3.81	14.62	0.116	0.100	0.143	0.195	0.115	0.168	0.261	0.208
130	5.81	14.74	6.68	-4.02	-6.14	4.72	6.44	15.14	0.080	0.196	0.204	0.196	0.179	0.206	0.274	0.237
140	6.69	15.31	6.12	-4.37	-5.98	4.66	7.11	15.50	0.150	0.196	0.236	0.128	0.124	0.126	0.122	0.176
150	7.74	15.45	6.11	-4.72	-5.56	4.86	8.35	16.00	0.146	0.199	0.152	0.137	0.172	0.167	0.289	0.231
160	8.39	16.59	5.89	-4.28	-5.37	5.38	9.72	16.45	0.178	0.191	0.223	0.204	0.095	0.102	0.167	0.223
190	11.18	16.85	3.20	-5.46	-4.34	5.80	13.02	17.54	0.189	0.321	0.214	0.250	0.309	0.356	0.369	0.313
200	12.47	17.96	3.58	-4.25	-4.45	5.97	14.39	16.52	0.256	0.431	0.173	0.424	0.390	0.223	0.356	0.219
210	14.55	18.26	4.08	-4.13	-3.82	5.92	14.88	16.64	0.270	0.342	0.272	0.316	0.343	0.236	0.263	0.421
220	15.69	18.34	3.95	-4.13	-3.84	5.70	15.96	16.80	0.505	0.582	0.552	0.540	0.490	0.562	0.622	0.668
230	16.69	16.93	2.79	-4.20	-3.73	6.41	16.69	15.88	1.275	0.957	0.770	1.328	0.738	1.406	1.292	0.691
290	22.27	15.07	3.43	-0.51	-2.33	9.17	24.78	13.03	1.232	1.314	0.919	1.678	1.233	0.935	1.186	1.133
300	23.71	15.80	1.22	-2.40	-0.53	7.13	23.27	14.56	0.854	0.655	1.163	0.940	0.842	0.606	0.931	0.751

Table 22 High preswirl, PR = 30%, ω = 10,200

f	Test Data								Uncertainties							
	Rzxx	Izxx	Rzxy	Izxy	Rzyx	Izyx	Rzyy	Izyy	Rzxx	Izxx	Rzxy	Izxy	Rzyx	Izyx	Rzyy	Izyy
20	-3.55	2.36	6.14	-0.67	-6.68	0.63	-3.29	2.69	0.145	0.196	0.094	0.085	0.143	0.088	0.061	0.091
30	-3.46	3.97	5.99	-0.93	-6.35	1.13	-3.02	4.19	0.182	0.153	0.103	0.102	0.153	0.122	0.090	0.110
40	-3.33	5.01	6.09	-0.97	-6.03	1.78	-2.32	5.13	0.380	0.340	0.139	0.143	0.351	0.316	0.179	0.167
50	-2.20	6.37	5.49	-1.07	-5.88	1.97	-1.71	5.80	0.148	0.147	0.157	0.081	0.139	0.107	0.157	0.132
70	-0.56	8.01	4.89	-1.57	-5.20	2.17	0.21	7.82	0.126	0.121	0.159	0.173	0.093	0.090	0.152	0.170
80	0.17	8.94	5.12	-1.58	-4.97	2.20	0.82	8.58	0.062	0.144	0.098	0.057	0.083	0.087	0.097	0.126
90	1.15	9.47	5.12	-1.89	-4.64	2.53	2.13	9.26	0.111	0.129	0.115	0.138	0.086	0.134	0.122	0.182
100	2.05	10.13	4.69	-2.18	-4.45	2.55	2.93	9.60	0.110	0.141	0.092	0.144	0.117	0.103	0.132	0.165
110	2.87	10.84	4.52	-2.28	-4.49	2.32	3.54	10.13	0.136	0.188	0.163	0.208	0.088	0.196	0.211	0.150
130	4.71	11.35	3.91	-2.50	-3.90	2.83	5.50	11.00	0.129	0.229	0.160	0.141	0.087	0.077	0.111	0.143
140	5.28	11.87	4.02	-1.80	-3.54	2.89	7.04	10.69	0.097	0.137	0.121	0.073	0.098	0.093	0.109	0.142
150	5.83	12.08	3.42	-1.43	-3.30	2.86	7.59	10.48	0.082	0.212	0.140	0.121	0.074	0.079	0.178	0.186
160	6.26	11.15	2.17	-2.96	-4.57	3.49	7.86	12.02	0.099	0.120	0.147	0.220	0.086	0.109	0.168	0.225
190	9.09	12.23	1.37	-1.85	-2.71	2.53	12.28	9.43	0.117	0.341	0.314	0.311	0.168	0.150	0.328	0.352
200	10.22	13.19	1.36	-1.59	-3.42	2.57	12.10	10.67	0.132	0.397	0.252	0.220	0.196	0.218	0.313	0.296
210	11.09	12.78	0.79	-2.18	-3.65	3.30	12.25	11.47	0.247	0.357	0.374	0.283	0.226	0.178	0.267	0.445
220	12.39	13.71	0.13	-1.52	-2.43	3.79	13.09	12.35	0.360	0.299	0.477	0.713	0.495	0.333	0.839	0.475
230	13.83	12.67	0.03	-0.94	-2.88	3.02	14.70	10.70	0.754	1.128	1.475	0.852	1.111	0.883	1.143	1.506
290	16.57	9.67	-2.91	1.35	-2.26	6.91	22.51	8.62	1.085	0.793	1.362	2.056	0.891	0.966	1.416	1.985
300	16.37	10.05	-1.50	1.74	-2.16	6.99	20.77	9.84	0.574	0.469	1.363	1.063	0.651	0.730	1.569	1.506

Table 23 High preswirl, PR = 30%, ω = 15,200

f	Rzxx	Izxx	Rzxy	Izxy	Rzyx	Izyx	Rzyy	Izyy	Rzxx	Izxx	Rzxy	Izxy	Rzyx	Izyx	Rzyy	Izyy
			Test Data									Uncertainties				
20	-7.91	4.93	5.86	-1.11	-6.19	1.15	-7.85	4.91	0.145	0.196	0.094	0.085	0.143	0.088	0.061	0.091
30	-7.03	7.02	5.73	-1.47	-5.94	1.55	-6.92	6.85	0.182	0.153	0.103	0.102	0.153	0.122	0.090	0.110
40	-6.71	7.77	5.29	-1.90	-5.26	2.56	-5.80	9.08	0.380	0.340	0.139	0.143	0.351	0.316	0.179	0.167
50	-4.80	10.66	5.22	-1.77	-5.40	2.11	-4.66	10.56	0.148	0.147	0.157	0.081	0.139	0.107	0.157	0.132
70	-2.29	13.46	4.90	-2.53	-4.83	2.65	-2.23	13.12	0.126	0.121	0.159	0.173	0.093	0.090	0.152	0.170
80	-0.85	14.48	4.61	-2.59	-4.59	2.84	-0.98	14.64	0.062	0.144	0.098	0.057	0.083	0.087	0.097	0.126
90	0.58	15.46	4.12	-2.63	-4.25	2.69	0.58	15.92	0.111	0.129	0.115	0.138	0.086	0.134	0.122	0.182
100	2.00	16.33	4.07	-3.22	-4.28	2.41	2.22	16.59	0.110	0.141	0.092	0.144	0.117	0.103	0.132	0.165
110	3.47	17.50	4.03	-3.26	-3.97	2.91	3.33	17.28	0.136	0.188	0.163	0.208	0.088	0.196	0.211	0.150
130	6.30	18.40	3.43	-3.13	-3.39	3.14	6.53	17.74	0.129	0.229	0.160	0.141	0.087	0.077	0.111	0.143
140	7.77	18.82	3.09	-3.49	-2.99	3.26	7.40	18.13	0.097	0.137	0.121	0.073	0.098	0.093	0.109	0.142
150	9.05	18.69	2.58	-3.37	-2.70	2.78	9.03	19.05	0.082	0.212	0.140	0.121	0.074	0.079	0.178	0.186
160	10.09	19.01	2.84	-1.94	-2.61	3.56	11.66	19.06	0.099	0.120	0.147	0.220	0.086	0.109	0.168	0.225
190	13.64	18.48	2.18	-3.43	-2.25	3.26	13.84	18.72	0.117	0.341	0.314	0.311	0.168	0.150	0.328	0.352
200	14.44	19.26	2.14	-3.60	-1.60	3.31	14.75	18.68	0.132	0.397	0.252	0.220	0.196	0.218	0.313	0.296
210	15.28	18.82	1.88	-3.44	-1.31	3.24	15.85	18.72	0.247	0.357	0.374	0.283	0.226	0.178	0.267	0.445
220	17.15	19.49	1.58	-3.45	-1.08	2.87	17.28	18.38	0.360	0.299	0.477	0.713	0.495	0.333	0.839	0.475
230	18.45	19.49	0.99	-3.54	-1.21	2.33	17.82	18.26	0.754	1.128	1.475	0.852	1.111	0.883	1.143	1.506
290	24.50	16.20	-0.28	-1.69	-2.51	3.96	24.84	14.82	1.085	0.793	1.362	2.056	0.891	0.966	1.416	1.985
300	25.13	16.12	-0.50	-1.01	-2.21	4.17	23.17	13.42	0.574	0.469	1.363	1.063	0.651	0.730	1.569	1.506

Table 24 High preswirl, PR = 30%, ω = 20,200

f	Rzxx	Izxx	Rzxy	Izxy	Rzyx	Izyx	Rzyy	Izyy	Rzxx	Izxx	Rzxy	Izxy	Rzyx	Izyx	Rzyy	Izyy
			Test Data									Uncertainties				
20	-5.01	3.18	9.83	-1.38	-9.38	1.66	-4.18	3.13	0.145	0.196	0.094	0.085	0.143	0.088	0.061	0.091
30	-4.70	4.77	9.40	-1.70	-8.89	1.73	-3.80	4.77	0.182	0.153	0.103	0.102	0.153	0.122	0.090	0.110
40	-3.38	5.64	8.51	-2.21	-9.33	1.97	-3.20	6.80	0.380	0.340	0.139	0.143	0.351	0.316	0.179	0.167
50	-2.05	7.11	8.89	-2.66	-8.40	2.81	-2.41	7.15	0.148	0.147	0.157	0.081	0.139	0.107	0.157	0.132
70	-0.64	9.38	7.74	-3.10	-7.44	2.77	-0.63	9.04	0.126	0.121	0.159	0.173	0.093	0.090	0.152	0.170
80	0.52	10.08	7.56	-3.57	-7.19	3.24	0.67	9.80	0.062	0.144	0.098	0.057	0.083	0.087	0.097	0.126
90	1.31	10.68	7.37	-3.66	-6.91	3.48	1.85	10.66	0.111	0.129	0.115	0.138	0.086	0.134	0.122	0.182
100	2.30	11.12	6.94	-3.53	-6.31	3.40	2.78	10.38	0.110	0.141	0.092	0.144	0.117	0.103	0.132	0.165
110	3.44	11.68	6.71	-4.34	-6.79	3.46	3.63	11.56	0.136	0.188	0.163	0.208	0.088	0.196	0.211	0.150
130	5.40	12.30	6.09	-4.28	-5.77	4.03	5.92	11.68	0.129	0.229	0.160	0.141	0.087	0.077	0.111	0.143
140	6.00	12.53	5.72	-4.03	-5.76	4.04	6.77	12.11	0.097	0.137	0.121	0.073	0.098	0.093	0.109	0.142
150	6.65	12.50	5.57	-4.19	-5.26	4.21	7.74	11.79	0.082	0.212	0.140	0.121	0.074	0.079	0.178	0.186
160	7.58	12.96	5.03	-4.42	-5.08	4.82	9.15	12.21	0.099	0.120	0.147	0.220	0.086	0.109	0.168	0.225
190	9.95	13.14	2.77	-5.30	-3.72	4.23	11.52	12.51	0.117	0.341	0.314	0.311	0.168	0.150	0.328	0.352
200	11.62	14.30	3.27	-4.28	-4.29	4.19	11.96	12.09	0.132	0.397	0.252	0.220	0.196	0.218	0.313	0.296
210	12.58	13.78	3.26	-4.19	-4.13	4.54	12.87	12.44	0.247	0.357	0.374	0.283	0.226	0.178	0.267	0.445
220	13.84	13.70	3.20	-3.88	-3.91	4.59	13.45	12.51	0.360	0.299	0.477	0.713	0.495	0.333	0.839	0.475
230	13.91	12.97	3.22	-3.32	-4.25	4.85	15.04	11.96	0.754	1.128	1.475	0.852	1.111	0.883	1.143	1.506
290	18.18	10.03	2.57	-1.14	-3.95	7.74	22.54	7.29	1.085	0.793	1.362	2.056	0.891	0.966	1.416	1.985
300	18.80	10.42	1.73	-3.11	-2.83	6.86	19.02	9.24	0.574	0.469	1.363	1.063	0.651	0.730	1.569	1.506

Table 25 High preswirl, PR = 40%, ω = 10,200

	Test Data								Uncertainties							
f	Rzxx	Izxx	Rzxy	Izxy	Rzyx	Izyx	Rzyy	Izyy	Rzxx	Izxx	Rzxy	Izxy	Rzyx	Izyx	Rzyy	Izyy
20	-3.41	2.74	6.15	-0.39	-5.81	0.55	-2.62	2.44	0.141	0.126	0.073	0.074	0.143	0.117	0.055	0.078
30	-2.71	3.57	5.78	-0.83	-5.71	0.99	-2.33	3.81	0.181	0.109	0.102	0.126	0.062	0.118	0.078	0.060
40	-2.31	4.57	5.71	-1.24	-5.57	1.70	-1.56	4.89	0.468	0.357	0.148	0.305	0.311	0.277	0.104	0.145
50	-1.41	5.94	5.43	-1.18	-5.53	1.49	-1.24	5.56	0.207	0.162	0.163	0.224	0.124	0.138	0.180	0.131
70	-0.18	7.75	5.16	-1.44	-4.90	1.72	0.33	7.47	0.150	0.162	0.226	0.233	0.090	0.143	0.227	0.150
80	0.54	8.40	4.79	-1.52	-4.45	2.01	1.09	7.95	0.100	0.087	0.183	0.150	0.074	0.076	0.091	0.147
90	1.08	8.83	4.40	-1.41	-4.59	1.93	1.85	8.95	0.163	0.133	0.140	0.185	0.119	0.097	0.182	0.164
100	1.86	9.83	4.91	-1.42	-4.44	2.16	2.57	9.59	0.213	0.112	0.228	0.300	0.130	0.158	0.250	0.172
110	2.73	10.44	4.35	-1.71	-4.24	2.25	3.84	10.20	0.256	0.221	0.343	0.356	0.209	0.215	0.247	0.386
130	4.32	11.54	4.75	-0.77	-3.50	2.51	5.79	10.38	0.122	0.184	0.249	0.244	0.118	0.082	0.136	0.212
140	5.07	11.29	3.27	-2.12	-3.81	2.67	6.21	11.48	0.156	0.198	0.266	0.342	0.145	0.160	0.308	0.214
150	5.21	11.64	2.58	-1.59	-3.64	3.00	6.94	11.88	0.101	0.162	0.233	0.233	0.141	0.095	0.197	0.221
160	6.79	12.11	6.72	-0.10	-3.62	2.28	9.57	8.22	0.145	0.195	0.347	0.523	0.068	0.103	0.171	0.277
190	9.46	11.83	-2.05	-2.34	-3.61	2.34	11.25	13.70	0.161	0.186	0.410	0.238	0.101	0.132	0.296	0.294
200	10.34	12.92	-0.30	-1.39	-3.22	2.02	11.48	12.80	0.209	0.256	0.363	0.240	0.148	0.148	0.199	0.247
210	10.83	13.01	0.10	-0.44	-3.23	2.80	12.59	12.31	0.223	0.412	0.529	0.537	0.219	0.219	0.304	0.350
220	12.14	13.83	0.39	-0.59	-3.02	2.92	13.52	11.60	0.364	0.298	0.587	0.844	0.365	0.333	0.879	0.546
230	12.77	12.85	-0.14	0.59	-2.91	2.89	14.59	12.51	0.594	0.863	1.829	0.964	0.716	0.658	1.274	1.532
290	15.82	10.27	-0.75	0.72	-2.30	6.40	21.14	9.25	0.756	0.768	1.817	1.800	0.855	0.473	1.558	1.829
300	15.73	9.94	-1.43	0.43	-2.31	5.62	16.99	9.14	0.597	0.597	0.975	1.445	1.390	1.083	2.296	2.051

Table 26 High preswirl, PR = 40%, ω = 15,200

	Test Data								Uncertainties							
f	Rzxx	Izxx	Rzxy	Izxy	Rzyx	Izyx	Rzyy	Izyy	Rzxx	Izxx	Rzxy	Izxy	Rzyx	Izyx	Rzyy	Izyy
20	-4.02	2.59	7.28	-0.59	-7.11	1.25	-2.71	2.58	0.141	0.126	0.073	0.074	0.143	0.117	0.055	0.078
30	-3.46	3.86	7.12	-0.78	-6.82	1.24	-2.47	3.78	0.181	0.109	0.102	0.126	0.062	0.118	0.078	0.060
40	-3.49	4.17	7.12	-1.23	-5.84	2.19	-2.05	5.11	0.468	0.357	0.148	0.305	0.311	0.277	0.104	0.145
50	-2.11	6.38	6.98	-1.28	-6.43	1.61	-1.45	6.23	0.207	0.162	0.163	0.224	0.124	0.138	0.180	0.131
70	-0.56	7.99	5.96	-1.74	-5.80	2.44	0.83	7.66	0.150	0.162	0.226	0.233	0.090	0.143	0.227	0.150
80	0.11	9.04	6.17	-1.70	-5.43	2.24	0.84	8.38	0.100	0.087	0.183	0.150	0.074	0.076	0.091	0.147
90	1.13	9.69	5.86	-2.20	-5.24	2.43	1.95	9.29	0.163	0.133	0.140	0.185	0.119	0.097	0.182	0.164
100	1.69	10.48	5.83	-2.10	-4.94	2.23	2.54	9.56	0.213	0.112	0.228	0.300	0.130	0.158	0.250	0.172
110	2.75	11.32	5.87	-2.44	-5.05	2.39	3.51	10.01	0.256	0.221	0.343	0.356	0.209	0.215	0.247	0.386
130	4.65	11.75	5.54	-2.26	-4.69	2.90	5.74	11.00	0.122	0.184	0.249	0.244	0.118	0.082	0.136	0.212
140	5.12	11.93	4.58	-2.49	-4.54	2.68	6.00	11.24	0.156	0.198	0.266	0.342	0.145	0.160	0.308	0.214
150	5.97	12.22	5.03	-2.72	-4.52	2.86	6.71	11.31	0.101	0.162	0.233	0.233	0.141	0.095	0.197	0.221
160	6.78	12.53	4.29	-2.85	-4.14	3.31	8.10	11.94	0.145	0.195	0.347	0.523	0.068	0.103	0.171	0.277
190	9.47	13.23	0.13	-3.23	-3.07	2.49	11.95	11.93	0.161	0.186	0.410	0.238	0.101	0.132	0.296	0.294
200	10.83	14.56	1.34	-1.82	-3.37	2.38	11.78	11.91	0.209	0.256	0.363	0.240	0.148	0.148	0.199	0.247
210	11.88	14.54	1.45	-2.06	-3.82	2.26	12.01	11.87	0.223	0.412	0.529	0.537	0.219	0.219	0.304	0.350
220	14.23	14.50	-0.79	-1.32	-3.63	1.91	13.94	13.25	0.364	0.298	0.587	0.844	0.365	0.333	0.879	0.546
230	14.97	15.23	-2.93	2.87	-1.47	1.45	19.66	15.14	0.594	0.863	1.829	0.964	0.716	0.658	1.274	1.532
290	16.52	12.03	-7.61	8.09	-1.91	6.33	29.38	11.06	0.756	0.768	1.817	1.800	0.855	0.473	1.558	1.829
300	16.68	12.58	-1.64	1.72	-0.83	6.46	19.98	8.74	0.597	0.597	0.975	1.445	1.390	1.083	2.296	2.051

Table 27 High preswirl, PR = 40%, ω = 20,200

f	Test Data								Uncertainties							
	Rzxx	Izxx	Rzxy	Izxy	Rzyx	Izyx	Rzyy	Izyy	Rzxx	Izxx	Rzxy	Izxy	Rzyx	Izyx	Rzyy	Izyy
20	-4.98	2.91	8.81	-0.94	-8.70	1.26	-3.80	3.02	0.141	0.126	0.073	0.074	0.143	0.117	0.055	0.078
30	-4.34	4.32	8.54	-1.17	-8.36	1.43	-3.36	4.43	0.181	0.109	0.102	0.126	0.062	0.118	0.078	0.060
40	-3.28	5.31	8.03	-1.89	-8.57	1.79	-2.88	5.91	0.468	0.357	0.148	0.305	0.311	0.277	0.104	0.145
50	-1.92	6.49	8.37	-2.19	-7.85	1.85	-2.62	6.51	0.207	0.162	0.163	0.224	0.124	0.138	0.180	0.131
70	-1.03	8.83	7.28	-2.15	-7.05	2.37	-0.25	8.46	0.150	0.162	0.226	0.233	0.090	0.143	0.227	0.150
80	0.32	10.00	7.66	-2.74	-6.82	2.69	0.64	9.19	0.100	0.087	0.183	0.150	0.074	0.076	0.091	0.147
90	1.39	10.32	6.80	-3.18	-6.40	2.44	1.34	9.99	0.163	0.133	0.140	0.185	0.119	0.097	0.182	0.164
100	1.90	10.66	6.39	-2.84	-6.34	2.66	2.36	10.64	0.213	0.112	0.228	0.300	0.130	0.158	0.250	0.172
110	2.95	11.64	6.55	-3.37	-6.32	3.14	3.86	11.09	0.256	0.221	0.343	0.356	0.209	0.215	0.247	0.386
130	4.61	12.34	6.46	-2.92	-5.74	3.25	5.58	11.33	0.122	0.184	0.249	0.244	0.118	0.082	0.136	0.212
140	5.30	12.79	6.00	-3.03	-5.86	3.64	6.44	12.26	0.156	0.198	0.266	0.342	0.145	0.160	0.308	0.214
150	6.06	12.80	5.49	-3.50	-5.25	3.76	7.35	11.92	0.101	0.162	0.233	0.233	0.141	0.095	0.197	0.221
160	7.52	13.32	5.45	-4.04	-5.08	3.72	8.13	11.89	0.145	0.195	0.347	0.523	0.068	0.103	0.171	0.277
190	9.19	13.54	1.17	-3.55	-4.40	3.60	11.86	12.89	0.161	0.186	0.410	0.238	0.101	0.132	0.296	0.294
200	10.77	14.36	2.20	-3.32	-4.42	3.55	11.75	12.49	0.209	0.256	0.363	0.240	0.148	0.148	0.199	0.247
210	11.31	14.16	2.16	-2.95	-5.11	3.85	11.75	12.68	0.223	0.412	0.529	0.537	0.219	0.219	0.304	0.350
220	13.21	14.70	1.45	-2.31	-4.77	3.88	14.01	13.45	0.364	0.298	0.587	0.844	0.365	0.333	0.879	0.546
230	13.51	13.67	0.96	-2.56	-4.63	4.69	14.78	13.27	0.594	0.863	1.829	0.964	0.716	0.658	1.274	1.532
300	16.59	11.48	0.17	-0.47	-3.37	7.91	20.37	9.98	0.597	0.597	0.975	1.445	1.390	1.083	2.296	2.051
310	16.24	10.96	-3.09	0.99	-1.68	8.43	21.58	7.85	0.505	0.539	1.094	1.126	0.308	0.773	1.319	1.193

Table 28 High preswirl, PR = 50%, ω = 10,200

f	Test Data								Uncertainties							
	Rzxx	Izxx	Rzxy	Izxy	Rzyx	Izyx	Rzyy	Izyy	Rzxx	Izxx	Rzxy	Izxy	Rzyx	Izyx	Rzyy	Izyy
20	-3.34	2.38	5.68	-0.39	-5.90	0.72	-2.80	2.40	0.252	0.425	0.235	0.087	0.074	0.103	0.045	0.092
30	-2.76	3.40	5.58	-0.72	-5.34	0.96	-2.42	3.51	0.267	0.139	0.123	0.198	0.170	0.140	0.138	0.073
40	-2.55	4.59	5.57	-0.73	-5.42	1.20	-2.03	4.75	0.380	0.342	0.165	0.139	0.287	0.285	0.112	0.100
50	-1.94	5.19	4.80	-1.08	-5.17	1.75	-0.92	5.50	0.202	0.188	0.174	0.177	0.166	0.141	0.174	0.179
70	-0.52	7.23	4.86	-1.33	-4.75	1.48	-0.09	6.84	0.262	0.299	0.360	0.344	0.238	0.238	0.383	0.354
80	0.06	8.10	4.72	-1.47	-4.59	1.70	0.56	7.71	0.125	0.121	0.138	0.071	0.185	0.154	0.204	0.236
90	0.85	8.61	4.36	-1.64	-4.26	1.79	1.16	8.60	0.218	0.190	0.243	0.177	0.140	0.120	0.149	0.170
100	1.58	9.26	4.45	-1.58	-4.13	1.88	2.43	8.92	0.214	0.145	0.192	0.226	0.151	0.154	0.184	0.331
110	2.32	9.94	3.96	-1.87	-4.49	1.74	3.05	10.03	0.317	0.228	0.336	0.297	0.388	0.271	0.411	0.424
130	3.72	10.61	3.96	-0.82	-3.83	2.04	5.40	10.30	0.253	0.208	0.263	0.288	0.122	0.130	0.212	0.137
140	4.94	11.15	3.93	-1.70	-3.59	2.11	5.99	10.47	0.092	0.116	0.277	0.280	0.150	0.203	0.278	0.309
150	6.05	11.12	4.19	-2.38	-3.68	1.38	5.91	9.82	0.175	0.316	0.435	0.292	0.106	0.134	0.246	0.267
160	6.42	12.48	4.45	2.45	-2.83	2.41	12.01	9.53	0.481	0.295	0.436	0.433	0.146	0.157	0.300	0.300
190	8.11	11.95	-0.24	-3.47	-2.85	2.29	9.76	11.32	0.208	0.339	0.575	0.454	0.299	0.307	0.553	0.285
200	9.07	12.99	0.27	-2.00	-3.11	2.51	10.54	11.32	0.178	0.406	0.589	0.397	0.231	0.321	0.413	0.279
210	10.13	13.56	-0.37	-1.01	-2.79	2.61	11.63	12.20	0.293	0.263	0.708	0.701	0.207	0.369	0.363	0.484
220	12.19	14.20	-1.01	-0.03	-2.78	2.05	13.37	12.49	0.767	0.420	1.029	1.015	0.693	0.648	1.153	1.149
230	12.79	12.17	-0.14	0.11	-3.38	2.91	13.76	12.23	1.323	0.771	1.746	2.861	0.732	1.235	2.586	1.445
300	15.86	10.64	-2.18	1.81	-1.26	5.48	16.54	10.22	0.931	0.909	1.507	1.675	1.509	1.513	1.595	1.848
310	16.54	9.98	-2.49	0.87	-1.34	6.87	21.49	9.04	0.637	0.931	1.358	1.265	0.711	0.941	1.435	1.001

Table 29 High preswirl, PR = 50%, ω = 15,200

f	Test Data								Uncertainties							
	Rzxx	Izxx	Rzxy	Izxy	Rzyx	Izyx	Rzyy	Izyy	Rzxx	Izxx	Rzxy	Izxy	Rzyx	Izyx	Rzyy	Izyy
20	-3.53	2.64	7.16	-0.55	-6.79	0.62	-2.86	2.45	0.252	0.425	0.235	0.087	0.074	0.103	0.045	0.092
30	-3.15	3.91	7.03	-0.90	-6.88	0.99	-2.63	3.73	0.267	0.139	0.123	0.198	0.170	0.140	0.138	0.073
40	-1.71	2.93	6.77	-1.37	-6.39	2.52	-2.20	5.06	0.380	0.342	0.165	0.139	0.287	0.285	0.112	0.100
50	-1.91	6.06	6.47	-1.35	-6.11	1.37	-1.43	6.03	0.202	0.188	0.174	0.177	0.166	0.141	0.174	0.179
70	-0.44	7.72	5.69	-1.81	-5.86	2.17	0.45	7.77	0.262	0.299	0.360	0.344	0.238	0.238	0.383	0.354
80	0.27	8.92	6.10	-1.90	-5.38	2.12	0.91	8.21	0.125	0.121	0.138	0.071	0.185	0.154	0.204	0.236
90	1.24	9.41	5.90	-2.30	-5.07	2.23	1.61	8.79	0.218	0.190	0.243	0.177	0.140	0.120	0.149	0.170
100	1.81	10.30	5.99	-2.02	-4.86	2.07	2.14	9.27	0.214	0.145	0.192	0.226	0.151	0.154	0.184	0.331
110	2.73	10.39	4.84	-2.56	-4.92	1.83	2.94	9.87	0.317	0.228	0.336	0.297	0.388	0.271	0.411	0.424
130	4.88	11.42	5.42	-2.46	-4.64	2.69	5.12	10.70	0.253	0.208	0.263	0.288	0.122	0.130	0.212	0.137
140	5.35	11.87	4.78	-2.51	-4.45	2.95	6.48	11.38	0.092	0.116	0.277	0.280	0.150	0.203	0.278	0.309
150	5.42	11.44	4.03	-2.11	-4.17	2.75	7.07	11.15	0.175	0.316	0.435	0.292	0.106	0.134	0.246	0.267
160	7.27	12.45	4.60	-3.01	-4.22	2.90	8.17	11.40	0.481	0.295	0.436	0.433	0.146	0.157	0.300	0.300
190	9.33	12.63	0.77	-3.29	-3.70	2.58	10.57	12.14	0.208	0.339	0.575	0.454	0.299	0.307	0.553	0.285
200	10.73	13.81	1.74	-1.99	-3.89	2.39	11.37	11.96	0.178	0.406	0.589	0.397	0.231	0.321	0.413	0.279
210	11.13	13.68	1.12	-2.41	-3.49	2.77	12.01	12.59	0.293	0.263	0.708	0.701	0.207	0.369	0.363	0.484
220	11.98	16.40	-3.14	-2.76	-2.79	2.43	15.35	14.49	0.767	0.420	1.029	1.015	0.693	0.648	1.153	1.149
230	17.37	16.65	-6.00	-1.84	-0.71	-0.43	15.08	18.89	1.323	0.771	1.746	2.861	0.732	1.235	2.586	1.445
290	20.24	11.05	-2.51	3.58	-3.84	3.81	26.14	9.61	1.136	1.833	2.889	3.140	1.455	0.940	3.150	2.309
300	18.17	10.92	-4.77	-0.90	-3.78	3.44	18.79	9.22	0.931	0.909	1.507	1.675	1.509	1.513	1.595	1.848

Table 30 High preswirl, PR = 50%, ω = 20,200

f	Test Data								Uncertainties							
	Rzxx	Izxx	Rzxy	Izxy	Rzyx	Izyx	Rzyy	Izyy	Rzxx	Izxx	Rzxy	Izxy	Rzyx	Izyx	Rzyy	Izyy
20	-4.29	2.88	8.67	-0.82	-8.06	0.80	-3.40	2.63	0.252	0.425	0.235	0.087	0.074	0.103	0.045	0.092
30	-3.54	4.08	8.35	-1.31	-8.12	1.23	-3.43	4.21	0.267	0.139	0.123	0.198	0.170	0.140	0.138	0.073
40	-2.77	5.16	8.04	-1.57	-7.56	1.94	-2.35	5.45	0.380	0.342	0.165	0.139	0.287	0.285	0.112	0.100
50	-1.93	6.73	8.00	-2.37	-7.31	1.92	-2.05	6.77	0.202	0.188	0.174	0.177	0.166	0.141	0.174	0.179
70	-0.49	8.27	6.91	-2.40	-7.08	2.13	-0.22	8.51	0.262	0.299	0.360	0.344	0.238	0.238	0.383	0.354
80	0.55	9.54	7.35	-2.72	-6.52	2.28	0.34	9.06	0.125	0.121	0.138	0.071	0.185	0.154	0.204	0.236
90	1.25	10.01	6.54	-2.55	-6.44	2.54	1.59	10.02	0.218	0.190	0.243	0.177	0.140	0.120	0.149	0.170
100	2.13	10.96	7.19	-2.80	-6.14	2.54	2.29	10.11	0.214	0.145	0.192	0.226	0.151	0.154	0.184	0.331
110	2.94	11.49	6.64	-3.12	-6.62	2.84	3.32	11.57	0.317	0.228	0.336	0.297	0.388	0.271	0.411	0.424
130	5.10	12.19	6.52	-3.15	-6.02	3.08	5.01	11.66	0.253	0.208	0.263	0.288	0.122	0.130	0.212	0.137
140	5.53	12.51	5.94	-3.10	-5.78	3.13	6.37	12.01	0.092	0.116	0.277	0.280	0.150	0.203	0.278	0.309
150	6.08	12.48	5.51	-3.28	-5.48	3.50	7.38	12.51	0.175	0.316	0.435	0.292	0.106	0.134	0.246	0.267
160	7.13	13.15	5.00	-3.59	-5.61	3.75	8.10	13.34	0.481	0.295	0.436	0.433	0.146	0.157	0.300	0.300
190	9.41	13.21	1.21	-4.19	-4.44	3.41	11.96	12.82	0.208	0.339	0.575	0.454	0.299	0.307	0.553	0.285
200	10.68	14.58	2.50	-2.99	-4.49	3.73	12.47	12.84	0.178	0.406	0.589	0.397	0.231	0.321	0.413	0.279
210	11.88	14.31	2.93	-3.45	-4.53	3.69	12.14	13.09	0.293	0.263	0.708	0.701	0.207	0.369	0.363	0.484
220	12.83	14.60	2.11	-2.86	-4.43	4.06	14.02	13.34	0.767	0.420	1.029	1.015	0.693	0.648	1.153	1.149
230	13.95	13.64	1.51	-2.16	-4.64	4.28	14.93	13.62	1.323	0.771	1.746	2.861	0.732	1.235	2.586	1.445
290	17.80	10.80	-0.38	0.27	-4.50	8.08	25.43	8.69	1.136	1.833	2.889	3.140	1.455	0.940	3.150	2.309
300	17.19	11.96	-0.05	0.92	-2.08	8.18	23.40	9.37	0.931	0.909	1.507	1.675	1.509	1.513	1.595	1.848

VITA

Brent Alan Seifert received his Bachelor of Science degree in mechanical engineering from Texas A&M University at College Station in May 2003. He received his Master of Science degree from Texas A&M University in December 2005. He can be reached at the following permanent address:

Brent Alan Seifert
11506 Amber Canyon Dr.
Houston, TX 77095